

TECHNISCHE UNIVERSITÄT MÜNCHEN

Lehrstuhl für Biofunktionalität der Lebensmittel

# Iron as environmental factor in the pathogenesis of Crohn´s disease-like ileitis

Tanja Verena Werner

Vollständiger Abdruck der von der Fakultät Wissenschaftszentrum Weihenstephan für Ernährung,  
Landnutzung und Umwelt der Technischen Universität München zur Erlangung des akademischen  
Grades eines

Doktors der Naturwissenschaften

genehmigten Dissertation.

Vorsitzende: Univ.-Prof. Dr. H. Daniel

Prüfer der Dissertation: 1. Univ.-Prof. Dr. D. Haller

2. apl. Prof. Dr. K. Schümann

Die Dissertation wurde am 21.06.2010 bei der Technischen Universität München eingereicht und  
durch die Fakultät Wissenschaftszentrum Weihenstephan für Ernährung, Landnutzung und Umwelt am  
08.10.2010 angenommen.

*Für meine Familie*

## PUBLICATIONS AND PRESENTATIONS

### Peer-reviewed original manuscripts and reviews

**Werner T\***, Shkoda A\*, Daniel H, Gunckel M, Rogler G, Haller D. Differential protein expression profile in the intestinal epithelium from patients with inflammatory bowel disease. *J Proteome Res.* 2007 Mar;6(3):1114-25. (\* authors contribute equally to the manuscript)

**Werner T**, Haller D. Intestinal epithelial cell signalling and chronic inflammation: From the proteome to specific molecular mechanisms. *Mutat Res.* 2007 Sep 1;622(1-2):42-57

**Werner T**, Shkoda A, Haller D. Intestinal epithelial cell proteome in IL-10 deficient mice and IL-10 receptor reconstituted epithelial cells: impact on chronic inflammation. *J Proteome Res.* 2007 Sep;6(9):3691-704.

**Werner T**, Hoermannsperger G, Schuemann K, Hoelzlwimmer G, Tsuji S, Haller D. Intestinal epithelial cell proteome from wild-type and TNFDeltaARE/WT mice: effect of iron on the development of chronic ileitis. *J Proteome Res.* 2009 Jul;8(7):3252-64.

**Tanja Werner**, Stefan Wagner, Dirk Haller. Die Bedeutung von Eisen bei chronisch entzündlichen Darmerkrankungen (CED). *Bauchredner* Ausgabe 1/2010

**Werner T**, Wagner SJ, Martínez I, Walter J, Kisling S, Chang JS, Schümann K, Haller D. Depletion of dietary iron prevents Crohn's disease-like ileitis affecting epithelial stress responses and the gut microbial ecology. GUT accepted

### Published Abstracts

**Werner T**, Schuemann K, Haller D. Low dietary iron inhibits chronic experimental ileitis and attenuates endoplasmic reticulum stress responses in intestinal epithelial cells. *Gastroenterology* 2008; 134(4): A254-A255

## Oral presentations

**Werner T**, Shkoda A, Daniel H, Gunckel M, Rogler G, Haller D. Intestinal epithelial cell proteome from patients with inflammatory bowel disease. 44. Wissenschaftlicher Kongress der Deutschen Gesellschaft für Ernährung, Halle-Wittenberg, Germany, March 8-9<sup>th</sup>, 2007

**Werner T**, Schümann K, Kollias G and Haller D. Effects of an iron-low diet on chronic ileitis. 45. Wissenschaftlicher Kongress der Deutschen Gesellschaft für Ernährung, Bonn, Germany, March 8-9<sup>th</sup>, 2007. March 13-14<sup>th</sup>, 2008

**Werner T**, Clavel T, Kisling S, Schümann K, Haller D. Dietary iron triggers chronic inflammation: impact on endoplasmic reticulum (ER)-stress and apoptosis signaling. 2nd Conference of the German Society of Hygiene and Microbiology “Microbiota, Probiota and Host”, Seon, Germany, April 23-25<sup>th</sup>, 2009

**Werner T**, Chang J, Kisling S, Schümann K, Binder U, Skerra A, Haller D. Iron-deficient diet and systemic iron repletion inhibited chronic ileitis targeting endoplasmic reticulum stress responses in the intestinal epithelium. 14<sup>th</sup> International Congress of Mucosal Immunology, Boston, USA, July 5-9<sup>th</sup>, 2009

## Poster presentations

**Werner T**, Shkoda A, Daniel H, Gunckel M, Rogler G and Haller D. Intestinal epithelial cell proteome from patients with inflammatory bowel disease. 5th Meeting of the European Mucosal Immunology Group, Prague, Czech Republic, October 5-7<sup>th</sup>, 2006

**Werner T** and Haller D. Adjuvant nutritional therapy in TNF<sup>ΔARE/WT</sup> mice with chronic ileitis. 44. Wissenschaftlicher Kongress der Deutschen Gesellschaft für Ernährung, Halle-Wittenberg, March 8-9<sup>th</sup>, 2007.

**Werner T**, Schulz N, Kollias G, Schuemann K and Haller D. Iron-low diet inhibits chronic ileal inflammation in  $TNF^{\Delta ARE/WT}$  mice by attenuating oxidative and endoplasmic reticulum (ER) stress. 2<sup>nd</sup> World Conference of Stress 2007, Budapest, Hungary, August 23-26<sup>th</sup>, 2007

**Werner T**, Schümann K, Kollias G, Haller D. Iron-low diet inhibits chronic ileal inflammation in  $TNF^{\Delta ARE/WT}$  mice by attenuating oxidative and endoplasmic reticulum (ER) stress. Digestive Disease Week 2008, San Diego, USA, May 17-22<sup>th</sup>, 2008

**Werner T**, Kollias G, Schuemann K, Haller D. Low dietary iron inhibits chronic experimental ileitis by attenuating endoplasmic reticulum and oxidative stress responses in intestinal epithelial cells. 6th Meeting of the European Mucosal Immunology Group, Mailand, Italy, October 8-10<sup>th</sup>, 2008

### Prices and travel grants

Poster price from the Deutsche Gesellschaft für Ernährung for:

**Werner T** and Haller D. Adjuvant nutritional therapy in  $TNF^{\Delta ARE/WT}$  mice with chronic ileitis. 44. Wissenschaftlicher Kongress der Deutschen Gesellschaft für Ernährung, Halle-Wittenberg, March 8-9<sup>th</sup>, 2007.

Travel grant from the Anneliese Pfannenbergs Stiftung 2008 for scientific conferences

Travel grant from the Deutsche Forschungsgemeinschaft for the Digestive Disease Week 2008, San Diego, USA, May 17-22<sup>th</sup>, 2008

Travel grant from the Society for immunology for the 14th International Congress of Mucosal Immunology, Boston, USA, July 5-9<sup>th</sup>, 2009

Travel grant from DANONE GmbH for the 14th International Congress of Mucosal Immunology, Boston, USA, July 5-9<sup>th</sup>, 2009

**TABLE OF CONTENTS**

|   |           |
|---|-----------|
| <b>PUBLICATIONS AND PRESENTATIONS.....</b>  | <b>3</b>  |
| <b>TABLE OF CONTENTS.....</b>   | <b>6</b>  |
| <b>ZUSAMMENFASSUNG .....</b>  | <b>9</b>  |
| <b>ABSTRACT .....</b>   | <b>11</b> |
| <b>1 INTRODUCTION.....</b>  | <b>12</b> |
| 1.1 The trace element iron.....   | 12        |
| 1.2 Iron in nutrition .....   | 12        |
| 1.3 Anatomy of the GI tract and the intestinal epithelium.....  | 13        |
| 1.4 The role of the intestinal epithelium in immunity.....  | 15        |
| 1.5 Iron metabolism in the GI tract .....   | 17        |
| 1.5.1 Iron metabolism in the circulation .....  | 18        |
| 1.5.2 Iron utilization in the cell.....   | 20        |
| 1.5.3 Regulation of cellular iron metabolism.....   | 21        |
| 1.5.4 Regulation of systemic iron metabolism.....   | 21        |
| 1.6 IBD: causes, consequences and the role of iron in intestinal inflammation .....   | 23        |
| 1.6.1 The clinical pictures Ulcerative colitis (UC) and Crohn´s disease (CD).....   | 23        |
| 1.6.2 Genetic factors in IBD: disturbances in microbial-host interaction, barrier function and immunity.....                | 24        |
| 1.6.3 Endoplasmic reticulum (ER) stress as possible trigger in the pathogenesis of IBD and its role in iron metabolism..... | 25        |
| 1.6.4 Iron as environmental parameter in the context of IBD.....  | 28        |
| 1.6.5 Iron and NF-κB .....  | 31        |
| 1.7 The TNF <sup>ΔARE/WT</sup> mouse model for chronic ileitis .....  | 33        |
| <b>2 AIMS OF THE WORK .....</b>   | <b>34</b> |
| <b>3 MATERIALS AND METHODS .....</b>  | <b>35</b> |
| Animals and Diets .....   | 35        |
| Isolation of murine primary IEC .....   | 35        |
| Proteome analysis .....   | 36        |
| Western blot analysis.....  | 38        |
| RNA isolation and measurement.....  | 39        |
| Immunohistochemical labelling .....   | 39        |
| TUNEL staining .....  | 40        |

|  |           |
|--|-----------|
| Ileal explant cultivation .....  | 41        |
| Cell culture, co-culture and stimulation .....   | 41        |
| Reverse transcription and Real-Time PCR.....   | 41        |
| ROS measurement .....  | 43        |
| Chromatin immunoprecipitation (ChIP) analysis.....   | 43        |
| Isolation of intraepithelial lymphocytes (IEL) and FACS staining.....  | 43        |
| Non-heme content, hematocrit and hemoglobin determination .....  | 44        |
| ELISA analysis .....   | 44        |
| Isolation of mesenteric CD8 $\alpha\beta$ <sup>+</sup> T cells.....  | 45        |
| Cell mediated cytotoxicity assay .....   | 45        |
| Statistical analysis.....  | 47        |
| <b>4 RESULTS.....</b>  | <b>48</b> |
| <b>4.1 Effects of an iron-deficient diet on chronic ileitis .....</b>  | <b>48</b> |
| 4.1.1 Epithelial cell proteome of iron-adequately and iron-deficiently fed WT and TNF <sup><math>\Delta</math>ARE/WT</sup> mice .....  | 50        |
| 4.1.1.1 Protein expression profiling of the ade WT-ARE-comparison: effects of chronic inflammation on the ileal epithelial cell proteome.....                                  | 51        |
| 4.1.1.2 Protein expression profiling of the ARE-comparison: effects of iron on the epithelial cell proteome under conditions of disease susceptibility.....                    | 53        |
| 4.1.1.3 Protein expression profiling of the WT-comparison: effects of iron on the epithelial cell proteome under normal conditions of non-susceptible mice .....               | 55        |
| 4.1.1.4 Protein expression profiling of the def WT-ARE-comparison: effects of iron on the epithelial cell proteome under non-inflamed but disease susceptible conditions ..... | 56        |
| 4.1.2 Focus on the overlap of regulated proteins between the ade WT-ARE-comparison and ARE-comparison .....  | 58        |
| 4.1.3 Bibliometric analysis of differentially regulated proteins from the ade WT-ARE- and the ARE-comparison .....   | 60        |
| 4.1.4 Up-regulation of proteins involved in inflammation, cell stress responses and apoptosis by the iron-adequate diet.....   | 63        |
| 4.1.5 Iron-mediated up-regulation of proteins involved in inflammation, cell stress responses and apoptosis <i>ex vivo</i> and <i>in vitro</i> .....                           | 66        |
| <b>4.2 Effects of short-term reduction of dietary iron in existing ileitis .....</b>   | <b>70</b> |
| <b>4.3 Effects of systemic iron repletion on chronic ileitis: focus on the epithelium.....</b>   | <b>71</b> |
| 4.3.1 Iron repletion maintained down-regulated ER stress and apoptosis-associated protein expression in IEC.....   | 72        |

|            |   |            |
|------------|---|------------|
| 4.3.2      | Ileal explants from the parenteral iron-repletion experiment confirmed the reduction of ER stress and apoptosis ..... | 74         |
| <b>4.4</b> | <b>Effects of systemic iron repletion on chronic ileitis: focus on immune cells and the gut microbiota .....</b>      | <b>76</b>  |
| 4.4.1      | Luminal ID and systemic iron repletion did not influence the phenotype of intraepithelial lymphocytes (IEL) .....     | 78         |
| 4.4.1.1    | Higher susceptibility towards cytotoxic T cell-induced apoptosis in an ER-stressed epithelium .....                   | 80         |
| 4.4.2      | Luminal iron rather than the inflammatory host response affect the gut microbiota.....                                | 82         |
| 4.4.2.1    | Iron-deficient diet induces significant alterations of the gut microbiota .....                                       | 82         |
| 4.4.2.2    | Highly significant associations between members of the gut microbiota and inflammation .....                          | 83         |
| <b>5</b>   | <b>DISCUSSION .....</b>   | <b>91</b>  |
| 5.1        | Effects of an iron-deficient diet on the ileal IEC proteome of WT and TNF <sup>ΔARE/WT</sup> mice .....               | 91         |
| 5.2        | Luminal iron as environmental factor in the pathogenesis of CD-like ileitis .....                                     | 94         |
| 5.3        | Outlook.....  | 99         |
|            | <b>LIST OF FIGURES.....</b>   | <b>100</b> |
|            | <b>LIST OF TABLES.....</b>  | <b>102</b> |
|            | <b>ABBREVIATIONS .....</b>  | <b>103</b> |
|            | <b>REFERENCES .....</b>   | <b>107</b> |
|            | <b>ACKNOWLEDGEMENTS.....</b>  | <b>117</b> |
|            | <b>CURRICULUM VITAE .....</b>   | <b>118</b> |
|            | <b>ERKLÄRUNG .....</b>  | <b>121</b> |

### ZUSAMMENFASSUNG

Chronisch entzündliche Darmerkrankungen (CED) sind rezidivierende, immunvermittelte Störungen des Gastrointestinaltraktes mit Morbus Crohn (MC) und Colitis ulzerosa als den beiden Hauptverlaufsformen. Bei der Pathogenese von CED spielt die genetische Prädisposition des Menschen als auch Umweltfaktoren eine Rolle. Ernährungsformen der westlichen Industrieländer werden als Umweltfaktor diskutiert, es gibt aber bislang keine klare Korrelation zwischen Ernährung bzw. einzelnen Nahrungsbestandteilen und der Entwicklung von CED. Das Ziel der vorliegenden Arbeit war die Untersuchung des Spurenelements Eisen als möglicher Umweltfaktor in der Pathogenese von MC.

Studien in  $\text{TNF}^{\Delta\text{ARE}/\text{WT}}$  Mäusen, einem Mausmodell für chronische Ileitis, haben gezeigt, dass das langfristige Füttern einer eisenarmen Diät nach dem Absetzen der Jungtiere von der Mutter die Entzündung im Darm verhindern kann. Die kurzfristige Gabe der eisenarmen Diät in bestehender Entzündung führte zu einer signifikanten Reduktion des Entzündungsgrades. Die systemische Eisengabe durch wöchentliches, intraperitoneales Spritzen einer Eisenlösung von eisenarm gefütterten  $\text{TNF}^{\Delta\text{ARE}/\text{WT}}$  Mäusen führte nicht zu einem Wiederauftreten der Entzündung. Dies deutet daraufhin, dass luminales Eisen der entscheidende Faktor in der Pathogenese von MC ist. Untersuchungen zur Aufklärung des Mechanismus haben gezeigt, dass die eisenarme Diät einen signifikanten Einfluss auf die Zusammensetzung der Darmmikrobiota hat. Intestinale Epithelzellen (IEZ) und die damit verbundene Barrierefunktion spielen eine wichtige Rolle bei der Erhaltung der Darmhomöostase, welche bei CED gestört ist. Eine Proteomanalyse isolierter primäre IEZ von entzündeten, eisenadäquat gefütterten  $\text{TNF}^{\Delta\text{ARE}/\text{WT}}$  Mäusen im Vergleich zu nicht-entzündeten, eisendefizient gefütterten  $\text{TNF}^{\Delta\text{ARE}/\text{WT}}$  Mäusen zeigte unterschiedlich regulierte Proteine, welche im Energiemetabolismus, in der Wirtsabwehr und bei Stressantwort eine Rolle spielen. Die Western blot Analyse bestätigte aktivierte oxidative und endoplasmatischer Retikulum (ER) Stressmechanismen und damit verbundene Apoptose. Beide Faktoren werden durch das Füttern der eisenarmen Diät wie auch der systemischen Eisengabe verhindert. Die Applikation der eisenarmen Diät hatte keinen Einfluss auf die Veränderung des Phänotypes von intraepithelialen Lymphozyten (IEL) bzw. führte nicht zu einer reduzierten Infiltration von  $\text{CD8}\alpha\beta^+$  IEL, welche hauptverantwortlich für die Entzündungsentstehung im  $\text{TNF}^{\Delta\text{ARE}/\text{WT}}$  Mausmodell sind. Co-Kultur Experimente mit einer intestinalen Epithelzelllinie und isolierten  $\text{CD8}\alpha\beta^+$  T-Zellen aus entzündeten  $\text{TNF}^{\Delta\text{ARE}/\text{WT}}$  Mäusen haben jedoch gezeigt, dass bestehender ER Stress in IEZ zu einer erhöhten T-Zell-induzierten Apoptose führt.

Die Ergebnisse dieser Arbeit deuten darauf hin, dass das Füttern einer eisenarmen Diät in Kombination mit systemischer Eisengabe die Entstehung der Dünndarmentzündung in einem Mausmodell, welches die MC-Erkrankung des Menschen widerspiegelt, verhindern kann. Der Mechanismus umfasst dabei die Veränderungen der Darmmikrobiota als auch die Verhinderung von Stressmechanismen und Apoptose im intestinalen Epithel. Dieser Ansatz könnte eine

Therapiemöglichkeit darstellen, die sowohl auf die Reduktion der Darmentzündung als auch der Verhinderung einer Anämie, welche bei  $\frac{1}{3}$  aller CED-Patienten auftritt, abzielt.

**ABSTRACT**

Inflammatory bowel diseases (IBD) including ulcerative colitis and Crohn's disease (CD) are spontaneously relapsing, immunologically mediated disorders of the gastrointestinal tract. Present etiologic theories of IBD imply the presence of environmental factors like smoking, luminal enteric bacteria or diet in a genetic susceptible host. Although western-like diets are discussed as a risk factor for the development of IBD, there is currently no sufficient evidence for a direct correlation between diet or dietary factors and IBD. The aim of the present work was to characterize the role of iron as environmental factor in the pathogenesis of CD-like ileitis.

Studies in  $TNF^{\Delta ARE/WT}$  mice, a mouse model resembling human CD-like ileitis, showed that long-term feeding of an iron-deficient diet after weaning period inhibited the development of chronic ileitis. In addition, short-term feeding of the iron-deficient diet in existing ileitis lead to a significant decrease in the histology score. Most importantly, systemic iron repletion by weekly applied intraperitoneal iron injections maintained the protective effect of the iron-deficient diet supporting a critical role for luminal iron in the pathogenesis of ileitis in  $TNF^{\Delta ARE/WT}$  mice. Experiments to elucidate the underlying mechanisms revealed a tremendous effect of luminal iron deprivation on the bacterial composition of the gut microbiota.

Intestinal epithelial cells (IEC) forming the gut barrier are important for maintenance of gut homeostasis which is disturbed in IBD. Proteome analysis of isolated primary IEC from inflamed, iron-adequately fed  $TNF^{\Delta ARE/WT}$  mice compared to non-inflamed iron-deficiently fed  $TNF^{\Delta ARE/WT}$  mice revealed significantly regulated proteins involved in energy homeostasis, host defense and stress responses. Western blot analysis showed activated oxidative as well as endoplasmic reticulum (ER) stress mechanisms and apoptosis. ER stress and apoptosis are absent in isolated primary IEC from iron-deficiently fed as well as iron-repleted  $TNF^{\Delta ARE/WT}$  mice. Luminal iron deprivation did not affect intraepithelial lymphocyte (IEL) phenotype or lead to a reduction of cytotoxic  $CD8\alpha\beta^+$  IEL, the major effector T cells in the  $TNF^{\Delta ARE/WT}$  mouse model. Interestingly, co-culture experiments with a small IEC line and isolated  $CD8\alpha\beta^+$  T cells from inflamed  $TNF^{\Delta ARE/WT}$  mice revealed that ER stress in IEC sensitized the epithelium towards cytotoxic T-cell induced apoptosis.

In conclusion, the results of the present thesis indicate that luminal iron deprivation in combination with systemic iron repletion inhibited the development of inflammation in  $TNF^{\Delta ARE/WT}$  mice, resembling human CD-like ileitis. The mechanisms mediated by the iron-deficient diet implied changes in the gut microbiota as well as inhibition of ER stress and apoptosis in the intestinal epithelium. This method may offer a new treatment possibility to reduce ileal inflammation and the onset of anemia which occurs in  $\frac{1}{3}$  of all IBD patients.

# 1 INTRODUCTION

## 1.1 The trace element iron

Iron is the fourth common trace element on earth and nearly essential for all living organisms. The two main forms of iron are the ferric form as  $\text{Fe}^{3+}$  and the ferrous form as  $\text{Fe}^{2+}$ . It is required for many cellular redox reactions, for oxygen transport, electron transfer, aerobic and anaerobic energy metabolism, growth, DNA-synthesis and as co-factor for many enzyme systems [1, 2]. The role of iron in haematology was already known in the 18<sup>th</sup> century, but its function in immunity was first described in the late 1960s and the beginning of the 70s by observations of an association between iron deficiency (ID) and infections [3, 4]. Iron can act as a catalyst for the production of reactive oxygen species (ROS) via the Fenton reaction. ROS are discussed in a variety of pathologies including inflammation and carcinogenesis by inducing tissue and DNA damage [5, 6]. Because of these damaging and toxic effects, iron metabolism in the human body is tightly regulated starting at the level of absorption in the gastrointestinal (GI) tract.

## 1.2 Iron in nutrition

In nutrition, 90% of iron is present in its anorganic forms as non-heme iron (ferrous and ferric compounds) and 10% of iron in its organic forms, most importantly as heme. A typical western diet contains 5-15mg non-heme iron and 1-5mg heme iron and provides approximately 6mg iron/1000 kcal. As the bioavailability of heme iron is 2-3 times higher than for non-heme iron, 20-35% of daily iron requirements are covered by heme iron [7]. Meat, fish and poultry are the main source for heme iron in form of haemoglobin and myoglobin [8]. In contrast to heme iron, the bioavailability of non-heme iron is very low due to complex formation with nutritional ligands like phosphates, phytates and oxalic acid as they can be found in cereals and vegetables [9]. The strong binding of those compounds to iron inhibits the absorption. The bioavailability of non-heme iron can be enhanced by complex formation with ascorbate, citrate, fumarate and amino acids as well as oligopeptides from meat digestion [10]. There are also modern factors including caseinophosphopeptides and fructo-oligosaccharides with prebiotic characteristics to fortify non-heme iron bioavailability. These complexes inhibit the formation of ferrous hydroxides in the gut lumen and therefore iron is still available for resorption. The resorption of heme iron is less influenced by nutritional ligands except for high luminal calcium concentration [11].

ID affects an estimated 2 billion people worldwide [12]. The high prevalence of ID in developing countries is due to unvaried plant-based diet. Therefore, food fortification may be

an effective strategy to overcome nutritional ID. There are a wide range of iron compounds for food fortification like ferrous gluconate, ferrous lactate, etc., but the World Health Organisation (WHO) recommends only ferrous sulphate, ferrous fumarate, ferric pyrophosphate and electronic iron powder [13]. This fortification has shown to be beneficial for anemic patients, but a general food fortification with iron might have negative effects for individuals suffering from gastrointestinal disorders because of its pro-oxidative and possible pro-inflammatory character.

### 1.3 Anatomy of the GI tract and the intestinal epithelium

The GI tract is divided into the upper and lower part. Mouth, pharynx, oesophagus and stomach belong to the upper GI tract, small intestine (duodenum, jejunum, ileum) and large intestine (cecum, colon, rectum) belong to the lower GI tract. The small intestine reaches a length of around 5-7 metres, the large intestine of approximately 1.5 metres. A schematic cross section through the small intestine is shown in Figure 1. From inside to the outside, the mucosa includes the epithelium, lamina propria and muscularis mucosa followed by the submucosa containing blood vessels, lymph streams and nerves reaching into the mucosa, enclosed by the circular and longitudinal muscle layer and the serosa as outer membrane [14].

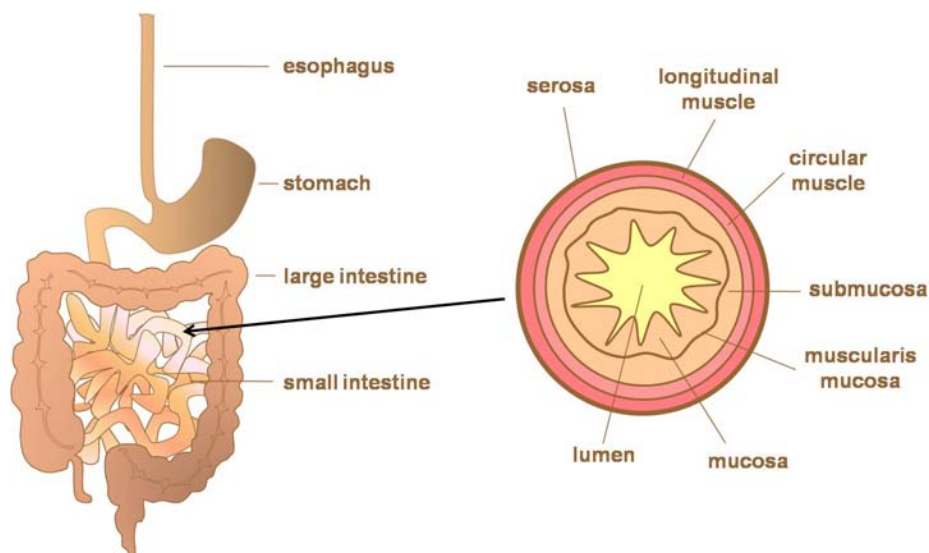


**Figure 1. Schematic illustration of the GI tract (left) and cross section of the small intestine (right).**

The GI tract with a surface area of approximately 300m<sup>2</sup> harbours around 10<sup>14</sup> bacteria of more than 1000 species, with low bacterial density in the upper GI tract, increasing numbers in the distal small intestine and highest numbers (10<sup>11</sup>-10<sup>12</sup> bacteria per g) in the colon as major bacterial pool [15]. The

function of the non-pathogenic, commensal microbiota includes among others the colonization of ecological niches to block pathogens, metabolization of dietary factors for energy supply of the host and influence on immune functions [16]. Because bacteria need iron for growth, function and survival, they secrete high affinity iron chelators called siderophores to solubilise iron from the environment before internalization [17]. In mice, iron supplementation was shown to increase colony forming units (CFU) of *M. tuberculosis* and human transferrin transgenic mice developed prolonged bacteraemia with *N. meningitidis* [18, 19]. Therefore, in the situation of inflammation, a host protective mechanism is to sequester iron. Consequentially, diets different in iron concentration influence the microbial composition from animals [20].

Only a single cell layer separates the organism from this enormous numbers of gut bacteria - the intestinal epithelium. Intestinal epithelial cells (IEC) which are bound by adherent and tight junction proteins represent a highly selective barrier between the rough gut lumen and the underlying immune cells. *In vitro* studies clearly demonstrate multiple damaging effects of iron on IEC affecting cell proliferation, caspase-3 activation (apoptosis) as well as lipid peroxidation via Nuclear Factor kappa B (NF- $\kappa$ B) activation [21-23]. The intestinal epithelium is a fast renewable cell system along the crypt-villus axis. The crypt region harbours the proliferating stem cells which can develop into four different types of IEC including enterocytes or absorptive cells, goblet cells, enteroendocrine cells, Paneth cells and the follicle-associated epithelium with microfold (M)-cells [24].

The enterocytes or absorptive cells are specialized for the transport of nutrients and barrier formation. Their apical membrane which is in contact with the lumen is closely covered with absorptive microvilli. Membrane-fixed glycoproteins form the brush border glycocalyx at the top of the microvillus for the absorption of digested nutritive substances [25]. Nearly 80% of IEC are enterocytes. They actively transport monosaccharides and amino acids and absorb monoglycerides and fatty acids by passive transport through the villus membrane. Goblet cells are the second most abundant IEC cell type with increasing numbers from the small to the large intestine. After stimulation, mucus can be released into the lumen to build a protective mucus layer over the epithelial cells preventing enormous inclusion of antigens and pathogens [26]. The Paneth cells are located in the crypt regions to produce antimicrobial defensins as part of the innate immune response and host defense mechanisms [27] to maintain epithelial integrity. The function of enteroendocrine cells implies the production of different hormones like cholecystokinin for stimulating the secretion of pancreatic enzymes or contraction of the gall bladder as well as secretin for the stimulation of pancreatic and biliary bicarbonate secretion [28].

Specialized IEC, the M cells, are the “door” for antigens to enter the organism. In difference to enterocytes, the brush border glycocalyx is absent on the apical surface of M cells. These cells transport microbes to antigen presenting cells (APC) in the underlying gut-associated lymphoid tissue (GALT) [25]. As most of the antigens enter the human body through the intestinal epithelium, the

GALT has to distinguish between the harmless food antigens, commensal bacteria and the harmful pathogens.

#### 1.4 The role of the intestinal epithelium in immunity

The GALT can be divided into two parts, the inductor site (Peyer's Patches in small intestine, colonic patches, mesenteric lymph nodes and isolated lymphoid follicles) and the effector site (epithelium and lamina propria). M cells translocate antigens to APC in the subepithelial dome (enriched APC region) of the Peyer's Patch (PP). PP are aggregations of lymphoid follicles, occurring only in the small intestine, primarily in the distal ileum [29]. As shown in Figure 2, the PP contains B-cell follicle and germinal centers surrounded by T cells. Afferent lymphatics connect mesenteric lymph nodes (MLN) to the PP and lamina propria (LP) [30].

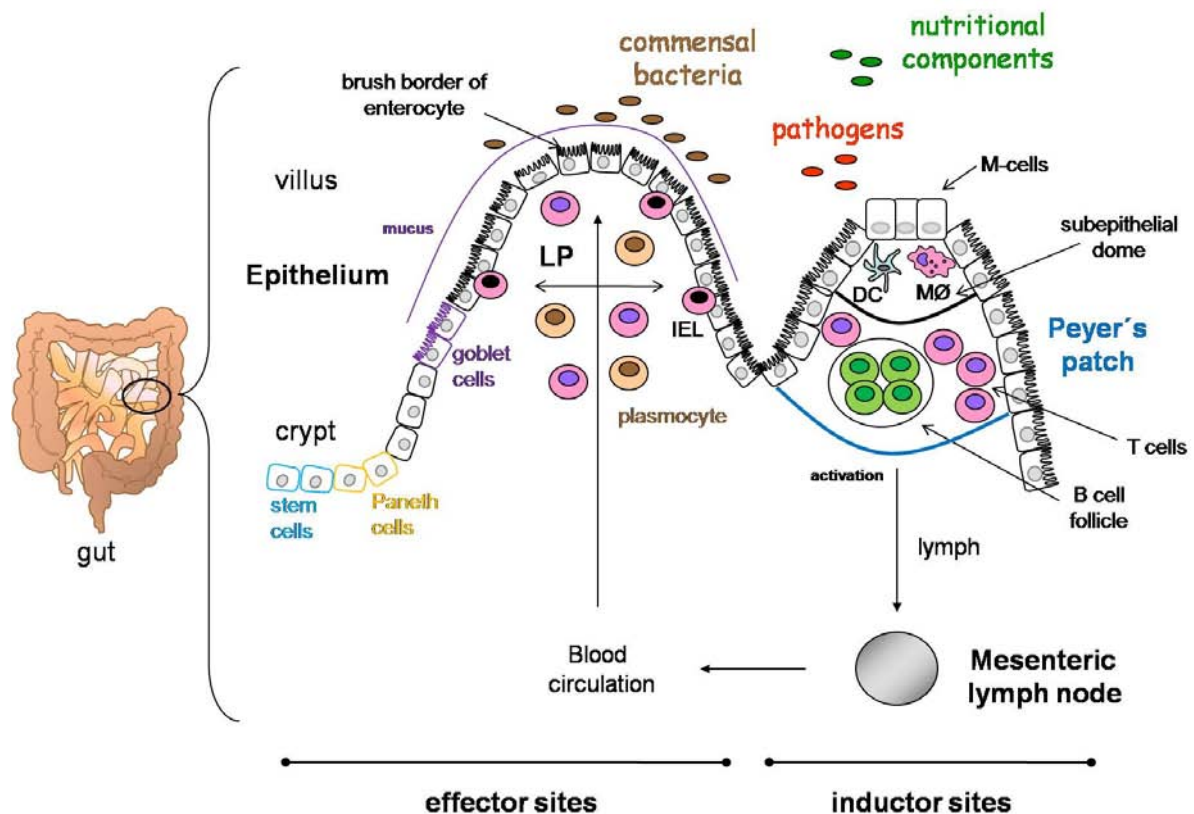


**Figure 2. Overview of the GALT (modified from Magelhaes 2007 [31] and Haller 2008 [32]).** LP: lamina propria; IEL: intraepithelial lymphocyte; DC: dendritic cell; MØ: macrophage

Antigen-loaded DC travel to lymph nodes where they activate the naive T cells to induce a cellular response. T lymphocytes can be divided into two main classes via the cell surface protein  $CD4^+$  or  $CD8^+$ . Naive  $CD4^+$  T cells can differentiate into helper T cells (Th1, Th2, and Th17), suppressor or memory T cells after activation, whereas  $CD8^+$  T cells differentiate into cytotoxic T cells. APC present fragmented peptides from virus and some bacteria (which replicate in the cytosol) via human major histocompatibility complex (MHC) class I whereas other bacteria and parasites are internalized via

endocytosis and then presented by MHC class II. The antigen presentation by MHC class I leads to the activation of cytotoxic CD8<sup>+</sup> T cells in contrast to the activation of CD4<sup>+</sup> T cells via antigen presentation by MHC class II molecules [33]. Activation of T cells by APC need the interaction of the T cell receptor with the antigen-loaded MHC and co-stimulatory molecules. These activated T cells remain in the lymph node, proliferate and differentiate to antigen-specific effector T cells. The differentiation of CD4<sup>+</sup> T cell subsets is dependent on the cytokine milieu. Th1 cells produce interleukin (IL)-2, interferon (IFN)- $\gamma$  and tumor necrosis factor (TNF)- $\alpha$  for T cell activation, cellular immunity and inflammation. Th2 cells produce anti-inflammatory IL-4, IL-5, IL-6 and IL-10 for initiating the humoral response via antibody production by B cells or antibody-secreting plasmocytes. The Th17 subset of T cells primarily secretes IL-6, IL-22 and IL-17.

After clonal expansion, effector T cells travel to the area of infection through the blood circulation. In the gut, LP plasmocytes mainly produce non-inflammatory, secretory immunoglobulin A (sIgA). Its role is the neutralisation of pathogens and their toxins as well as the exclusion from antigens entering the epithelium [34]. Every sixth cell in the epithelium and mucosa is a lymphocyte. These intraepithelial lymphocytes (IEL) are continuously associated with the intestinal epithelium and represent the first immune cells to delete pathogen-infected IEC [35] to maintain mucosal integrity.

In the early 60ies, clinical observations lead to the association between ID and immunity. ID reduced the proportion of total T cells, helper T cells as well as cytotoxic and suppressor T cells in mice spleen without affecting CD4<sup>+</sup>/CD8<sup>+</sup> ratios (this could also be observed for peripheral blood [36]). Anergy, a state of unresponsiveness of T cells by an incomplete activation of the T cell receptor (lack of co-stimulatory signals from the APC) was described in humans and animals suffering from ID. Beside this, ID lead to a decreased secretion of IL-2 and IFN- $\gamma$ , restricted lymphocyte proliferative response towards mitogens/antigens, reduced antibody-dependent cytotoxicity as well as reduced thymus weight [37]. For murine splenic B cells, ID targeted B cell numbers and reduced the proliferative response after lipopolysaccharide (LPS) stimulation. ID in rats affected IEC numbers containing sIgA which may have an influence on mucosal immunity.

The epithelial layer as a barrier, the production of mucus, defensins and other antimicrobial peptides by the above mentioned IEC types display a physical shield to prevent interactions between IEC and microorganisms. Moreover, there is accumulating evidence that IEC contribute to the initiation and regulation of innate and adaptive defense mechanisms by directly interacting with LP DC, LP lymphocytes (LPL) and IEL [38, 39] and are therefore considered to be a constitutive component of the mucosal immune system. IEC themselves constitutively express, or can be induced to express, co-stimulatory molecules [40, 41] and components of the MHC including class II, classical I and non-classical class Ib MHC molecules [42, 43], Toll-like receptors (TLR) and nucleotide-binding oligomerization domain (NOD) protein receptors [44, 45] as well as inflammatory and chemoattractive cytokines [46].

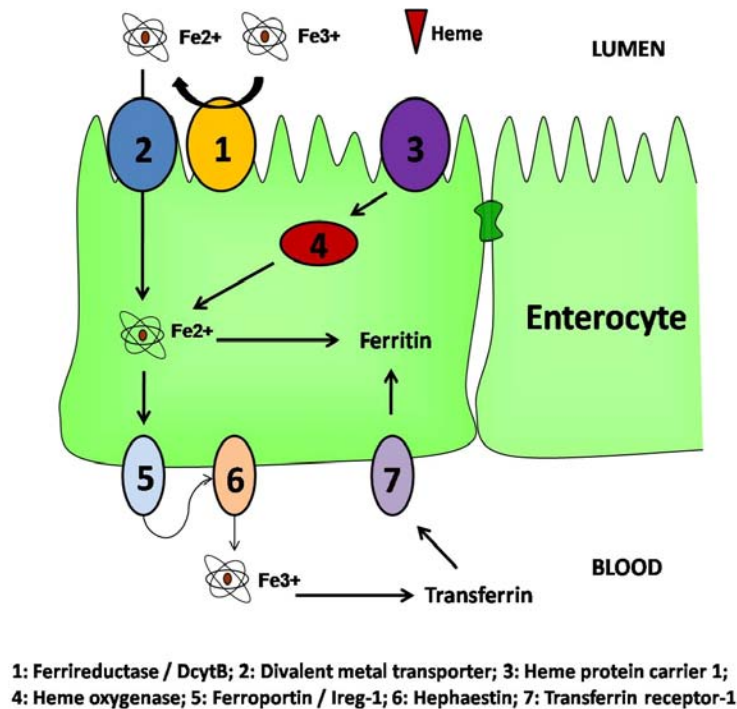
The mechanism how the intestinal immune system distinguishes between harmless commensal bacteria and pathogens is still unknown. Both bacterial groups express similar microbial associated molecular pattern (MAMP), also known as pathogen associated molecular pattern (PAMP) in the context of pathogens. The intestinal immune system recognizes bacteria via pattern recognition molecules (PRM) or so called pattern recognition receptors (PRR) including the two main forms in the gut, TLR and NOD [31]. In case of pathogens, the host's intestinal immune system initiates an innate immune response to defeat the invaders. This results in an activation of the pro-inflammatory NF- $\kappa$ B signalling pathway and therefore to the up-regulation of pro-inflammatory chemokines and cytokines including TNF and IL. The initiation also includes among others the recruitment of phagocytic cells and diverse growth factors for the activation and proliferation of immune cells [47].

To prevent this pathogen-induced immune response towards non-pathogenic luminal antigens from commensal bacteria or food, the immune system has developed a way of non-responsiveness – the oral tolerance. The inhibition of the systemic immune response to non-pathogenic antigens includes the deletion of antigen-specific T cells as well as induction of anergy. Additionally, PP contain antigen-specific regulatory T cells which produce anti-inflammatory transforming growth factor- $\beta$  (TGF- $\beta$ ) and IL-10 to maintain gut homeostasis [48].

### **1.5 Iron metabolism in the GI tract**

In nutrition, 90% of iron is present in its anorganic forms as non-heme iron (ferrous and ferric compounds) and 10% of iron in its organic forms, most importantly as heme. The bioavailability of heme iron is higher than that of non-heme iron. Beside this, the bioavailability of non-heme iron is dependent on other dietary factors including e.g. phytic acid and polyphenols [10].

The main absorption of iron occurs in the duodenum. Because most of the iron appears in its oxidized form as Fe<sup>3+</sup> without bioavailability, the ferrereductase reduces iron to the transportable Fe<sup>2+</sup> form.



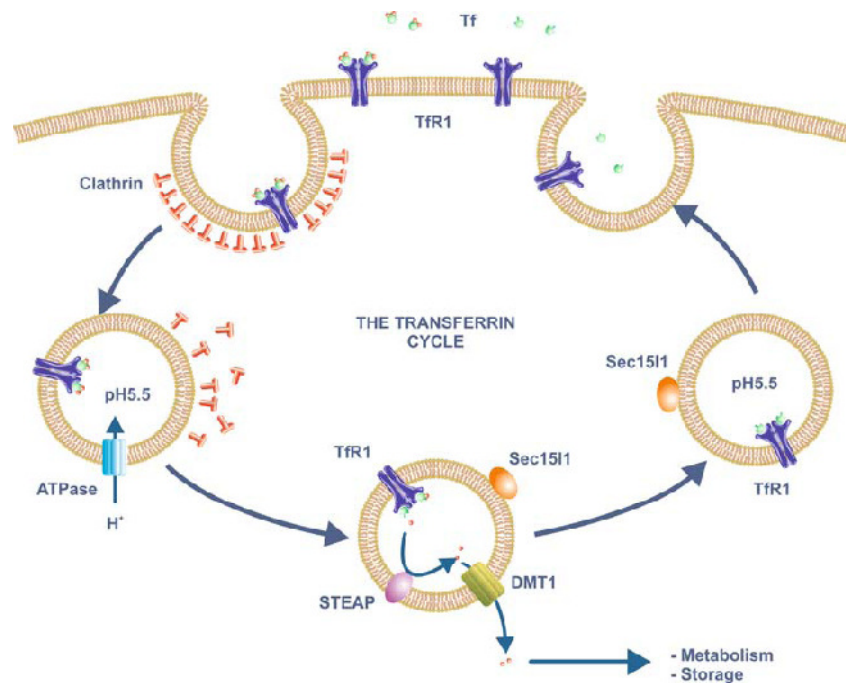
**Figure 3. Schematic overview of iron absorption, storage and transport in the enterocyte (modified from Gomollón et al. [49]).**

Figure 3 shows a possible mechanism, where the apical located ferrereductase duodenal cytochrom B (DcytB) reduces  $\text{Fe}^{3+}$  to  $\text{Fe}^{2+}$  to allow the import of ferrous iron via the brush-border membrane anchored divalent metal transporter DMT-1 which also transports other ions (zinc, copper, cobalt and cadmium) [50]. The heme iron is taken up by a not completely understood mechanism via a heme protein carrier HPC-1. In the enterocyte, the heme oxygenase (HO) degrades heme to a linear tetrapyrrol biliverdin under release of  $\text{Fe}^{2+}$  and carbon monoxide [51]. Keel et al. recently demonstrated that the duodenal heme exporter feline leukemia virus subgroup c receptor (FLVCR) may export functional heme into the circulation [52]. The iron storage form in the enterocyte is  $\text{Fe}^{2+}$  bound to ferritin. The iron export from the enterocyte includes ferroportin and hephaestin. Ferroportin (also known as Ireg-1) is localized at the basolateral membrane of polarized epithelial cells to export iron from the enterocyte into the system [53].

### 1.5.1 Iron metabolism in the circulation

Once exported from enterocytes, hephaestin oxidizes iron to  $\text{Fe}^{3+}$  as it can be bound to plasma transferrin only in the ferric form. Both, ferroportin and hephaestin are located not only in the duodenum, the expression can be detected in the whole gut, especially in crypt more than villus enterocytes [54]. In many tissues, the main plasma ferrereductase is the copper-dependent ceruloplasmin whereas hephaestin is the homolog of ceruloplasmin in the small intestine.

Transferrin contains two binding sites for one iron atom each. Non-iron bound transferrin is also called apo-transferrin, whereas binding of one iron atom leads to monoferric-transferrin and occupancy of both binding sites leads to diferric-transferrin. Physiological conditions include 30-40% of occupied binding sites, therefore, transferrin-bound iron is the crucial body iron pool. The transferrin-bound iron uptake is a receptor-mediated endocytosis mechanism (Figure 4). When transferrin-bound iron binds to the transferrin receptor 1 (TfR1) at the plasma membrane, the complex is internalized in clathrin-coated pits building endosomes after dissociation from clathrin. To release iron from transferrin, an ATPase acidifies the endosome. Because of the high-affinity binding of iron to transferrin, endosomal ferric reductases (proteins of the STEAP family) reduce iron to its ferrous form which then can leave the endosome via DMT-1. The TfR1 and apotransferrin is recycled and apotransferrin dissociates after reaching the cell surface [55].



**Figure 4. Transferrin-bound iron uptake via the TfR1 (from Anderson and Vulpe [55]).**

Sec151 is like the TfR1 localized in the endosome. The exact role of this protein is not completely investigated but mice with a mutation in Sec151 show a defective transport of transferrin-bound iron to immature erythroid cells [56]. Therefore, Sec151 seems to play a regulative role in the recycling of endosomes.

Besides the high-affinity TfR1-mediated uptake of diferric-transferrin, also low affinity uptake exists. Iron uptake in immature erythroid cells is exclusively mediated via the TfR1 pathway whereas hepatocytes and enterocytes can use high as well as low affinity uptake. The homolog of TfR1, the TfR2 seems to be responsible for low affinity iron uptake [57] but not as the only possibility because some cells use the low-affinity process without expressing TfR2 [58].

The uptake of non-transferrin-bound iron from the plasma into the cell is not well elucidated but DMT-1 seems to play a role in this process but not as the only route especially for hepatocytes [59].

The main part of plasma iron is not bound to transferrin, it is localized in hemoglobin of circulating red blood cells. Macrophages phagocytose aging erythrocytes and HO releases iron from heme to be exported into the plasma via natural resistance-associated macrophage protein-1 (NRAMP-1; similar to DMT-1) to bind to transferrin. This pathway is the most important pathway to release iron into the circulation. The liver-produced haptoglobin binds plasma hemoglobin whereas free heme in the plasma is bound by hemopexin [60, 61]. The haptoglobin-hemoglobin complex can be taken up by macrophages via CD163 and receptor-mediated endocytosis [62], the hemopexin-heme complex is taken up by cells including hepatocytes, macrophages or other cell types via CD91 and high or low affinity binding [63].

### **1.5.2 Iron utilization in the cell**

After uptake, iron in its storage form is bound to ferritin. There are some hypothesis, in which way up-taken iron trafficks to the mitochondria for utilization or to ferritin for storage but the exact mechanism is unknown. Iron with its catalyzing potential may be bound to citrate or intracellular proteins [64] to avoid the formation of ROS or it is bound to specific chaperones as they exist for copper [65]. Shi et al. lately identified the poly (rC) binding protein 1 (PCBP1) which delivers iron to ferritin in *S. cerevisiae* and has a similar function in mammalian cell lines [66]. Because PCBP1 is ubiquitously expressed in mammalian cells, the role as general iron chaperone seems to be likely.

Many enzymes incorporate iron centers in form of heme or iron-sulfur (Fe-S) clusters, produced in the mitochondrion [67, 68]. The way of iron trafficking to the mitochondria is not exactly known as mentioned above but iron uptake into the mitochondrion seems to be mediated by the iron importer mitoferrin (Mfrn), a member of the mitochondrial solute carrier family (Slc25). The homolog Mfrn 2 is expressed in many non-erythroid tissues and may have a similar function whereas Mfrn is mainly expressed in erythroid cells [69]. Erythrocytes are responsible for oxygen transport in the circulation and this transport is dependent on heme as binding site for oxygen. For heme biosynthesis in immature erythroid cells, iron has to be transported to the mitochondria. One proposal for this transport is the direct contact between the endosome and the mitochondrion to transfer iron into the mitochondrion [70] but this has to be further investigated. Fully biosynthesized heme and Fe-S cluster abandon the mitochondrion through the heme exporter ATP-binding cassette (ABC) transporter ABCB10 or the Fe-S cluster transporter ABCB7 respectively, since the integration into proteins occurs in the cytoplasm.

### 1.5.3 Regulation of cellular iron metabolism

Because of the toxic and pro-oxidative effects of iron, body iron levels have to be tightly controlled. Simplified, when iron is required, iron import is increased while export decreases. ID leads to the up-regulation of TfR1 and DMT-1 accompanied by reduced expression of ferroportin. If iron supply is sufficient, the opposite effects occur leading to the down-regulation of TfR1 and DMT-1 as well as enhanced ferritin expression.

There are two distinct mechanisms involved in the regulation of iron metabolism – the iron responsive element (IRE) / iron regulatory protein (IRP) system and the role of liver-derived hepcidin. IRP1 and IRP2 are able to bind to stem loop structures (IRE) in the mRNA of proteins involved in iron metabolism. Depending on the position of the IRE in the mRNA untranslated region (UTR), the binding of IRP induces a translational block (5′) or stabilization for proceeding translation (3′) [71, 72]. The TfR1 mRNA contains multiple IRE in the 3′ UTR leading to stabilization of the mRNA when iron is needed. In contrast, the mRNA of ferritin has one IRE in the 5′ UTR inducing a translation block after IRP binding [73]. This interaction implies a simultaneous increase in iron uptake and decrease in iron storage. Other proteins with IREs are DMT-1 (3′ UTR) [74], ferroportin (5′ UTR) [75] and the rate limiting enzyme for heme biosynthesis aminolevulinic acid synthase (5′ UTR) [76].

The regulation of IRP1 and IRP2 themselves is different. IRP1 in an iron-sufficient state contains a Fe-S cluster (then named cytosolic aconitase). Under ID, the Fe-S cluster is removed which then enables the binding to IREs. Iron-repleted situations imply ubiquitination and proteasomal degradation of IRP2 whereas ID induces stabilization and the ability of IRE binding [72]. Not all iron transporting proteins are under the regulation of IRE/IRP. Hypoxia via the hypoxia-inducible factors (HIF) and pro-inflammatory cytokines also control transcription of e.g. TfR1 [77, 78].

The quickest mechanism to answer towards changes in iron metabolism is the internalization, stabilization, changes of proportion or degradation of transporters as it can be seen for DMT-1 [79], TfR2 [80], TfR1 [81] as well as ferroportin [82]. The removal of plasma-membrane located ferroportin is mediated by the binding of hepcidin.

### 1.5.4 Regulation of systemic iron metabolism

First attempts to explain the regulation of iron metabolism involved the crypt programming model.

Duodenal crypts internalize transferrin-bound iron via the TfR1 or 2 from the plasma. The absorbed iron regulates the expression of DMT-1 and ferroportin and therefore, the enterocyte has been “programmed” to take up a certain amount of iron after reaching the villus tip as mature absorptive cell [49, 54].

The identification of the liver-derived peptide hepcidin contributed substantially to the understanding of iron regulation and to a change of view of the crypt programming model. Because of the structural

similarity to defensins and cathelicidins, it has antimicrobial and antifungal properties against Gram-negative and Gram-positive bacteria as well as yeast but the biological importance of this function is not clear [83]. Hepcidin regulates the iron release into the plasma by binding to ferroportin leading to internalization and proteasomal degradation of the iron exporter. This affects iron release from intestinal enterocytes, macrophages, hepatocytes and placental cells [84]. In case of ID, hepcidin levels are low to enable iron plasma release. Several situations like hypoxia, increased erythropoiesis as well as pregnancy are also iron-requiring situations with decreased hepcidin levels.

Hepcidin is encoded by the hepcidin antimicrobial peptide (HAMP) gene. When body iron levels are high, hepcidin levels are also high to retain iron in the cell, but under ID, hepcidin levels decrease to allow iron entry from enterocytes or macrophages into the circulation. Expression of the HAMP gene is influenced by HFE (encoding a protein of the MHC class I), Tfr2 and hemojuvelin (HJV also known as HFE2), proteins which are located in the membrane of hepatocytes (Figure 5).

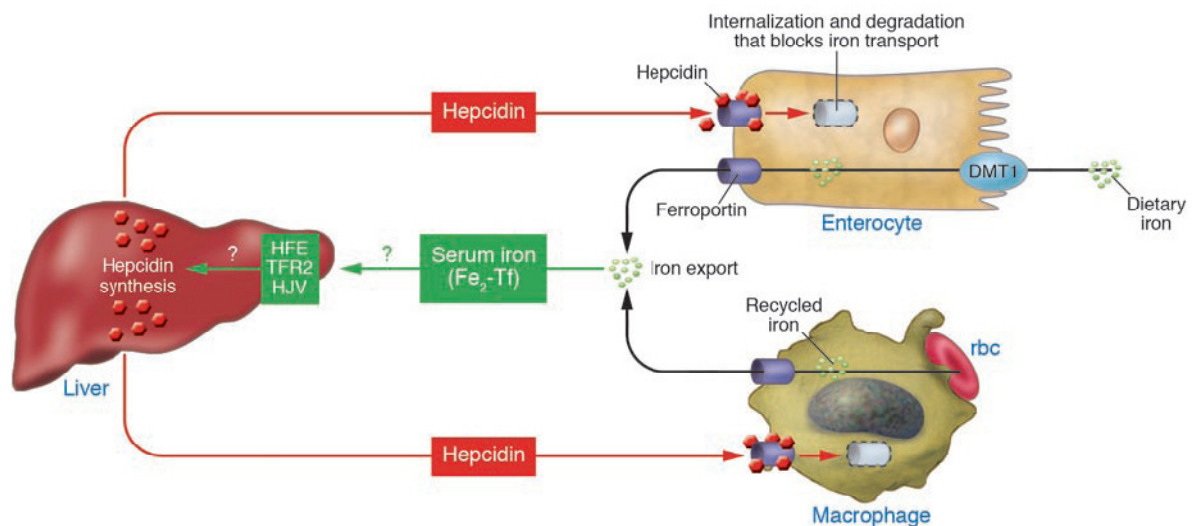


**Figure 5. Overview of the regulation of systemic iron metabolism (from Vaulont et al. [85]).**

Although the exact role of HFE and Tfr2 are still unknown, they may function as iron sensors by recognizing transferrin-bound iron as indicator for body iron status and therefore influence hepcidin expression. This assumption is supported by the results of HFE and Tfr2 knock out (k.o.) mice which develop hepatic iron overload and increased transferrin saturation [86, 87] also known as hemochromatosis. HJV signals through the bone morphogenetic protein (BMP)/SMAD pathway, with BMP6 as possible positive regulator of hepcidin [88]. Mutation in the HJV gene of mice target iron accumulation in liver, heart and pancreas accompanied by a failure to express HAMP and therefore hepcidin [89, 90]. This disease pattern is known as juvenile hemochromatosis. In all known types of hemochromatosis, the hepcidin/ferroportin axis is the main factor in the disturbed iron homeostasis and an explanation for the pathology of iron overload.

HJV k.o. mice do not respond with HAMP expression after application of dietary or injected iron, but they still up-regulate HAMP expression in response to inflammation. In inflammation, hepcidin expression is increased to retain iron in the cell leading to the unavailability of iron for invading pathogens as a mechanism for host protection [91, 92]. The release of cytokines after infection or inflammatory processes influence HAMP expression and therefore hepcidin levels. IL-6 is a potent inducer of hepcidin *in vitro* and *in vivo* as well as IL-1 $\alpha$  and IL-1 $\beta$  [93, 94], but the exact mechanism behind is still unclear. This response of iron metabolism towards inflammation has protective effects on the one hand, but may lead to the development of anemia of chronic disease (ACD) as it can be observed for diseases including tuberculosis, bacterial endocarditis, but also noninfectious inflammatory disorders like rheuma or inflammatory bowel disease (IBD).

### **1.6 IBD: causes, consequences and the role of iron in intestinal inflammation**

#### **1.6.1 The clinical pictures Ulcerative colitis (UC) and Crohn's disease (CD)**

IBD with UC and CD as main disease forms are spontaneously relapsing, immunologically mediated disorders of the GI tract. Both disorders affect people in approximately equal female/male proportion with a combined mean frequency of 5–200 cases per 100.000 European and North American inhabitants [95]. UC and CD differ in their clinical picture.

UC displays a non-transmural, continuous inflammatory disorder which is restricted to the colon. Due to the side of appearance, UC can occur as proctitis, left-sided colitis affecting the sigmoid colon with/without descending colon or pancolitis. In some UC patients also the distal ileum is involved (backwash ileitis). The main symptoms include bloody diarrhea, fever, abdominal pain and cramping accompanied by distorted crypt architecture and crypt abscesses. On immune response and cytokine level, UC seems to display a Th2-type mediated disease with IL-5 and IL-13 as main secreted cytokines [96].

CD displays a transmural, discontinuous inflammatory disorder that can affect the entire GI tract from the mouth to the anus. Most commonly, CD occurs in the terminal ileum, followed by colon, ileal colon and upper GI tract. The clinical symptoms include diarrhea, fever, abdominal pain, obstructions as well as fissures and skip lesions [97]. On immune response and cytokine level, CD seems to display a Th1-type mediated disease with IL-12, TNF and IFN- $\gamma$  as main secreted cytokines [96].

### **1.6.2 Genetic factors in IBD: disturbances in microbial-host interaction, barrier function and immunity**

The genetic background or the genetic susceptibility of the host, environmental factor including diet, smoking and life style habits as well as the gut microbiota are discussed in the etiology of IBD. This interplay of genetic and environmental factors is clearly demonstrated by concordance studies in twins. Different studies showed a pooled concordance in monozygotic twins of 37.3% for CD and 10% for UC. For dizygotic twins, the pooled concordance for CD is 7% and for UC 3% [98-100]. Therefore the genetic seems to play a more important role in CD than UC. A meta-analysis of genome-wide scans leads to the identification of more than 30 susceptible loci for CD [101].

The NOD2/caspase recruitment domain-containing protein (CARD) 15 gene was the first susceptibility gene reported in the context only with CD. How mutations in the NOD2 gene enhance intestinal inflammation is not clear but the associated reduced ability clearing invading pathogens may lead to a dysregulation in innate immunity. Autophagy-related protein (ATG) 16L1 and immunity-related guanosine triphosphatase (IRGM) associated with autophagy are further candidate genes affecting bacterial recognition and clearance. These susceptibility genes support the hypothesis of disturbances in microbial-host interactions in IBD patients.

Altered barrier function with increased permeability has been reported for IBD patients [102]. In CD, this includes the up-regulation of pore-forming Claudin 2, decreased and redistributed tight junction components and increased IEC apoptosis [103]. In addition, CD patients also show increased bacterial translocation [104]. However, the loss of tolerance towards the commensal bacteria seems to be one of the main events in the pathogenesis of IBD. CD as well as UC patients show defects in oral tolerance induction including also healthy relatives [105]. The recently reported production of antibodies against bacterial glycans further support the “loss of tolerance” hypothesis in IBD [106].

Colonization of the gut by commensal bacteria has effects on nutritional and defensive function through the modulation of gene expression [107]. As different genes may be influenced by different bacteria, manipulating host microbiota may offer a possibility to treat intestinal pathophysiology. Iron is essential for bacterial growth and development. Changes in dietary iron may therefore be a possible target to manipulate host microbiota. Yet little is known about how intestinal bacteria target protective and detrimental signal transduction pathways in genetically susceptible hosts.

As already described in 1.2 and 1.3, IEC are part of the first line defense via the production of mucus, antimicrobial peptides and defensins as well as sIgA. Mucus, produced by Goblet cells, has protective functions regarding the inhibition of a direct bacteria-IEC contact. The loss of Goblet cells as it occurs in UC is accompanied by reduced mucin production (also occurring in CD) [108].

CD patients have defective antimicrobial peptide production (human  $\alpha$  defensin 5, human  $\beta$  defensin 2) accompanied by dysfunctions in bacterial killing [109-111]. This decreased production of human  $\alpha$  defensin 5 by ileal Paneth cells is strongly associated with the mutations in the IBD susceptibility gene

NOD2/CARD15. In addition, sIgA is necessary for neutralisation of bacteria and in case of pathogens their toxins as well as the exclusion of antigens entering the epithelium. IBD patients show decreased concentration of IgA in faecal content as further point in defective first line defence mechanisms [112].

The disturbances in microbial-host interaction, microbial killing and barrier function may furthermore contribute to disorders in immune responses as it can be observed in IBD. Other susceptibility genes including organic cation transporter (OCTN), discs large homolog (DLG) 5, intercellular adhesion molecule (ICAM)-1, TLR-4 and the IL-23 Receptor (IL-23R) participate in the regulation of innate immune responses [113]. B lymphocytes may play a role by the already mentioned production of antibodies against bacterial glycans of commensal bacteria. However, a variety of defects in T cells have been associated with IBD. Studies showed resistance towards T cell apoptosis, excess of Th1 and Th17 cytokine responses in CD as well as defects in regulatory T cell activation and function, latest being important for the maintenance of gut homeostasis [114-118].

Various CD4<sup>+</sup> regulatory T cells seem to be involved in the suppression of mucosal immune responses. The anti-inflammatory cytokine IL-10, produced by Tr1 cells, is discussed in the suppression of responses towards commensal bacteria [119]. Therefore, a lack of IL-10 in the IL-10<sup>-/-</sup> mouse model leads to the development of a Th1-type CD-like disease. Animal models display a good possibility to get further insights and examine mechanisms contributing to the pathogenesis of IBD. The classification determines between antigen-specific (a.o. Ovalbumin/transfercolitis/OVA transgenic mice), inducible (dextrane sulfate sodium (DSS)), genetic (IL-10<sup>-/-</sup>, TNF<sup>ΔARE/WT</sup>), adoptive transfer (RAG2<sup>-/-</sup>) and spontaneous (Samp1/YIT) animal models [120].

### **1.6.3 Endoplasmic reticulum (ER) stress as possible trigger in the pathogenesis of IBD and its role in iron metabolism**

Besides the already known genetic and environmental factors which play a role in the pathogenesis of IBD, recent studies also implicate a link to stress responses in IEC and the development of IBD.

The ER is responsible for the correct folding, posttranslational modifications and secretion of proteins [121]. This organelle is sensitive towards changes in physiology and biochemical processes including imbalances in the redox potential (oxidative stress), but also infections or energy deficiency. These stimuli may lead to a reduced folding capacity in the ER and misfolded proteins can accumulate, which then activates the unfolded protein response (UPR) [122]. In detail, the major chaperone (helperproteins for the correct folding) glucose-regulated protein-78 (grp-78) dissociates from the three transmembrane domains to activate the UPR, followed by different downstream signalling cascades known as ER stress pathways. Figure 6 illustrates an overview of these pathways.

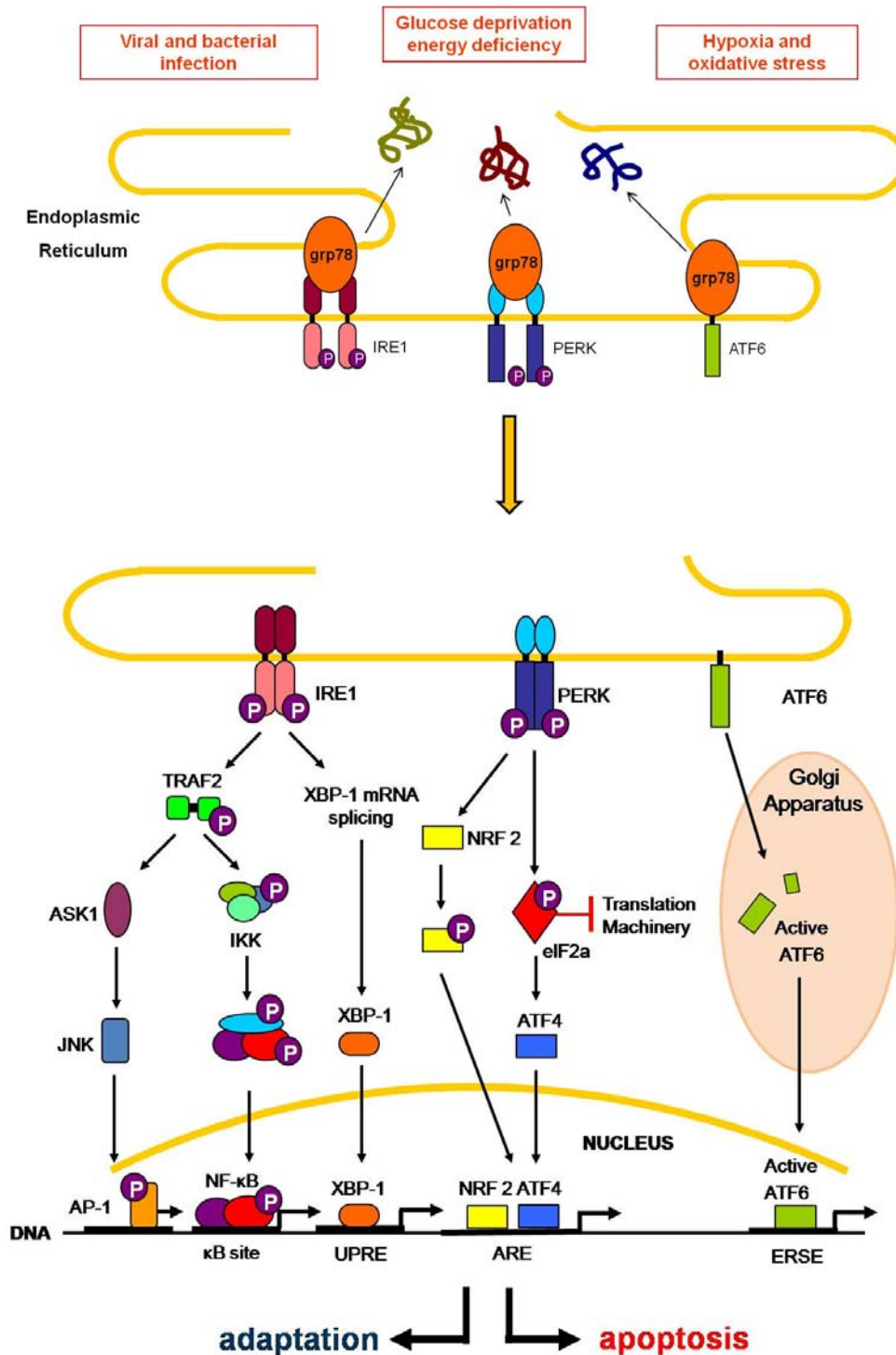


Figure 6. Overview of ER stress pathways.

Inositol-requiring enzyme 1 (IRE1) consists of IRE1 $\alpha$  and IRE1 $\beta$ . After dissociation of grp-78, IRE1 is autophosphorylated and dimerizes. The endonuclease activity of IRE1 splices the X-box protein 1 (XBP1) by removing 26 bases from the transcript. The spliced form of XBP1 can translocate into the nucleus and binds to UPR elements (UPRE) to activate the transcription of chaperones, co-chaperones, genes involved in protein degradation (to restore ER function) or the negative feedback factor for the

pancreatic ER kinase-like ER-associated kinase (PERK) pathway P58<sup>IPK</sup>. The activation of IRE1 also leads to a complex formation of the cytoplasmic part of IRE1 with the adaptor protein TNF receptor-associated factor 2 (TRAF2) and the mitogen-activated protein kinase kinase (MAPKK) apoptosis signal-regulating kinase 1 (ASK1). This complex formation implicates phosphorylation and activation of JNK and therefore the induction of pro-apoptotic pathways. It has been shown that the activation of TRAF2 leads to the induction of NF- $\kappa$ B and associated gene expression [123].

The second pathway is mediated by PERK. After dimerization and autophosphorylation, PERK is able to phosphorylate the eukaryotic translation initiation factor 2 $\alpha$  (eIF2 $\alpha$ ; p-eIF2 $\alpha$ ) leading to a general inhibition of protein translation. This stop of the translational machinery is important for cell survival to protect the ER by decreasing nascent protein arrival. PERK is also able to phosphorylate the nuclear related factor 2 (NRF2) to initiate gene expression involved in counteracting oxidative stress, e.g. HO-1 or HIF-1 $\alpha$  by binding to antioxidative response elements (ARE). Some genes with specific sequences are excluded from the translational stop like the activating transcription factor 4 (ATF4). ATF4 translocates into the nucleus and also binds to ARE to induce gene expression involved in redox reaction and stress response as well as amino-acid metabolism and protein secretion. ATF4 not only has a pro-survival character as it also induces the transcription factor cAMP response element-binding transcription factor (C/EBP) homologues protein (CHOP) which is known to promote apoptotic cell death. As a negative feedback mechanism, ATF4 induces the expression of growth-arrest DNA damage gene 34 (GADD34) which dephosphorylates eIF2 $\alpha$  to abrogate the translational stop.

The third ER stress pathway is mediated by ATF6. After grp-78 dissociation, ATF6 travels to the Golgi apparatus where it is transformed into its active form by cleavage. After translocation into the nucleus, ATF6 binds to ER stress response element (ERSE) to initiate the expression of grp-78, grp-94, grp-58 as well as CHOP and XBP1. As there is no evidence linking ATF6 to ER stress induced apoptosis, ATF6 is seen as a pro-survival factor to counteract ER stress.

ER stress and the UPR include pro- and anti-apoptotic pathways and there is a tight regulation between adaptation or apoptosis. If ER stress cannot be solved and continues, this may result into the induction of apoptosis. The phenomenon ER stress in the context of IBD was first described by Shkoda et al. showing induction of grp-78 protein expression in IBD-patients as well as IL-10<sup>-/-</sup> mice [124]. In addition, Kaser et al. showed that the loss of ER-associated transcription factor XBP-1 was linked to a Paneth cell dysfunction leading to an increased risk for IBD [125]. Heazlewood et al. revealed mucin depletion by the loss of ER stressed goblet cells as component of the pathogenesis of human colitis leading to a depleted mucus barrier, increased epithelial permeability and ER stress triggered local mucosal inflammation [126]. The lack of the ER stress related transcription factor IRE-1 $\beta$  in the intestinal epithelium was associated with an increased sensitivity to dextran sodium sulfate colitis [127].

Recent studies implicate a role of ER stress in iron metabolism. Faye et al. showed that iron-fed C57BL/6 mice had decreased liver and serum haptoglobin which participates in many biological

processes and during the acute-phase responses including inflammation [128]. This decrease may be mediated via iron-induced oxidative stress which alters ER environment. The iron-fed C57BL/6 mice showed decreased mRNA and protein levels of grp-78, so the authors assume that the loss of grp-78 as assisting chaperone for protein folding leads to the incorrect folding and degradation of haptoglobin.

Iron-overload by intraperitoneal injections of iron-dextran in rats resulted in tissue injury accompanied by the induction of grp-78 as well as ER stress-associated induction of pro-apoptotic caspase 12 [129]. Lou et al. assume that ER stress may play an important role in iron-induced tissue injury and that ROS are a responsible factor in mediating ER stress in the context of iron-overload cellular injury.

The iron-overload disease hereditary hemochromatosis (HH) occurs because of a mutation in the HFE gene leading to deregulated iron metabolism. Recent studies revealed that the induction of the UPR is a feature of HH and might be responsible for the genesis of immunological abnormalities which are associated with HH [130].

Sato et al. showed increased metallothionein (MT) expression, a metal-binding protein, after induction of ER stress and enhanced grp-78 mRNA expression in the liver of MT-null mice suggesting that MT attenuates the expression of grp-78 and therefore might prevent ER stress [131]. Recently, it has been reported that ER stress directly controls iron metabolisms through the induction of hepcidin expression accompanied by hypoferremia and the development of anemia of chronic inflammation (ACI) [132], a major problem in IBD patients.

### **1.6.4 Iron as environmental parameter in the context of IBD**

Whereas the interplay between genetic susceptibility and environmental factors are responsible for the disease onset, trace elements like iron are also discussed in the pathogenesis of IBD [133]. One third of IBD patients develop anemia due to an inappropriate intake or loss of iron affecting life quality (a.o. fatigue, nausea, anorexia, weight loss, dizziness, tinnitus, reduced attention). Anemia can occur because of ID or as anemia of chronic inflammation/disease (ACI/D) mostly mediated by pro-inflammatory IL-6 which induces hepcidin production leading to a decrease of iron export from cells [134].

In active CD, absorption of orally administered iron was impaired and correlated with IL-6 and C-reactive protein (CRP) serum levels as well as urine hepcidin levels leading to the suggestion that oral iron in active IBD may be of limited benefit [135]. Other IBD-related pro-inflammatory cytokines like TNF and IFN- $\gamma$  have been associated with the pathogenesis of ACI [136, 137]. Additionally, CD patients seem to prefer low-fiber non-iron fortified cereals to relieve intestinal symptoms and show lower intake of ascorbic and phytic acid (to improve iron bioavailability) which may also contribute to an increased risk for ID [138]. Furthermore, used drugs in IBD including sulphasalazine or 5-Aminosalicylic acid (ASA) to down-regulate inflammatory processes have been associated with hemolytic anemia [139]. From all these risk factors it seems to be obvious that iron levels have to be corrected in IBD patients.

Body iron status can be measured and monitored by different factors including serum ferritin levels, transferrin saturation and iron utilization by erythropoiesis expressed as cellular hemoglobin content of reticulocytes (CHR) and proportion of hypochromic red cells (% HYPO) as well as hemoglobin and hematocrit. The classification of ID anemia is depending on these factors. Since inflammation influences acute phase proteins like ferritin, categorization of ID differentiates between active and non-active IBD (Table 1) [140, 141].

**Table 1. Degree of ID evaluated by serum ferritin or transferrin saturation (from [140])**

|   | Serum Ferritin<br>[ $\mu\text{g/l}$ ] | Transferrin Saturation<br>[%] |
|---|---------------------------------------|-------------------------------|
| Depleted iron stores in healthy adults or patients with quiescent IBD | < 30                                  | < 16                          |
| Depleted iron stores during active IBD                                | < 100                                 | < 16                          |
| Adequate iron stores  | > 100                                 | 16 - 50                       |
| Potential iron overload   | > 800                                 | > 50                          |

Oral or parenteral iron supplementation are common alternatives for the treatment of ID. Oral preparations contain iron in form of Fe-(II)-salts like Fe-(II)-sulfate, Fe-(III)-polymaltose-complexes or heme-iron-polypeptides. Oral application of iron salts is a cheap but ineffective treatment of IBD-associated anemia. Limited resorption, high iron demand and low compliance are considering factors against oral iron treatment. Oral iron therapy is poorly tolerated by IBD patients [142, 143]. There is accumulating evidence in these chronically inflamed patients that oral iron supplementation may contribute to inflammatory processes and tissue pathology because of the pro-oxidative capacity of iron. Inflamed mucosa from IBD patients already show an imbalance in ROS production and anti-oxidative defense mechanism including total peroxyl radical scavenging capacity, reduced glutathione as well as ascorbic acid levels [144]. Increased reactive oxygen intermediates (ROI), DNA oxidation products as well as elevated iron levels in combination with decreased copper and superoxide dismutase (Cu-Zn SOD) activity were found in mucosal biopsies of CD patients. Elevated mucosal iron levels were also detected in UC patients [145]. IBD patients suffer from an increase in mucosal ROS production, measured by luminal-amplified chemiluminescence. For UC, this increase is in proportion to disease activity [146]. Application of an iron chelator on mucosal UC biopsies significantly decreased luminal-amplified chemiluminescence pointing to a possible therapeutic use [147].

Erichsen et al. showed that oral supplementation of CD patients with ferrous fumarate lead to an increasing trend of the disease activity index accompanied by diarrhea, abdominal pain and nausea. Additionally, patients had significantly decreased plasma-reduced cysteine as well as plasma-reduced glutathione as possible oxidative stress markers [148]. Also in healthy individuals, iron supplementation lead to a 40% increase in fecal ROS accompanied by luminal oxidative stress [149].

Therefore, administration of antioxidative vitamin E and C to CD patients resulted in lower plasma oxidative stress levels [150].

As the pro-inflammatory effect of oral iron administration is not fully proven in humans, animal models display a clear picture. Oral iron supplementation in DSS, dinitro-benzene-sulphonic acid (DNBS) as well as 2,4,6-trinitrobenzene sulfonic acid (TNBS) induced colitis resulted in enhanced histology [151-156]. This increase in inflammation in DSS + iron treated rats was due to higher expression levels of pro-inflammatory cytokines including TNF, IL-1, IL-6 as well as NF- $\kappa$ B activity [153]. In addition, DSS + iron led to increased oxidative stress measurable by myeloperoxidase (MPO) activity and lipid peroxidases (LPO) accompanied by lower plasma levels of antioxidative vitamin A and  $\alpha$ -tocopherol. Interestingly, simultaneous administration of iron and vitamin E in DSS-colitis ameliorated the effect, but did not affect oxidative stress [154]. Reifen et al. showed increased colitis score after iron supplementation which could be inhibited by the concurrent application of 5-aminosalicylic acid and/or lycopene involving oxidative stress-induced damage [157].

In a spontaneous mouse model of IBD, the IL-10<sup>-/-</sup> mouse, oral as well as rectal iron supplementation lead to spontaneously increased pro-inflammatory cytokine expression (IL-1, IL-6, TNF, IFN- $\gamma$ ) in the colonic mucosa as well as after LPS-stimulation. Iron-treated IL-10<sup>-/-</sup> mice also showed higher neutrophil numbers, without increased histology [158].

Barollo et al. showed that iron deprivation diminished macroscopic damage score in DNBS-treated rats and correlates with a decrease in DNA adducts (oxidative DNA damage). Furthermore, iron supplementation increased the damage score as well as production of DNA adducts [159]. The iron manipulation was accompanied with changes in other tract elements like zinc and copper which may also be involved in the pathogenesis of IBD. In another study, Barollo et al. also showed protective effects of an iron chelator on the degree of colitis and DNA damage [160].

Severe anemia and intolerability of oral iron preparations among others are indications for intravenous iron treatment. Intravenous iron preparations are Fe-(III)-complexes including low-molecular weight iron dextrane, iron gluconate, iron sucrose and ferric carboxymaltose. Advantages and disadvantages of the different intravenous preparations are listed in Table 2 [140, 161].

**Table 2. Preparations for intravenous iron therapy (modified from [161])**

|   | Iron dextran        | Iron gluconate | Iron sucrose   | Ferric carboxymaltose                         |
|---|---------------------|----------------|----------------|---|
| Complex stability                       | high                | low            | moderate       | high  |
| Acute toxicity                          | low                 | high           | medium         | low   |
| Test dose required                      | yes                 | no             | only in Europe | no  |
| Maximal dose                            | 20mg/kg body weight | 62.5mg         | 500mg          | 1000mg  |
| infusion time                           | 5h                  | 30min          | 3.5h           | 15min   |
| Risk of dextran-induced anaphylaxis     | yes                 | no             | no             | no  |
| Relative risk of serious adverse events | moderate            | low            | lowest         | not available                                 |
| positive aspect                         |                     |                |                | almost physiological pH-value, low osmolarity |

Because of the proven efficacy and tolerability for the treatment of ID anemia by intravenous iron [162] this route of iron administration is preferable and recommended [140].

### 1.6.5 Iron and NF- $\kappa$ B

Iron seems to play an important role in TNF secretion and NF- $\kappa$ B activation in different diseases and most importantly in IBD. The transcription factor NF- $\kappa$ B is a key player in immune as well as inflammatory processes and apoptosis. As shown in Figure 7, after cell stimulation by pro-inflammatory cytokines like TNF or IL-1 $\beta$ , TLR as well as antigen receptors (T or B cell receptor), NF- $\kappa$ B is activated by phosphorylation and proteasomal degradation of the inhibitor of  $\kappa$ B (I $\kappa$ B) [163]. The activation is mediated through the I $\kappa$ B-kinase (IKK) complex which consists of IKK $\alpha$ , IKK $\beta$  and IKK $\gamma$ , latest also called NF- $\kappa$ B essential modulator (NEMO). The active heterodimer consisting of the subunits p50 and p65 (RelA) translocates into the nucleus to induce expression of inflammatory genes (cytokines, chemokines, adhesion molecules and inhibitors of apoptosis) [164].

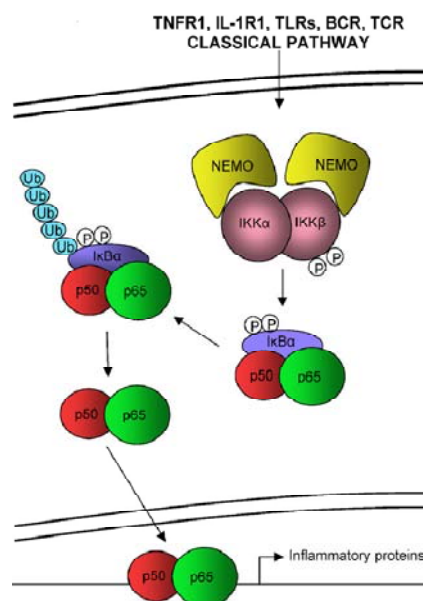


**Figure 7. Classical pathway of NF-κB activation (from Gloire et al. [163]).**

Several studies have shown that  $H_2O_2$  can induce NF-κB activation, but this is highly cell-type specific [165]. If this effect is mediated by  $H_2O_2$  itself or  $OH^-$  which appears through the Fenton reaction in the presence of  $Fe^{2+}$  is not clear. The involvement of ROS in TNF induced NF-κB activation is controversially discussed. Some antioxidants inhibit TNF induced NF-κB activation [166, 167], but it also has been reported that the ROS inhibitor N-Acetylcysteine (NAC) as well as the antioxidant epigallocatechin-gallate (EGCG) failed to do so [168]. Additionally, in mouse alveolar epithelial cells,  $H_2O_2$  reduced NF-κB activation [169].

TNF binding to its receptor (TNFR1) does not only mediate NF-κB activation, but also JNK activation. Whereas NF-κB activation leads to anti-apoptotic processes, JNK is a mediator for apoptosis. Here, the role of ROS in JNK activation is well characterized. NF-κB down-regulates JNK activation by suppressing TNF-induced ROS accumulation [170, 171]. The prolonged JNK activation could be inhibited by the pre-treatment with NAC.

Iron can also directly activate NF-κB. In rat Kupffer cells, iron stimulation ( $Fe^{2+}$ ) lead to an increased TNF protein release by activation of inhibitor κB kinase (IKK), NF-κB and TNF promoter activity which may aggravate liver injury as it has been shown *in vivo* [172]. Therefore, iron chelation to inhibit NF-κB activation might be protective against iron-mediated liver injury. As already mentioned in the previous paragraph, Carrier et al. showed an increase in TNF expression as well as NF-κB activity when mice with DSS-induced colitis where fed with a high iron diet.

Iron deprivation as inhibitor of oxidative stress might be beneficial also in other diseases like atherosclerotic vascular disease. In a mouse model of local inflammation, iron chelation was shown to inhibit LPS-induced nicotinamide adenine dinucleotide phosphate (NADPH) oxidase-mediated oxidative stress, NF-κB-activation and adhesion molecule expression (vascular cell adhesion molecule (VCAM)-1, ICAM-1) as important factors for the development of atherosclerosis [173]. Furthermore,

iron chelation therapies are a.o. discussed in the context of myelodysplastic syndromes and cancer [174, 175].

### **1.7 The TNF<sup>ΔARE/WT</sup> mouse model for chronic ileitis**

Heterozygous TNF<sup>ΔARE/WT</sup> mice show impaired regulation of TNF synthesis by deletion of a repeated octanucleotide AU-rich motif in the 3'-untranslated region of the TNF gene [176]. This genetic variation results in enhanced mRNA stability and increased TNF production accompanied by the development of a severe ileitis closely resembling the immune- and tissue-related phenotype of human CD with ileal involvement. Disease onset is detectable after week 4 of age and the inflammatory score increases with age. Besides the progress of ileitis, TNF<sup>ΔARE/WT</sup> mice develop clinical evidence of chronic polyarthritis with joint swelling and distortion of paw morphology. Backcrossing of TNF<sup>ΔARE/WT</sup> to recombinae activating gene (RAG)-1<sup>-/-</sup> mice abrogated ileitis but not polyarthritis. Therefore, the presence of T and B cells seems to play a major role in the pathogenesis of IBD in the TNF<sup>ΔARE/WT</sup> model. Ratio of T-cell subsets in thymus and peripheral blood are not affected by the TNF overproduction. Disease progression is characterized by splenomegaly and a significant increase of CD11b<sup>+</sup> myeloid cells as well as CD8<sup>+</sup> T lymphocytes with enhanced expression levels of CD44, CD69 and CD25 [177]. This indicates that CD8<sup>+</sup> T lymphocytes are in an activated/memory state. The murine small intestinal IEL compartment contains CD8α<sup>+</sup> cells which are the resident population restricted to the epithelium and CD8αβ<sup>+</sup> cells which migrate into the epithelium after peripheral antigen exposure. In TNF<sup>ΔARE/WT</sup> mice, a loss of CD8α<sup>+</sup> and increasing numbers of CD8αβ<sup>+</sup> IEL as major effector cell population is responsible for the disease progression [178].

Exclusion of CD4<sup>+</sup> T cells resulted in disease exacerbation whereas elimination of MHC-I/CD8<sup>+</sup> T cell responses lead to delayed onset and attenuation of IBD. Crossing the TNF<sup>ΔARE/WT</sup> allele to IL12p40 or IFN-γ deficient background alleviated intestinal inflammation whereas IL4<sup>-/-</sup> had no influence on disease progression. Therefore, Th1 cytokines are important factors in the onset of TNF-induced IBD. As iron has an effect on TNF and NF-κB activation, the TNF<sup>ΔARE/WT</sup> mouse may display an excellent opportunity to test iron-mediated effects and mechanisms in the context of inflammation and IBD.

## 2 AIMS OF THE WORK

The aim of this work was to characterize the role of dietary and systemic iron as environmental factor on chronic ileitis in the TNF<sup>ΔARE/WT</sup> mouse model with regard to ER stress responses and apoptosis in the intestinal epithelium.

Currently, there is no clear evidence for a direct correlation between diet or dietary factors and IBD. Trace elements like iron are discussed in the pathogenesis of CD but mechanistically data are missing. In animal models, various negative effects of luminal iron administration concerning enhanced histology, increasing pro-inflammatory cytokine levels as well as tissue and DNA damage have been reported, but iron in human IBD is predominantly mentioned in the context of the development of anemia and ACI/ACD. The pro-oxidative character of iron may cause tissue damage via ROS production affecting the integrity of the intestinal epithelium. Since the intestinal epithelium represents the border line between luminal environment and underlying immune cells, IEC dysfunction and disturbed IEC homeostasis participate in the pathogenesis of IBD. There is accumulating evidence that not only oxidative stress but also ER stress in IEC has a pivotal role in disease development and progression and that ER stress controls iron metabolism. Therefore, a major aspect of the present work was to elucidate the role of luminal and systemic iron on chronic ileitis in a murine CD-like animal model focusing on ER stress responses and apoptosis in the intestinal epithelium. Additional *ex vivo* and *in vitro* studies as well as analysis of the microbiota and immune cells should help to understand the mechanisms, how iron may influence pathology and participating factors in the development of chronic intestinal inflammation.

### 3 MATERIALS AND METHODS

#### Animals and Diets

Conventionally raised wild type (WT) and heterozygous  $TNF^{\Delta ARE/WT}$  mice (a generous gift from Kollias G., Institute for Immunology, Biomedical Sciences Research Center “Al. Fleming”, Greece) on a C57BL/6 background received an iron-adequate diet after weaning (Altromin C1000, containing 180mg Fe/kg added as iron sulphate) (Altromin, Lage, Germany). At the age of seven weeks, WT and  $TNF^{\Delta ARE/WT}$  mice were randomly separated into two groups receiving either an iron-adequate or an iron-deficient diet (Altromin C1038, containing <10mg Fe/kg; N = 10/group). Mice were killed by cervical dislocation at the age of 18 weeks (feeding experiment). In addition, conventionally raised  $TNF^{\Delta ARE/WT}$  mice at the age of 17 weeks were transferred from an iron-adequate diet to an iron-deficient diet for additional four weeks. Mice were then killed at the age of 21 weeks (short-term feeding experiment). Finally, conventionally raised WT and  $TNF^{\Delta ARE/WT}$  mice at the age of seven weeks were separated into iron-adequate or iron-deficient diet groups. After an initial dose finding study, the mice fed on an iron-deficient diet received weekly intraperitoneal (IP) injections of 90 $\mu$ mol Fe as  $Fe(NO_3)_3$ -complexed with nitrilotriacetic acid (NTA) in a 1:2 ratio [FeNTA(1:2)] (10mM stock solution: 38mg NTA (Bioanalytic, Umkirch/Freiburg, Germany) 51mg  $NHCO_3$  (Merck, Darmstadt, Germany), 40mg  $Fe(NO_3)_3 \cdot 9H_2O$  (Bioanalytic, Umkirch/Freiburg, Germany), 10ml 0.9% NaCl (Roth, Karlsruhe, Germany)) to replete the iron status to iron-adequate levels. Iron-adequate control mice received corresponding sham-injections of physiological saline (0.9% NaCl) (injection experiment). Iron injections were adjusted individually to body weight. In all experiments, tissue sections of the distal ileum were fixed in 10% neutral buffered formalin. Histological changes (score 0 – 12) were scored in paraffin-embedded, hematoxylin and eosin (H&E) stained ileal sections in a blinded fashion by assessing the degree of lamina propria mononuclear cell infiltration, crypt hyperplasia, goblet cell depletion and architectural distortion as previously described [179].

#### Isolation of murine primary IEC

Primary IEC from the ileal epithelium of all mice from the feeding, short-term feeding and injection experiment were purified as previously described [180]. Ileal tissue was cut into pieces and incubated at 37°C in Dulbecco’s modified Eagle’s medium (DMEM) (Invitrogen, Carlsbad, USA) containing 5% FCS (Invitrogen, Carlsbad, USA) and 1mM dithiothreitol (DTT) (Roth, Karlsruhe, Germany) for 30min. The remaining tissue was incubated in 30ml PBS (1X) (Invitrogen, Carlsbad, USA) containing 1.5mM EDTA (Roth) for additional 10min. The supernatants were filtered, centrifuged for 5min at 400g and the cell pellet was resuspended in DMEM containing 5% FCS. Finally, the primary IEC suspension was purified by centrifugation through a 20%/40% discontinuous Percoll gradient (GE Healthcare, Uppsala, Sweden) at 600g for 30min. After centrifugation, IEC were obtained between the

percoll phases, resuspended and centrifuged (2min, 1000g). After discharging supernatant, the remaining pellet was dissolved in either 800µl trizol (Qiagen, Maryland, USA) for RNA isolation or 250µl lysis buffer (7M urea, 2M thiourea, 2% CHAPS, 1% DTT) (all from Roth, Karlsruhe, Germany) for further analysis including Western blot or proteome analysis.

### **Determination of protein concentration**

The isolated IEC in lysis buffer were treated with ultrasonic impulses for homogenisation (10 times, amplitude 35, cycle 0.5) and vortexed before, in between, and at the end of a 30-60min rest on ice for complete lysis. After centrifugation (30min, 14000rpm, 4°C), the supernatant was transferred to a fresh tube. The protein concentration was measured using the Bradford assay (Roth, Karlsruhe, Germany). After preparation of the protein standard solution (BSA 2mg/ml) (Applichem, Darmstadt, Germany), the standard curve was assessed including the following concentrations 0, 2, 4, 8, 12, 16, 20, 40 [µg/µl], using 2µl lysis buffer, 200µl dye reagent and the according amounts of standard solution and PBS in order to obtain a total amount of 1000µl per single standard step. 2µl of each sample was diluted in 798µl PBS and incubated with 200µl dye reagent. After vortexing and incubation for 5min, standard solutions and samples were applied for OD measurement (600nm) (Eppendorf, Hamburg, Germany).

## **Proteome analysis**

### **Sample preparation for 2D-PAGE and gel analysis**

Purified primary IEC from iron-adequately and iron-deficiently fed WT as well TNF<sup>ΔARE/WT</sup> mice were lysed in 200µl buffer containing 7M urea, 2M thiourea, 2% CHAPS, 1% DTT, 4% protease inhibitor (Roche Diagnostics, Mannheim, Germany) and 2% Pharmalyte (Amersham Biosciences, Freiburg, Germany). Homogenization of the cell extracts was achieved by ultrasonication (amplitude 35, cycle 0.5) using 10 impulses on ice. The lysed cells were then centrifuged for 30min at 10000g at 4°C. The total protein concentrations of the solubilised proteins in the supernatants were determined using the BIO-RAD protein assay (Munich, Germany) and used for further analysis or stored at -80°C.

Immobilized pH-gradient strips (IPG, pH 3-10, 18cm, Amersham Biosciences, Freiburg, Germany) were rehydrated overnight in 350µl buffer (8M urea, 0.5% CHAPS, 15mM DTT, 0.5% IPG buffer) and 250µg of total protein was cup loaded onto the strip. Isoelectric focusing (IEF) in the first dimension and sodium-dodecyl-sulfate polyacrylamide gel electrophoresis (SDS-PAGE) in the second dimension were performed. IEF was run by a GE Healthcare Ettan IPGphor 3 (Munich, Germany) unit under the following conditions: 500V (1min, gradient), 4000V (1.5h, gradient), 8000V (28000Vh, Step-n-hold). Subsequent to the first dimension and before loading onto SDS-PAGE gels, strips were incubated for 15min in equilibration-buffer (1.5M Tris-HCL (Applichem), pH 8.8, 6M urea, 2% SDS (Applichem), 1% DTT) followed by additional equilibration in buffer for another 15min (1.5M Tris-HCL, pH 8.8, 6M urea, 2% SDS, 4% iodoacetamide (Applichem)).

SDS-PAGE gel electrophoresis was performed in a BIO-RAD PROTEAN® plus Dodeca™ Cell with 5mA per gel for 2h followed by 13-15mA per gel overnight using 12.5% SDS-polyacrylamide gels (1mm-thick). For protein staining, gels were fixed in 40% ethanol (CLN Nierle, Niederhummel, Germany) and 10% acetic acid (Applichem) for 8h followed by an overnight exposure to a Coomassie solution containing 10% (NH<sub>4</sub>)<sub>2</sub>SO<sub>4</sub> (Applichem), 1% phosphoric acid (Fluka, Sigma Aldrich), 25% methanol (Zefa Laborservice, Harthausen, Germany) and 0.625% Coomassie Brilliant blue G-250 (Applichem). Destaining of the gels was performed in bidistilled water (bd.H<sub>2</sub>O) until the background was completely clear. All 10 gels from iron-adequately and iron-deficiently fed WT (N = 10) as well as TNF<sup>ΔARE/WT</sup> mice (N = 10) were simultaneously subjected to all steps of 2D-gel electrophoresis including IEF, SDS-PAGE, Coomassie Brilliant Blue staining and quantitative analysis in order to minimize variability between samples.

Coomassie-stained gels were scanned (GS-800 Calibrated Densitometer, BIO-RAD) and analyzed by ProteomWeaver software (Definiens, Munich, Germany) including background subtraction and volume normalization. Reference gels from the iron-adequately and iron-deficiently fed WT as well as TNF<sup>ΔARE/WT</sup> mice were generated and compared with the gels from the IEC samples from each group. Spots with at least 1.5 fold differences in protein intensity, a significant Mann-Whitney-U test ( $p < 0.05$ ) and present in at least 3 out of 5 (or 2 out of 4 respectively) gels were picked for further MALDI-TOF-mass spectrometry (MS) analysis.

### **Trypsin digestion of protein spots and MALDI-TOF MS**

Coomassie-stained spots were picked, washed alternately in acetonitrile (Roth) and 50mM NH<sub>4</sub>HCO<sub>3</sub>, dried and then digested using 0.1μg sequencing grade modified trypsin (Promega, Mannheim, Germany) in 50mM NH<sub>4</sub>HCO<sub>3</sub> (Roth). The dried spots were rehydrated for 1h at 4°C by adding 6μl of 0.02μg/μl trypsin and incubated overnight at 37°C. Finally, 7μl of 1% trifluoroacetic acid (TFA, Sigma, Germany) were added and the tryptic peptide fragments were extracted using ultrasonication for 15min at room temperature (RT). Supernatants were stored at -80°C or directly used for MALDI-TOF-MS analysis.

MS analysis was performed according to the method of Bruker Daltonics (Leipzig, Germany) using the Autoflex Control software and the mass spectrometer from Bruker Daltonics. Briefly, 1.5-2μl of the extracted protein sample together with 2μl of 0.1% TFA was spotted onto the target using the thin-layer affinity HCCA AnchorChip™ preparation by Bruker Daltonics. Proteins were identified by using the Mascot Server 1.9 (Bruker Daltonics) based on mass searches in the Matrix Sciences Mascot Database (MSDB) database within murine sequences only. The search parameters allowed the carboxyamidomethylation of cysteine and one missing cleavage. The minimum score of 61 and a mass accuracy of ± 100 ppm were selected as criteria for positive identification of proteins.

### Western blot analysis

Purified primary IEC (pooled for each group) from the correlating animal experiments, from organ culture experiments or Mode-K cells were lysed in 1x Laemmli buffer (12.5ml Tris-HCl, 8ml 10% SDS, 7.9g Glycerol (Applichem), 7.7mg DTT, 1.25ml 0.5% Bromphenole (Roth), 50ml H<sub>2</sub>O). After a 5min heating step (95°C), equal protein amounts (20-50µg) were subjected to electrophoresis (15mA per gel) on 7, 10 or 15% SDS-PAGE gels due to the size of the protein of interest. Protean Mini cell was used according to the manufacturer's instructions (BIO-RAD). The size of proteins was confirmed with the Precision Plus protein dual color standards (Fermentas, St. Leon-Rot, Germany). Proteins were blotted on PVDF membranes (Millipore, Schwalbach, Germany) using a Trans Blot SD Semi Dry Transfer Cell (24V, 47min) (BIO-RAD) and semi-dry blotting buffer (25mM Tris (Roth), 192mM glycine (Applichem), 20% methanol (v/v)). Short incubation of blotted membranes in 0.5% ponceau S (w/v) (Roth) in 1 % acetic acid (v/v) was used as control for presence of proteins. Membranes were washed with dest. H<sub>2</sub>O followed by Tris buffered saline (TBS) (20 mM Tris, 137 mM NaCl (Roth)) supplemented with 0.1 % tween 20 (v/v) (TBST) (Serva, Heidelberg, Germany). Membranes were blocked with 5% dry milk (w/v) (Roth) in TBST for 1h at RT on a rocking shaker. All used antibodies were diluted in this blocking reagent in different dilutions as needed.

**Table 3. List of used antibodies**

|                                   |                                 |
|-----------------------------------|---------------------------------|
| CD3                               | Santa Cruz, Heidelberg, Germany |
| β-actin                           | Cell Signalling, Danvers, USA   |
| catalase                          | Santa Cruz, Heidelberg, Germany |
| p-Rel A                           | Santa Cruz, Heidelberg, Germany |
| HIF-1α                            | Novus, Cambridge, UK            |
| HO-1                              | Stressgen, Ann Arbor, USA       |
| grp-78                            | Sigma Aldrich, Germany          |
| p-eiF2α                           | Cell Signalling, Danvers, USA   |
| VCP                               | Cell Signalling, Danvers, USA   |
| cleaved caspase 3 (cc3)           | Cell Signalling, Danvers, USA   |
| CD71 / Transferrin receptor (TfR) | Santa Cruz, Heidelberg, Germany |
| anti-rabbit IgG                   | Dianova, Hamburg, Germany       |
| anti-mouse IgG                    | Dianova, Hamburg, Germany       |
| anti-goat IgG                     | Dianova, Hamburg, Germany       |

The antiserum for mouse intelectin 1 was a generous gift from Shoutaro Tsuji (Division of Cancer Therapy, Kanagawa Cancer Center Research Institute, 1-1-2 Nakao, Asahi-ku, Yokohama-shi Kanagawa, 241-0815, Japan).

After incubation of first antibody (either 1h at RT or overnight at 4°C on a rocking shaker), membranes were washed with TBST (3 times, 10min each) on a rocking shaker. Secondary antibodies (anti-rabbit IgG, anti-mouse IgG or anti-goat IgG) were also diluted in blocking reagent and applied on the membrane for 1h at RT on a rocking shaker. Subsequently, membranes were washed (3 times,

10min each) and proteins were detected using an enhanced chemiluminescence light (ECL) detection kit as recommended by the manufacturer (GE Healthcare, Munich, Germany).

### **RNA isolation and measurement**

Samples for RNA isolation (IEC, Mode-K cells, T cells) were kept in 200 - 800µl trizol or 350µl RLT buffer.

For the isolation of trizol-kept samples: After incubation (5min, RT), 40 – 160µl chloroform (Applichem) were added and samples were shaken for 15sec. After 3min incubation at RT, samples were centrifuged (12000rpm, 30min, 4°C) and the top layer was transferred to a fresh tube. After addition of 100 – 400µl isopropyl alcohol (CLN Nierle), the samples were incubated at -20°C overnight. On the next day, samples were centrifuged (12000rpm, 30min, 4°C) and supernatant was removed. 1ml 75% ethanol was added followed by centrifugation (8000rpm, 10min, 4°C). Again, supernatant was carefully removed and samples were air-dried (~ 5min) until the pellet turned transparent. Pellets were resuspended in 20µl DEPC (Applichem) H<sub>2</sub>O. The RNA concentration and purity (A260:A280 ratio) was determined by spectrophotometric analysis (Nanodrop photometer, Peqlab, Erlangen, Germany).

For the isolation of RLT buffer-kept samples: RNA was isolated by using the RNeasy® Mini Kit (Quiagen, Hilden, Germany) according to the manufacturer's instructions. Briefly, samples in RLT buffer were mixed with 350µl 70% ethanol and applied onto RNeasy columns. After 3 centrifugation steps (8000g, 15sec, RT) with application of 350µl of RW1 buffer and 2 times 500µl of RPE buffer, samples were centrifuged again (8000g, 2min, RT). Afterwards, columns were centrifuged without buffer (18000g, 1min, RT), followed by the addition of 50µl RNase-free H<sub>2</sub>O and centrifugation (8000g, 1min, RT). Last step was repeated with the collected flow-through. The RNA concentration and purity (A260:A280 ratio) was determined by spectrophotometric analysis (Nanodrop photometer).

### **Immunohistochemical labelling**

Paraffin-embedded tissue from distal ileum segments of TNF<sup>ΔARE/WT</sup> mice were cut in 5µm slides, transferred onto microscope slides (Roth) and paraffin was melted at 60°C for 10min, followed by automatically deparaffinization in a Leica ST5020 (Wetzlar, Germany). For antigen unmasking, slides were shortly boiled in EDTA (1mM, pH 8.0) followed by 15min subboiling. For staining, slides were washed in distilled H<sub>2</sub>O (dH<sub>2</sub>O) (3 times, 5min), incubated in 3% H<sub>2</sub>O<sub>2</sub> (Neolab, Heidelberg, Germany) for 10min, followed by 2 washing steps in dH<sub>2</sub>O for 5min each. Slides were blocked with blocking buffer (TBST with 5% normal goat serum) for 60min, followed by direct application of diluted (in antibody dilution buffer containing TBST with 1% BSA and 0,3% Triton-X100 (Roth)) grp-78 antibody overnight at 4°C. After 3 washing steps with PBS (5min each), slides were incubated with diluted biotinylated anti-rabbit secondary antibody (Sigma Aldrich) for 30min at RT. After 3

washing steps (5min each), slides were incubated with DAB substrate (Sigma Aldrich) and staining monitored. Slides were immersed in dH<sub>2</sub>O and counterstained with methyl green (Applichem) for 10min. After washing twice (5min each), slides were dehydrated first in 95% ethanol (twice, 10min each), second in 100% ethanol (twice, 10min each), third in xylene (twice, 10min each) (Mediate, Burgdorf, Germany). Slides were mounted (mounting medium: Vectashield, Burlingame, USA).

### **TUNEL staining**

Paraffin-embedded tissue from distal ileum segments of TNF<sup>ΔARE/WT</sup> mice were deparaffinized by putting tissue slides in 3 changes of xylene (5min each), 2 changes of 100% ethanol (5min each), once in 95% ethanol, once in 70% ethanol (3min each) and last change in PBS (5min). TUNEL staining was performed by using the ApopTag® Peroxidase In Situ Apoptosis Detection Kit according to the manufacturer's instructions (Chemicon, Millipore).

Freshly diluted Proteinase K (20μg/ml) (Roth, Karlsruhe, Deutschland) was directly applied onto the specimen (~60μl/5 cm<sup>2</sup>, 15min, RT). After washing step in dH<sub>2</sub>O (2 times, 2min each) in a coplin jar, slides were quenched in 3% H<sub>2</sub>O<sub>2</sub> (diluted in PBS) for 5min at RT. After washing steps in PBS (2 times, 5min each) in a coplin jar, excess liquid was gently tapped off and Equilibration Buffer (~75μl/5 cm<sup>2</sup>) was directly applied onto the specimen for at least 10sec. Again, excess liquid was gently tapped off and Working Strength TdT Enzyme (~55μl/5 cm<sup>2</sup>) was directly applied onto the specimen for 1h at 37°C in a humidified chamber. Slides were transferred into a coplin jar containing Working Strength Stop/Wash Buffer with slight agitation for 15sec and another incubation for 10min at RT. After washing steps (3 times, 1min each) in PBS, excess liquid was gently tapped off and Anti-Dioxigenin Conjugate (~65μl/5cm<sup>2</sup>) was directly applied onto specimen. After incubation (30min, RT) in a humidified chambers, slides were washed (4 times, 2min each, RT) in a coplin jar. Excess liquid was gently tapped off and specimen were completely covered with Peroxidase Substrate (~75μl/5 cm<sup>2</sup>). To determine optimal staining time (3 – 6min), color development was monitored under the microscope. After staining time, slides were washed in dH<sub>2</sub>O (3 times, 1min each) in a coplin jar before 5min incubation at RT in dH<sub>2</sub>O. Counterstaining was performed with 0.5% methyl green (w/v) in a coplin jar (10min, RT). After incubation, slides were washed in 3 changes of dH<sub>2</sub>O in a coplin jar by dipping the slides 10 times each in the first and second washing step, followed by 30sec without agitation in the third wash. Specimen were dehydrated by moving each slide through 3 changes of xylene (2min each) and mounted under a glass coverslip in a mounting medium (Merck). Covered slides were viewed under the microscope to assess apoptotic processes.

### **Ileal explant cultivation**

Distal ileum segments (4x4mm size) from WT and TNF<sup>ΔARE/WT</sup> mice were cut open and cultivated (37°C, 5% CO<sub>2</sub> atmosphere) with serosal side down on costar Netwell inserts (500uM/l, Corning incorporated life sciences, Acton, USA) containing 1.8ml of DMEM medium (0.5% FCS, 1% antibiotics/antimycotics (AA)) (Invitrogen, Carlsbad, USA) with or without FeNTA (500μM) or TNF (50ng/ml) (Biosource, Invitrogen) in the lower compartment. 10μl of medium was applied to the luminal side of each tissue piece. After 24h cultivation, tissue pieces were submerged in 100μl lysis buffer, mashed in a homogeniser and centrifuged (14000g, 20min, 4°C). Protein concentration of supernatants was measured by spectrophotometric analysis (Nanodrop photometer).

### **Cell culture, co-culture and stimulation**

The murine IEC line Mode-K (passage 10-30) was grown in a humidified 5% CO<sub>2</sub> atmosphere at 37°C to confluency in 12- or 24-well tissue culture plates (Cell Star, Greiner bio-one, Frickenhausen, Germany) as previously described [181]. Where indicated, the confluent epithelial cell monolayers were stimulated with FeNTA (500μM), N-acetyl-L-cysteine (NAC; Sigma Aldrich) (2.5 or 5mM) or TNF (10ng/ml) at different time points. For co-culture experiments, BrdU labeled (Cellular DNA Fragmentation Enzyme-linked Immunosorbent Assay (ELISA), Roche, Mannheim, Germany) Mode-K cells (16h) were cultured in 12-well plates and incubated with 0.5μg/ml Tunicamycin (Tm) for 6h in RPMI 1640 medium (Gibco / Invitrogen) supplemented with 10% FCS and 1% AA (RPMI 1640 full medium), where indicated. Cells were washed with PBS and activated (mixed with two anti-CD3/CD28 MicroBeads per T cell (Miltenyi Biotec, Bergisch Gladbach, Germany) or non-activated CD8αβ T cells were added in a ratio of 1:1 (2.5x10<sup>5</sup> T cells) in 500μl RPMI 1640 full medium. The cells were co-cultured for up to 72h. After each 24h, the cells were visualized by microscope and supernatant was taken to measure cell mediated cytotoxicity (Cellular DNA Fragmentation ELISA).

### **Reverse transcription and Real-Time PCR**

RNA from Mode-K cells or T cells was extracted using trizol Reagent or RNA easykit (Quiagen) as described under RNA isolation. 1μg of total RNA was used for transcription to cDNA. The adequate amount of RNA for 1μg was mixed with 1μl Oligo-dT (500ng/μl) and filled up with PCR-H<sub>2</sub>O to 12μl. After incubation for 5min at 65°C in a thermocycler (Biometra, Göttingen, Germany), 8μl of a solution containing 4μl of 5x First Strand Buffer, 2μl of 0.1M DTT, 1μl of RNase Out (40U/μl) (Invitrogen) and 1μl MMLV-reverse transcriptase (200U/μl) were added to each sample. For cDNA generation, the mixture was incubated for 60min at 37°C using a thermocycler, followed by heating to 99°C for 1min.

For samples with very low amounts of RNA (T cells), MMLV was replaced by SuperScript III (Invitrogen) with higher sensitivity. The adequate amount of RNA for 50-100ng was mixed with 1µl Oligo-dT (500ng/µl), 1µl of desoxyribonucleoside triphosphate mixture (10mM) and filled up with PCR-H<sub>2</sub>O to 13µl. After incubation for 5min at 65°C in a thermocycler, followed by 1min on ice, 7µl of a solution containing 4µl of 5x First Strand Buffer, 1µl of 0.1M DTT, 1µl of RNase Out (40U/µl) and 1µl of SuperScript III (200U/µl) were added to each sample. Using a thermocycler for cDNA generation, the mixture was incubated for 1h at 50°C, followed by heating to 70°C for 15min and cool-down to 10°C.

Real-time PCR was performed from 1µl cDNA in glass capillaries with a Light Cycler™ system (Roche) or 96-well plates with a LightCycler 480 System (Roche) respectively, using the specific SYBR or UPL primers as previously described (14).

**Table 4. List of used primers with sequences (SYBR and UPL)**

| Primer        | Forward Sequence           | Reverse Sequence            |
|---------------|----------------------------|-----------------------------|
| 18s (SYBR)    | 5'-cggctaccacatccaaggaa    | 5'-gctggaattaccgcgct        |
| GAPDH (UPL)   | 5'-tgtctgtctttgtccttgagagg | 5'-aggggtgggacagacag        |
| HO-1 (SYBR)   | 5'- acatccaagccgagaa       | 5'- agcgggtatatgcgtg        |
| Grp-78 (SYBR) | 5'- tgacaaaaccgcctg        | 5'- caatgtccgcctcctg        |
| Grp-78 (UPL)  | 5'-ctgaggcgtatttggaaag     | 5'-tcatgacattcagtcagcaa     |
| GrzmB (UPL)   | 5'-gctgctcactgtgaaggaagt   | 5'-tggggaatgcattttacat      |
| IFN-γ (UPL)   | 5'-ggaggaactggcaaaaaggat   | 5'-ttcaagacttcaaagagtctgagg |
| TfR (UPL)     | 5'-gctttgggtgctggtgtt      | 5'-ctgctgggtctaaatccatctt   |
| TNF (UPL)     | 5'-tgccatgtctcagcctcttc    | 5'-gaggccatttgggaactct      |

The amplified product was detected by the presence of a SYBR green fluorescent signal. The universal probe library (UPL) and the LightCycler 480 System implies usage of a combination of specific primers with single hydrolysis probes. These probes contain 2 labels, a fluorescence reporter and a dark quencher, inproximately to each other. During PCR, the polymerase cleaves the probe when annealed to its target sequence, separating reporter and quencher. The reporter is no longer quenched and emits a measurable fluorescence signal when exited.

Melting curve analysis and gel electrophoresis was used to document the amplicon specificity. The crossing point of the log-linear portion of the amplification curve was determined. The relative induction of gene mRNA expression was calculated using the following equation: ED<sub>crossing point</sub> (control samples - treated samples) and normalized for the expression of 18S or GAPDH.

### **ROS measurement**

Mode-K cells were grown to 90-99% confluency. Cells were stimulated with FeNTA (500 $\mu$ M) for 3h with or without pre-incubation of NAC for 24h (2.5 and 5mM). After incubation, 5-(and-6)-chloromethyl-2'.7'-dichlorodihydrofluorescein diacetate, acetyl ester (CM-H<sub>2</sub>DCFDA; Invitrogen, Oregon, USA) was added for 40min (final concentration: 10 $\mu$ M). Medium was removed and cells were washed twice with cancer buffer (137mM NaCl, 5.4mM KCl (Neolab), 2.8mM CaCl<sub>2</sub>\*2H<sub>2</sub>O (Merck, Darmstadt, Germany), 1.0mM MgSO<sub>4</sub>\*H<sub>2</sub>O (Neolab), 10mM Hepes (Merck), 10mM glucose (Roth), bdH<sub>2</sub>O to 1l, pH 7.4). After washing steps, cells were incubated in 1ml cancer buffer (20min, 37°C). Photometric measurement of ROS production was performed by using Flourescan Askent software (Thermo Fisher Scientific, Germany) at wave length of 485/538 nm for up to 120min (every 10min).

### **Chromatin immunoprecipitation (ChIP) analysis**

After the treatment of Mode-K cells with FeNTA (500 $\mu$ M) and/or TNF (10ng/ml) for 6h, cells were fixed by adding formaldehyde (Roth) to a final concentration of 1%. Nuclear extraction and ChIP were performed by using the ChIP-IT Enzymatic kit from Active Motif (Carlsbad, USA) as described by the manufacturer. Extracts were normalized according to their DNA concentration, and immunoprecipitations were carried out overnight at 4°C using 5 $\mu$ l anti-NRF2 (Santa Cruz), anti-XBP-1 (Santa Cruz) and ATF6 (Santa Cruz) antibodies. Immune complexes were collected with salmon-sperm saturated protein A/G agarose for 30min and washed 3 times in high salt buffer, followed by 3 washes with no salt buffer. DNA cross-links of the immune complexes were reverted by heating, followed by proteinase K digestion. The DNA was extracted with phenol-chloroform and precipitated in ethanol. DNA isolated from an aliquot of the total nuclear extract was used as loading control for the PCR (input control). PCR was performed with total DNA (1 $\mu$ l, input control) and immunoprecipitated DNA (1 $\mu$ l) using the grp-78 promoter-specific primers (see Table 2) as previously described [182]. The length of the amplified product was 230bp. The PCR products (10 $\mu$ l) were subjected to electrophoresis on 2% agarose (Roth) gels.

### **Isolation of intraepithelial lymphocytes (IEL) and FACS staining**

WT and TNF<sup>ΔARE/WT</sup> mice from the injection experiment were sacrificed and small intestine was removed. Mesenteric fat and lymph node were trimmed off. Small intestine was cut open longitudinally and washed with Hank's balanced salt solution (HBSS) (PAA, Cölbe, Germany), supplemented with 2% FBS 3 to 4 times to flush out fecal residues. Digestion buffer (5mM EDTA, 1mM DTT, 10% FBS) was freshly prepared before use and prewarmed in 37°C water bath until use.

Small intestine was cut into 0.5-1cm pieces and incubated with 5 ml digestion buffer in a horizontal shaker (Thermo Fisher, Scientific) at 200rpm speed, 37°C, for 15min. Gut tissue was digested twice to release the IEL. Pooled IEL from each mouse were placed on ice for 10min to separate the tissue debris from cells. Supernatant was carefully removed and centrifuge at 350g, 4°C, for 5min. Pellets were resuspended in 2ml FACS buffer (5% FBS, 2mM EDTA, PBS) and applied onto a nylon wool fiber column (Kisker, Steinfurt, Germany) to remove adherent cells and tissue debris. IEL ( $10^6$  cells) were used for the immunophenotyping by FACS analysis. Antibodies used for the 6 colour surface staining were: CD3APC-Cy7 (BD Pharmingen, Heidelberg, Germany), CD8 $\alpha$ APC (Milteny Biotect), CD8 $\beta$ FITC (BD Pharmingen), CD4PE-Cy7 (BD Pharmingen), TCR $\alpha\beta$ PE (Serotec, Düsseldorf, Germany), CD69PerCPy7 (BD Pharmingen) and CD25-APC (BD Pharmingen). 100.000 cells were acquired from the LSR II (BD Bioscience) and analyzed using the BD FACSDiva software.

### **Non-heme content, hematocrit and hemoglobin determination**

Non-heme iron content in liver was determined from WT and TNF<sup>ΔARE/WT</sup> mice. Liver samples were cut in pieces (approximately 1mm<sup>3</sup>) and 30mg of tissue samples were dissolved in acid-mix (6M HCl, 20% TCA (v/v)). After incubation (65°C, 20h) and centrifugation (3000rpm, 3min), the non-heme iron content was measured photometrically by using a commercial kit (Feren-B, Bioanalytic, Umrich/Freiburg, Germany).

Hematocrit and hemoglobin concentrations were measured using the microhematocrit method (No. 749311, Brand, Wertheim, Germany; Hematocrit-centrifuge 2104, Hettlich, Tuttlingen, Germany) and the cyanmethemoglobin method (reagent: Bioanalytic 4001, Umrich, Freiburg, Germany; photometer: UV-DK-20, Beckmann, Munich, Germany), respectively.

### **ELISA analysis**

Protein concentrations were determined in medium (lower compartment) of cultivated explants and supernatants of co-culture experiments by mouse-specific TNF, granzyme B and IFN- $\gamma$  ELISA kits, according to the manufacturer's instructions (R&D Systems, Wiesbaden, Germany).

### **Isolation of mesenteric CD8 $\alpha\beta$ <sup>+</sup> T cells**

Mesenteric lymph nodes (MLN) were dissected and immediately stored in cold RPMI 1640 full medium. MLNs from up to 3 mice were pressed through a 70 $\mu$ M cell strainer (BD Falcon, Belgium), resuspended in 10ml RPMI 1640 full medium and centrifuged for 5min at 4°C. The pellet was washed in 10ml MACS buffer (PBS, 0.5% BSA, 2mM EDTA, pH 7.2) After centrifugation (350g, 4°C), pellet was resuspended in 5ml red blood cell lysis buffer (0.8% NH<sub>4</sub>Cl (Sigma Aldrich), 0.1% KHCO<sub>3</sub> (Neolab), 0.0037% Na<sub>2</sub>EDTA\*3H<sub>2</sub>O (Applichem) in H<sub>2</sub>O, pH 7.2) and incubated for 5min at RT. The reaction was stopped by adding 15ml MACS buffer. After filtering (70 $\mu$ M mesh) and centrifugation (5min, 350g), pellet was resuspended in 200 $\mu$ l FcR blocking solution (10% FcR Blocking Reagent (Miltenyi Biotec) in MACS buffer and incubated for 10min at 4°C. 1.5 $\mu$ g FITC labeled anti-CD8 $\beta$  antibody (FITC Rat Anti-Mouse CD8b.2, BD Pharmingen) were added and incubated for 10min at 4°C. Cells were washed with 10ml MACS buffer, centrifuged and resuspended in 400 $\mu$ l MACS buffer, containing 10% Anti-FITC MicroBeads (Miltenyi Biotec). Cells were incubated for 10min on ice, washed and resuspended in 1ml MACS buffer. Labeled CD8 $\alpha\beta$ <sup>+</sup> T cells were isolated by magnetic cell separation technology using MS Columns (Miltenyi Biotec) according to the manufacturer's instructions. Purity was checked using the BD LSR II Flow Cytometer.

### **Cell mediated cytotoxicity assay**

In order to quantify cell mediated cytotoxicity, the Cellular DNA Fragmentation ELISA (Roche, Germany) was used. The principle of the method is based on the measurement of BrdU labeled DNA fragments in the supernatant of apoptotic and necrotic cells as a non-radioactive alternative to the chromium-51 [<sup>51</sup>Cr] release assay. The assay was performed according to the manufacturer's standard protocol.

### **Pyrosequencing of cecal microbiota**

#### **DNA extraction**

The experiment was performed at the Department of Food Science and Technology from the University of Nebraska by Prof. Jens Walter and Inés Martínéz.

DNA extraction was performed as previously described [183]. Briefly, approximately 1 g of cecal content was diluted 1 to 10 in Phosphate Buffered Saline (PBS, pH7) and the cells were washed three times. Cell pellets were homogenized in 750  $\mu$ l lysis buffer (200 mM NaCl, 100 mM Tris [pH 8.0], 20 mM EDTA, 20mg/ml lysozyme) and transferred to a microcentrifuge tube containing 300 mg of 0.1-mm zirconium beads (BioSpec Products). Samples were then

incubated at 37°C for 30 min. 85 µl of a solution of 10% sodium dodecyl sulfate solution and 40 µl of proteinase K (15mg/ml) were added and samples were incubated for an additional 15 min at 60°C. 500 µl of phenol-chloroform-isoamyl alcohol (25:24:1) were added, and the samples were homogenized in a MiniBeadbeater-8 (BioSpec Products) at maximum speed for 2 min, immediately cooled on ice and then subjected to centrifugation at 10,000 x g for 5 min. The extraction was performed twice with phenol-chloroform-isoamyl alcohol (25:24:1) and twice with chloroform-isoamyl alcohol with centrifugation at 14,000 x g for 5 min; DNA was recovered by ethanol precipitation at -20°C. The DNA pellets were dried for 30 min at RT and later re-suspended in 100 µl of Tris-HCl buffer (10 mM, pH 8.0).

### **Gastrointestinal microbial analysis by pyrosequencing**

Gut microbiota composition was analyzed by 454 pyrosequencing of the 16S rRNA gene from the DNA extracts. The V1-V2-V3 region provides excellent resolution of most bacterial phyla and it performs well in high-throughput analyses. The 16S primers were modified to work with the Roche-454 Titanium adapter sequences and contain the A or B Titanium sequencing adapter (shown in italics), followed immediately by a unique 8-base barcode sequence (BBBBBBB) and finally the 5' end of primer. As forward primers, we did use a mixture (4:1) of the primers B-8FM (5'—*CCTATCCCCTGTGTGCCTTGGCAGTCTCAGAGAGTTTGATCMTGGCTCAG*) and B-8FMBifido (*CCTATCCCCTGTGTGCCTTGGCAGTCTCAGAGGGTTCGATTCTGGCTCAG*). As the reverse primer, the primer A-518R (5'—*CCATCTCATCCCTGCGTGTCTCCGACTCAGBBBBBBBATTACCGCGGCTGCTGG*—3') was used. Each sample was amplified with uniquely bar-coded primers, which allowed us to mix PCR products from multiple animals in a single run, followed by bioinformatic assignation of the sequences to their respective samples via the barcode. The PCR mixture contained 1 µl of forward primer mix, 1 µl of reverse primer, 0.25 µl of Ex-Taq polymerase (TaKaRa Bio, USA), 1.5 µl of the sample, 6.25 µl of Ex-Taq buffer, 5 µl of deoxynucleotides and 37 µl of double distilled sterile water were used for the reaction. The thermocycling program used was an initial denaturing step for 5 min at 95°C, followed by 30 cycles of denaturing at 95°C for 45 sec, annealing at 57°C for 45 sec and extension at 72°C for 2 min, with a final step at 72°C for 10 min. The PCR products were quantified using a software appropriate for gel quantification (Genesnap, Syngene USA).

The sequences obtained were binned according to their barcode using the Ribosomal Database Project (RDP) Pyrosequencing Pipeline (<http://pyro.cme.msu.edu/>) Initial Process with default parameters except for the minimum sequence length that was set up at 300 bp [184]. The quality approved sequences were trimmed to 400 bp. The resulting sequences were submitted to the RDP Classifier web tool for taxa assignment. In addition, sequences were aligned in the RDP Aligner web tool and later clustered with the Complete Linkage Clustering tool from RDP, using a 97% cutoff for maximum distance. Finally, microbial diversity was calculated using the Rarefaction tool provided by RDP (<http://rdp.cme.msu.edu/>).

### **Statistical analyses**

The impact of diet and genotype on the gut microbiota of the mice was analyzed with ANOVA analysis using a 3 x 2 factorial design. The bacterial groups were treated as proportions relative to the total amount of sequences present in each sample. Moreover, normalization of the bacterial groups was performed when necessary by calculating the arcsin of the square root of the proportion.

In order to investigate possible associations between bacterial populations and inflammation, Pearson multiple correlations were performed with the proportions of all individual bacterial taxa and OTUs, and the histology scores obtained with TNF<sup>ΔARE/WT</sup> mice using GraphPad Prism version 5.00 (GraphPad Software, San Diego, CA).

### **Statistical analysis**

Statistical tests were performed using unpaired t-test or One-Way ANOVA followed by Holm-Sidak test. Differences were considered significant if values were <0.05 (\*), <0.01 (\*\*), or <0.001 (\*\*\*).

## 4 RESULTS

### 4.1 Effects of an iron-deficient diet on chronic ileitis

WT (N = 10) and TNF<sup>ΔARE/WT</sup> mice (N = 10) at the age of 7 weeks were fed with an iron-adequate or an iron-deficient diet for additional 11 weeks (feeding experiment; Figure 8). Assuming an average food intake of 3g/mouse/day, this feeding pattern resulted in food-derived iron intake of approximately 0.54 mg iron in the iron-adequate group and 0.03 mg iron in the iron-deficiently fed group. Mice were sacrificed at the age of 18 weeks by cervical dislocation and samples were collected.

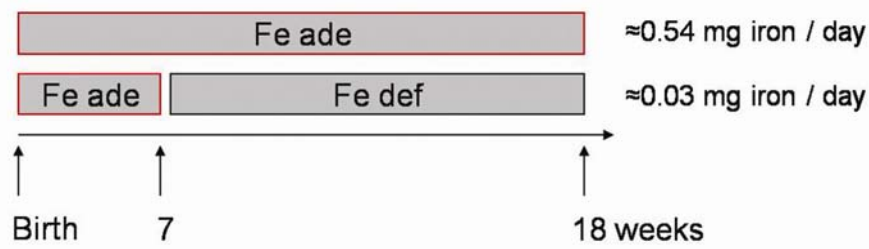


**Figure 8. Experimental setup of the feeding experiment**

Histological examination (score 0 - 12) of distal ileal segments revealed severe signs of tissue pathology in the iron-adequately fed TNF<sup>ΔARE/WT</sup> mice (score  $8.30 \pm 0.91$ ) compared to iron-deficiently fed TNF<sup>ΔARE/WT</sup> mice ( $2.30 \pm 0.76$ ) (Figure 9, bar chart). Hematoxylin and Eosin (H&E) staining of representative paraffin-embedded distal ileal segments from the iron-deficiently fed TNF<sup>ΔARE/WT</sup> mice illustrated the reduced transmural infiltration of immune cells, crypt hyperplasia and villus atrophy compared to the iron-adequately fed TNF<sup>ΔARE/WT</sup> mice (Figure 9, pictures). Both WT groups (iron-adequate:  $1.20 \pm 0.29$ ; iron-deficient:  $1.10 \pm 0.42$ ) showed no signs of tissue pathology. Numbers in parentheses represent average histological score  $\pm$  standard deviation.

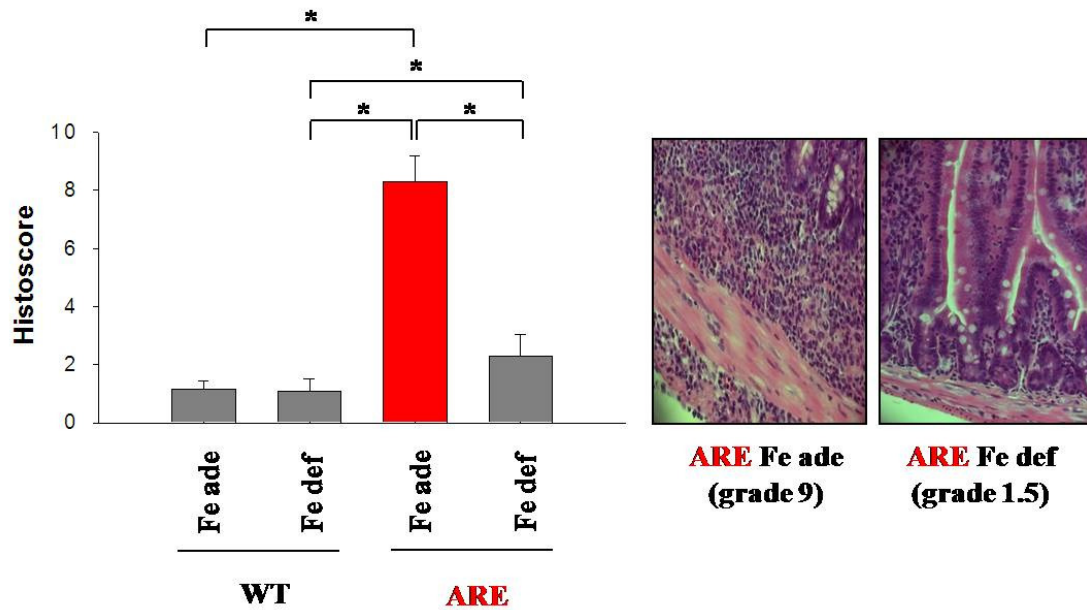


**Figure 9. Histology of the feeding experiment.** Histological analysis of iron-adequately and iron-deficiently fed WT and  $TNF^{\Delta ARE/WT}$  mice (bar chart) and representative H&E-staining of ileal segments from both  $TNF^{\Delta ARE/WT}$  groups (pictures).

In order to characterize the effect of the iron-deficient diet on different organs of WT and  $TNF^{\Delta ARE/WT}$  mice, Schümann et al. measured the non-heme iron content in liver and spleen demonstrating significant differences [185] between the iron-adequate and the iron-deficient diet. There were no significant differences in non-heme iron content of the ileum (data not shown). Interestingly, inflammation per se did not influence iron stores as the non-heme iron content did not differ between WT and  $TNF^{\Delta ARE/WT}$  mice.

Hemoglobin (Hb) and hematocrit (Hc) blood levels of  $TNF^{\Delta ARE/WT}$  decreased significantly when comparing the iron adequate diet with the iron-deficient diet [185]. As there are no reference ranges available for Hb and Hc values of mice, only the 2 diets can be compared without assessing the anemic status.

#### 4.1.1 Epithelial cell proteome of iron-adequately and iron-deficiently fed WT and TNF<sup>ΔARE/WT</sup> mice

To investigate the effect of inflammation and dietary low iron in healthy WT mice and under the condition of chronic ileitis in the TNF<sup>ΔARE/WT</sup> mouse model, protein expression profiling was prepared for all possible comparison between the 4 groups (Figure 10) including iron-adequately fed WT vs. iron-adequately fed TNF<sup>ΔARE/WT</sup> mice (ade WT-ARE-comparison), iron-adequately fed TNF<sup>ΔARE/WT</sup> vs. iron-deficiently fed TNF<sup>ΔARE/WT</sup> mice (ARE-comparison), iron-adequately fed WT vs. iron-deficiently fed WT mice (WT-comparison) and iron-deficiently fed WT vs. iron-deficiently fed TNF<sup>ΔARE/WT</sup> mice (def WT-ARE-comparison), respectively. First named group in the comparisons served as control.

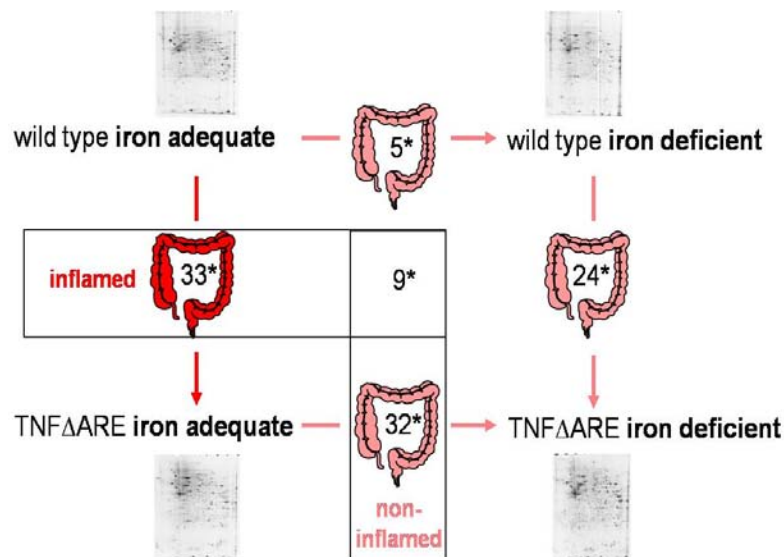


**Figure 10. Overview of all performed proteome comparisons including numbers of significantly regulated proteins (\*).**

We applied all steps of 2D gel electrophoresis including IEF, SDS-PAGE and Coomassie Brilliant Blue staining to all 10 WT / TNF<sup>ΔARE/WT</sup> gels simultaneously to minimize the variability between the samples. Protein spots with at least 1.5-fold change in the average steady-state expression level, a significant Mann-Whitney-U test ( $p < 0.05$ ) and a presence in at least half of the analyzed gels were submitted to MALDI-TOF-MS analysis. We produced duplicates for the set of the iron-adequately as well as the iron-deficiently fed TNF<sup>ΔARE/WT</sup> mice gels ( $N = 5$  for each diet, in technical duplicates) to assess the repeatability of 2D gel electrophoresis. We obtained 88% reproducibility, i.e. 88% of the significantly regulated proteins could be found in both set of gels for the comparison between iron-adequately and iron-deficiently fed TNF<sup>ΔARE/WT</sup> mice.

The absence of T-cell contamination in all groups confirmed the purity of the IEC isolation (Figure 11).

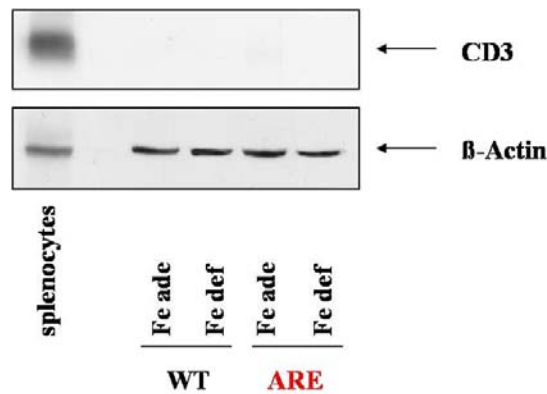


**Figure 11. Absence of CD3+T-cell contamination as confirmation for IEC purity.** Western blot analysis was performed with 25  $\mu$ g total protein derived from splenocytes and pooled IEC samples from 5 iron-adequately (Fe ade) or iron-deficiently fed (Fe def) WT and 5 iron-adequately or iron-deficiently fed  $TNF^{\Delta ARE/WT}$  mice, respectively, using immunoreactive CD3 and  $\beta$ -actin.

#### 4.1.1.1 Protein expression profiling of the ade WT-ARE-comparison: effects of chronic inflammation on the ileal epithelial cell proteome

To exclusively ascertain the effect of severe inflammation in the ileum on epithelial cell proteome independent of the iron diet, we first performed 2D gel electrophoresis from non-inflamed WT and inflamed  $TNF^{\Delta ARE/WT}$  mice fed with an iron-adequate diet which reflects the normal food composition for mice (each N = 5). We identified 33 differentially regulated proteins (Table 5), 30 up- and 3 down-regulated. Seventy-four % of these regulated proteins have catalytic activity, 25% are involved in catabolic procedures and 29% in ATP-binding. This may support the theory of energy deficiency under the condition of chronic inflammation by counteracting through up-regulation of these proteins for energy production.

**Table 5. ade WT-ARE-comparison: differentially regulated proteins in IEC from iron-adequately fed  $TNF^{\Delta ARE/WT}$  mice compared to iron-adequately fed WT mice**

| Gene ID | Accession Number | Name of Protein   | MM (Da) | pI    | SC (%) | RF   | F (WT) | F (ARE)  |
|---------|------------------|---|---------|-------|--------|------|--------|----------|
| 18477   | PRDX1_MOUSE      | Peroxiredoxin-1   | 22.7    | 10.26 | 38     | 2.18 | 1/5    | 4/5      |
| 16691   | K2C8_MOUSE       | Keratin, type II cytoskeletal 8                                   | 53.2    | 5.28  | 48     | 2.40 | 2/5    | 4/5      |
| 18648   | PGAM1_MOUSE      | Phosphoglycerate mutase 1   | 28.8    | 6.82  | 53     | 3.92 | 4/5    | 3+1xns/5 |
| 227231  | CPSM_MOUSE       | Carbamoyl-phosphate synthase [ammonia], mitochondrial [Precursor] | 165.7   | 6.50  | 40     | 2.06 | 2/5    | 3/5      |
| 11465   | Q9QZ83           | Gamma actin-like protein  | 41.3    | 5.48  | 44     | 2.31 | 1xns/5 | 4+1xns/5 |

## RESULTS

| Gene ID | Accession Number | Name of Protein                                | MM (Da) | pI   | SC (%) | RF   | F (WT)   | F (ARE)  |
|---------|------------------|--|---------|------|--------|------|----------|----------|
| 11429   | ACON_MOUSE       | Aconitate hydratase, mitochondrial [Precursor] | 86.2    | 8.92 | 32     | 1.81 | 2xns/5   | 2/5      |
| 21881   | TKT_MOUSE        | Transketolase                                  | 61.1    | 6.57 | 43     | 3.15 | 2/5      | 2/5      |
| 54128   | DHR11_MOUSE      | Dehydrogenase/reductase SDR family member 11   | 28.0    | 6.00 | 58     | 2.35 | 1/5      | 2/5      |
|         | Pmm2_MOUSE       | Phosphomannomutase 2                           | 28.2    | 5.73 | 45     |      |          |          |
| 72042   | COTL1_MOUSE      | Coactosin-like protein                         | 15.9    | 5.09 | 32     | 2.10 | 0/5      | 2+1xns/5 |
| 11461   | Q61276           | A-X actin                                      | 39.5    | 5.73 | 25     | 2.14 | 2/4      | 2/5      |
| 56431   | DEST_MOUSE       | Dextrin  | 18.7    | 9.27 | 32     | 1.87 | 2/5      | 3+1xns/5 |
| 14120   | F16P2_MOUSE      | Fructose-1,6-bisphosphatase isozyme 2          | 37.2    | 5.84 | 38     | 1.77 | 1+1xns/5 | 3+1xns/5 |
| 21454   | TCPZ_MOUSE       | T-complex protein 1 subunit zeta               | 58.3    | 6.71 | 42     | 2.13 | 0/5      | 4/5      |
| 16429   | ITL1A_MOUSE      | Intellectin-1a/b                               | 35.4    | 9.00 | 40     | 3.00 | 2+1xns/5 | 3/5      |
| 19166   | PSA2_MOUSE       | Proteasome subunit alpha type 2                | 26.0    | 9.11 | 51     | 2.41 | 0/5      | 2+3xns/5 |
| 16828   | LDHA_MOUSE       | L-lactate dehydrogenase A chain                | 36.7    | 8.83 | 54     | 3.20 | 1+1xns/5 | 3+1xns/5 |
| 227613  | TBB2C_MOUSE      | Tubulin beta-2C chain                          | 50.8    | 4.68 | 28     | 2.01 | 0/5      | 2+1xns/5 |
| 12631   | COF1_MOUSE       | Cofilin-1                                      | 18.7    | 9.19 | 52     | 2.37 | 1/5      | 3/5      |
| 20655   | SODC_MOUSE       | Superoxide dismutase [Cu-Zn]                   | 16.0    | 6.04 | 45     | 2.67 | 1+1xns/5 | 1+2xns/5 |
| 268373  | PPIA_MOUSE       | Peptidyl-prolyl cis-trans isomerase A          | 18.0    | 9.16 | 50     | 2.06 | 2+1xns/5 | 3/5      |
| 622402  | Q9JLI0           | Aldo-keto reductase a                          | 37.6    | 6.22 | 44     | 2.04 | 1+2xns/5 | 1/5      |
| 11637   | KAD2_MOUSE       | Adenylate kinase isoenzyme 2, mitochondrial    | 26.7    | 7.79 | 51     | 1.82 | 0/5      | 2+2xns/5 |
| 67738   | PPID_MOUSE       | 40 kDa peptidyl-prolyl cis-trans isomerase     | 32.4    | 9.98 | 21     | 2.47 | 1+1xns/5 | 3+1xns/5 |
| 225913  | DAK_MOUSE        | Dihydroxyacetone kinase                        | 59.9    | 6.48 | 36     | 2.31 | 3+1xns/5 | 3+2xns/5 |
| 18103   | NDKB_MOUSE       | Nucleoside diphosphate kinase B                | 18.8    | 9.30 | 58     | 1.96 | 3/5      | 4/5      |

## RESULTS

| Gene ID | Accession Number       | Name of Protein  | MM (Da) | pI   | SC (%) | RF    | F (WT)   | F (ARE)  |
|---------|------------------------|--|---------|------|--------|-------|----------|----------|
| 18813   | PA2G4_MOUSE            | Proliferation-associated protein 2G4                                   | 44.0    | 6.44 | 30     | 1.95  | 0/5      | 4/5      |
| 269523  | TERA_MOUSE<br>(Q8BSR6) | Transitional endoplasmic reticulum ATPase (valosin containing protein) | 89.9    | 5.00 | 21     | 3.17  | 0/5      | 2/5      |
| 23972   | Q5BKP4                 | 3'-phosphoadenosine 5'-phosphosulfate synthase 2                       | 70.9    | 7.93 | 24     | 3.64  | 1/5      | 2/5      |
| 22143   | TBA2_MOUSE             | Tubulin alpha-2 chain  | 50.8    | 4.68 | 36     | 3.86  | 0/5      | 1+2xns/5 |
| 11674   | ALDOA_MOUSE            | Fructose-bisphosphate aldolase A                                       | 39.7    | 9.26 | 46     | 4.89  | 1+1xns/5 | 1+1xns/5 |
| 12359   | CATA_MOUSE             | Catalase   | 59.9    | 8.53 | 27     | -2.38 | 2+2xns/5 | 1+2xns/5 |
| 27384   | AK1CD_MOUSE            | Aldo-keto reductase family 1 member C13                                | 37.6    | 6.46 | 33     | -2.09 | 2+ns/5   | 1+1xns/5 |
| 14085   | FAHD1_MOUSE            | Fumarylacetoacetate hydrolase domain-containing protein 1              | 24.8    | 8.81 | 50     | -2.13 | 1/5      | 3/5      |

### 4.1.1.2 Protein expression profiling of the ARE-comparison: effects of iron on the epithelial cell proteome under conditions of disease susceptibility

Histological examination of  $TNF^{\Delta ARE/WT}$  mice revealed the absence of inflammation after applying an iron-deficient diet. To further characterize the protective effect of an iron-deficient diet in a disease susceptible model for ileitis, we analyzed the epithelial cell proteome from 5 single inflamed iron-adequately fed  $TNF^{\Delta ARE/WT}$  mice and 5 single non-inflamed, iron-deficiently fed  $TNF^{\Delta ARE/WT}$  mice. As shown in Table 6 we identified 32 differentially regulated proteins including 9 down-regulated and 23 up-regulated. Four of these proteins could only be detected in replicate no. 1 including cytokeratin 19, intelectin 1, catalase and mitochondrial creatine kinase, 29 proteins were found in both sets of gels (reproducibility ~88%). Thirty-two % are mitochondrial proteins, mostly up-regulated, with the highest regulation factor of 12.87 for hydroxymethylglutaryl-CoA (HMG-CoA) synthase. This protein is one of the major enzymes for cholesterol biosynthesis, thus important for energy homeostasis and stability of plasma membranes suggesting a protective role in maintaining barrier function of the intestinal epithelium.

## RESULTS

**Table 6. ARE-comparison: differentially regulated proteins in IEC from iron-deficiently fed TNF<sup>ΔARE/WT</sup> mice compared to iron-adequately fed TNF<sup>ΔARE/WT</sup> mice**

| Gene ID | Accession Number | Name of Protein                                     | MM (kDa) | pI   | SC (%) | RF    | F (ARE)  | F (ARE Fe ↓) |
|---------|------------------|---|----------|------|--------|-------|----------|--------------|
| 11429   | Q505P4           | Aconitase 2   | 86.2     | 8.92 | 31     | -2.22 | 3+1xns/5 | 2/5          |
| 11931   | BAB26846         | ATP synthase subunit beta                           | 56.3     | 7.05 | 44     | -2.63 | 3/3      | 2/4          |
| 15516   | A29317           | Hsp90   | 92.7     | 4.59 | 38     | -2.94 | 2/4      | 4/5          |
| 108037  | Q99K87           | Serine hydroxymethyl transferase 2                  | 56.2     | 9.51 | 33     | -2.63 | 3+1xns/5 | 2+1xns/4     |
| 20341   | Q91X87           | Selenium binding protein 1                          | 56.0     | 5.28 | 43     | -3.45 | 2+2xns/5 | 3/5          |
| 20342   | AAB25841         | Selenium binding protein 2                          |          |      |        |       |          |              |
| 22004   | S23256           | Tropomyosin beta                                    | 33.0     | 4.48 | 45     | -2.86 | 3/3      | 1/4          |
| 56463   | BAC40105         | Staphylococcal nuclease domain-containing protein 1 | 102.7    | 7.31 | 40     | -2.70 | 3+1xns/4 | 0/5          |
| 16669   | JQ0028           | Cytokeratin 19 - mouse*                             | 44.5     | 5.15 | 27     | -2.27 | 2+2xns/5 | 3+1xns/5     |
| 16429   | JE0328           | Intelectin*   | 35.4     | 9.00 | 31     | -2.08 | 4+1xns/5 | 2xns/4       |
| 14827   | ISMSSS           | Protein disulfide-isomerase                         | 57.4     | 4.62 | 47     | 1.98  | 4+1xns/5 | 4/5          |
| 14864   | B28946           | Glutathione S-transferase mu3                       | 25.9     | 8.77 | 66     | 3.17  | 3+1xns/5 | 4/4          |
| 14862   | S33860           | Glutathione S-transferase mu 1                      | 26.1     |      |        |       |          |              |
| 230163  | ALDOB_MOUSE      | Fructose-bisphosphate aldolase B                    | 39.8     | 9.44 | 32     | 1.91  | 39571    | 2/4          |
| 11370   | Q5NCV8           | Long-chain specific acyl-CoA dehydrogenase          | 71.2     | 9.60 | 43     | 1.60  | 39573    | 3/4          |
| 225913  | Q8VC30           | Dihydroxyacetone kinase                             | 59.9     | 6.48 | 39     | 1.66  | 3+1xns/5 | 3+2xns/5     |
| 14079   | FABPI_MOUSE      | Fatty acid-binding protein                          | 15.0     | 7.58 | 44     | 2.41  | 3+2xns/5 | 5/5          |
| 16204   | ILBP_MOUSE       | Gastrotropin  | 14.4     | 5.86 | 46     | 2.42  | 3+1xns/4 | 4/4          |
| 14120   | Q9QXD7           | Fructose-1.6-bisphosphatase                         | 37.2     | 5.84 | 40     | 1.85  | 2/3      | 4/4          |
| 15356   | B55729           | Hydroxymethylglutaryl-CoA synthase                  | 53.1     | 8.49 | 34     | 12.87 | 0        | 3/5          |
| 15107   | Q8K149           | Hydroxyacyl-coenzyme A dehydrogenase                | 32.0     | 7.88 | 34     | 1.57  | 5/5      | 3/3          |
| 14555   | AAH05756         | Glycerol-3-phosphate dehydrogenase [NAD+]           | 57.6     | 6.36 | 47     | 1.72  | 4/5      | 5/5          |
| 109801  | LGUL_MOUSE       | Lactoylglutathione lyase                            | 20.1     | 5.12 | 37     | 1.79  | 5/5      | 4+1xns/5     |
| 66809   | Q6PG82           | Keratin 20  | 49.0     | 5.10 | 50     | 1.61  | 3/3      | 5/5          |
| 16691   | AAA37551         | Cytokeratin 8                                       | 53.2     | 5.28 | 45     | 2.90  | 1+1xns/3 | 3/5          |

## RESULTS

| Gene ID | Accession Number | Name of Protein   | MM (kDa) | pI   | SC (%) | RF   | F (ARE)  | F (ARE)  |
|---------|------------------|---|----------|------|--------|------|----------|----------|
| 14085   | AAH26949         | Fumarylacetoacetate hydrolase domain-containing protein 1 | 25.5     | 8.81 | 44     | 1.95 | 2+1xns/5 | 2+1xns/5 |
| 51798   | Q5M8P6           | Enoyl coenzyme A hydratase 1                              | 36.4     | 8.81 | 40     | 2.19 | 2+2xns/5 | 3+1xns/4 |
| 11668   | AAH54386         | Aldehyd dehydrogenase 1                                   | 54.9     | 4.91 | 27     | 4.41 | 3/5      | 2/4      |
| 110826  | BAB22076         | Electron transferring flavoprotein. beta polypeptide      | 27.5     | 9.47 | 45     | 1.72 | 2+2xns/5 | 1+2xns/4 |
| 21991   | TPIS_MOUSE       | Triosephosphate isomerase                                 | 26.9     | 7.80 | 48     | 1.83 | 2/5      | 2+2xns/5 |
| 18477   | A48513           | Peroxiredoxin 1   | 22.4     | 9.19 | 50     | 2.24 | 2+1xns/4 | 1+2xns/4 |
| 20655   | SODC_MOUSE       | Superoxide dismutase [Cu-Zn]                              | 15.9     | 6.40 | 39     | 2.79 | 1+2xns/5 | 2+3xns/5 |
| 12359   | CATA_MOUSE       | Catalase*   | 59.9     | 8.53 | 36     | 1.73 | 2+2xns/5 | 1+2xns/5 |
| 12716   | S24612           | Creatine kinase*  | 47.4     | 9.28 | 36     | 2.45 | 4/5      | 2xns/4   |

### 4.1.1.3 Protein expression profiling of the WT-comparison: effects of iron on the epithelial cell proteome under normal conditions of non-susceptible mice

We investigated the epithelial cell proteome from the 5 single iron-adequately fed WT mice with the 5 single iron-deficiently fed WT mice. We identified 5 down-regulated proteins (Table 7) including valosin containing protein, glutamate dehydrogenase, isocitrate dehydrogenase 1, acyl-CoA dehydrogenase and aconitase 2. Most of these proteins are involved in energy metabolism which may reflect lower energy levels under the condition of ID. Interestingly, aconitase 2 contains a  $Fe_4S_4$ -cluster in the active center and was hence identified as down-regulated in the WT and in the ARE-comparison under the iron-deficient diet responding to the low-iron diet.

**Table 7. WT-comparison: differentially regulated proteins in IEC from iron-deficiently fed WT mice compared to iron-adequately fed WT mice**

| Gene ID | Accession Number | Name of Protein                               | MM (kDa) | pI   | SC (%) | RF    | F (WT)   | F (WT Fe ↓) |
|---------|------------------|---|----------|------|--------|-------|----------|-------------|
| 269523  | Q8BSR6           | Valosin containing protein                    | 90.0     | 4.97 | 38     | -2.44 | 3/4      | 3/5         |
| 14661   | S16239           | Glutamate dehydrogenase precursor             | 61.6     | 8.84 | 48     | -2.33 | 3/4      | 3/5         |
| 15926   | Q8C338           | Isocitrate dehydrogenase 1 (NADP+), soluble   | 47.0     | 6.88 | 53     | -2.22 | 4+1xns/5 | 2/4         |
| 11409   | I49605           | Acyl-CoA dehydrogenase precursor, short chain | 45.2     | 9.66 | 40     | -2.04 | 2+xns/5  | 3+1xns/5    |
| 11429   | Q505P4           | Aconitase 2                                   | 86.2     | 8.92 | 44     | -2.50 | 3/4      | 1/5         |

#### 4.1.1.4 Protein expression profiling of the def WT-ARE-comparison: effects of iron on the epithelial cell proteome under non-inflamed but disease susceptible conditions

To complete all possible comparison between the 4 different groups, we performed proteome analysis for the comparison of the 5 iron-deficiently fed WT and the 5 non-inflamed, iron-deficiently fed  $TNF^{\Delta ARE/WT}$  mice. We identified 24 exclusively up-regulated proteins (Table 8) and investigated biological activity and biological function. Sixty-three % of the proteins have catalytic activity in specific oxidoreductase or lyase activity, 75% with binding activity predominantly for ion and protein binding. Interestingly, as up-regulated identified galectin 2 was shown to induce apoptosis in activated T-cells in vivo ameliorating acute and chronic murine colitis [186] suggesting also an effect on chronic ileitis.

**Table 8. def WT-ARE-comparison: differentially regulated proteins in IEC from iron-deficiently fed  $TNF^{\Delta ARE/WT}$  mice compared to iron-deficiently fed WT mice**

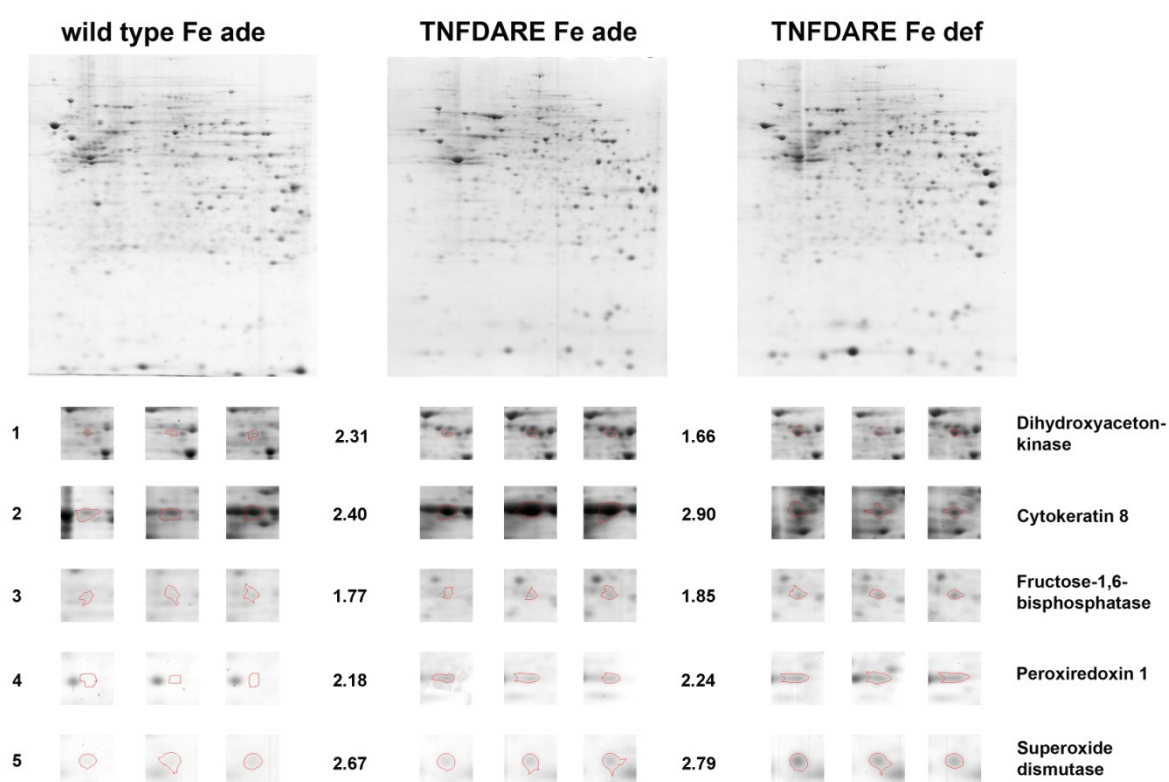
| Gene ID        | Accession Number | Name of Protein                         | MM (kDa)     | pI   | SC (%) | RF   | F (WT) | F (ARE) |
|----------------|------------------|---|--------------|------|--------|------|--------|---------|
| 11931          | P56480           | ATP synthase subunit beta               | 56.3         | 5.07 | 30     | 2.17 | 2/4    | 3/5     |
| 11461<br>11465 | Q61276<br>Q9QZ83 | Actin beta<br>Actin gamma               | 42.1<br>42.1 | 5.20 | 21     | 4.79 | 0/4    | 5/5     |
| 14121          | Q9QXD6           | Fructose 1,6-bisphosphatase isoenzyme 2 | 37.2         | 5.80 | 30     | 2.66 | 0/4    | 4/5     |
| 19186          | Q9D841           | Proteasome activator complex            | 28.8         | 5.70 | 49     | 1.84 | 2/4    | 5/5     |

## RESULTS

| Gene ID | Accession Number | Name of Protein                          | MM (kDa) | pI    | SC (%) | RF   | F (WT)   | F (ARE)  |
|---------|------------------|--|----------|-------|--------|------|----------|----------|
| 16796   | Q61792           | LIM / SH3 domain protein 1               | 30.4     | 6.70  | 32     | 3.21 | 0/4      | 2+1xns/5 |
| 12462   | P80318           | TCP-1 gamma                              | 61.2     | 6.30  | 17     | 3.34 | 0/4      | 3+1xns/5 |
| 230163  | ALDOB_MOUSE      | Fructose bisphosphate aldolase B         | 39.9     | 10.40 | 24     | 2.56 | 1/4      | 4/5      |
| 22349   | Q62468           | Villin 1                                 | 93.3     | 5.70  | 24     | 2.65 | 0/4      | 4/5      |
| 72692   | Q921F4           | Heterogeneous nuclear ribonuclear L      | 60.7     | 6.70  | 26     | 2.37 | 2/4      | 5/5      |
| 20867   | Q60864           | Stress induced phosphoprotein            | 63.2     | 6.40  | 16     | 2.34 | 2+1xns/4 | 3+1xns/5 |
| 28000   | Q99KP6           | Pre-mRNA processing factor               | 55.7     | 6.10  | 17     | 1.86 | 1/4      | 2+2xns/5 |
| 109264  | Q8BMF3           | NADP-dependent malic enzyme              | 64.6     | 7.80  | 32     | 2.87 | 0/4      | 5/5      |
| 12359   | CATA_MOUSE       | Catalase                                 | 60.0     | 8.60  | 29     | 1.82 | 4/4      | 4/5      |
| 15926   | Q8C338           | Isocitrate dehydrogenase cytoplasmic     | 47.0     | 6.50  | 50     | 2.42 | 0/4      | 3/5      |
| 23983   | P60335           | Poly(rC)-binding protein 1               | 38.0     | 6.80  | 42     | 2.16 | 1/4      | 2/5      |
| 171210  | Q9QYR9           | Acyl-coenzyme A thioesterase 2           | 49.9     | 7.10  | 29     | 2.26 | 0/4      | 4/5      |
| 26897   | O55137           | Acyl-coenzyme A thioesterase 1           | 46.3     | 6.12  | 21     |      |          |          |
| 20322   | Q64442           | Sorbitol dehydrogenase                   | 40.6     | 6.60  | 37     | 2.48 | 2/4      | 4/5      |
| 14555   | P13707           | Glyceraldehyde-3-phosphate dehydrogenase | 36.1     | 9.20  | 43     | 4.09 | 2/4      | 2/5      |
| 14873   | O09131           | Glutathione transferase omega            | 27.7     | 7.70  | 28     | 1.75 | 4/4      | 2/5      |
| 18648   | PGAM1_MOUSE      | Phosphoglycerate mutase 1                | 28.9     | 6.80  | 56     | 2.19 | 2/4      | 5/5      |
| 268373  | P62938           | Peptidyl-prolyl cis-trans isomerase      | 18.1     | 9.10  | 37     | 1.58 | 3/4      | 4/5      |
| 107753  | Q9CQW5           | Galectin-2                               | 15.0     | 7.90  | 62     | 2.64 | 3/4      | 3+1xns/5 |
| 21351   | Q93092           | Transaldolase                            | 37.5     | 6.70  | 23     | 2.18 | 3/4      | 3+1xns/5 |
| 27384   | Q8VC28           | Aldo-keto reductase                      | 37.6     | 6.80  | 26     | 1.54 | 3/4      | 5/5      |

### 4.1.2 Focus on the overlap of regulated proteins between the ade WT-ARE-comparison and ARE-comparison

Covering the significant differentially regulated proteins from the comparison between ade WT-ARE-comparison (reflects the protein changes under condition of inflammation) and the proteins of the ARE-comparison (inhibition of inflammation by the iron-deficient diet), we found an overlap of 9 proteins. Figure 12 shows representative gels from the different groups (big gels) and the regulated protein spots (small cut outs) for the 5 in both comparison up-regulated proteins including dihydroxyacetone kinase (Dak), cytokeratin 8, fructose-1.6-bisphosphatase, peroxiredoxin-1 and superoxide dismutase.



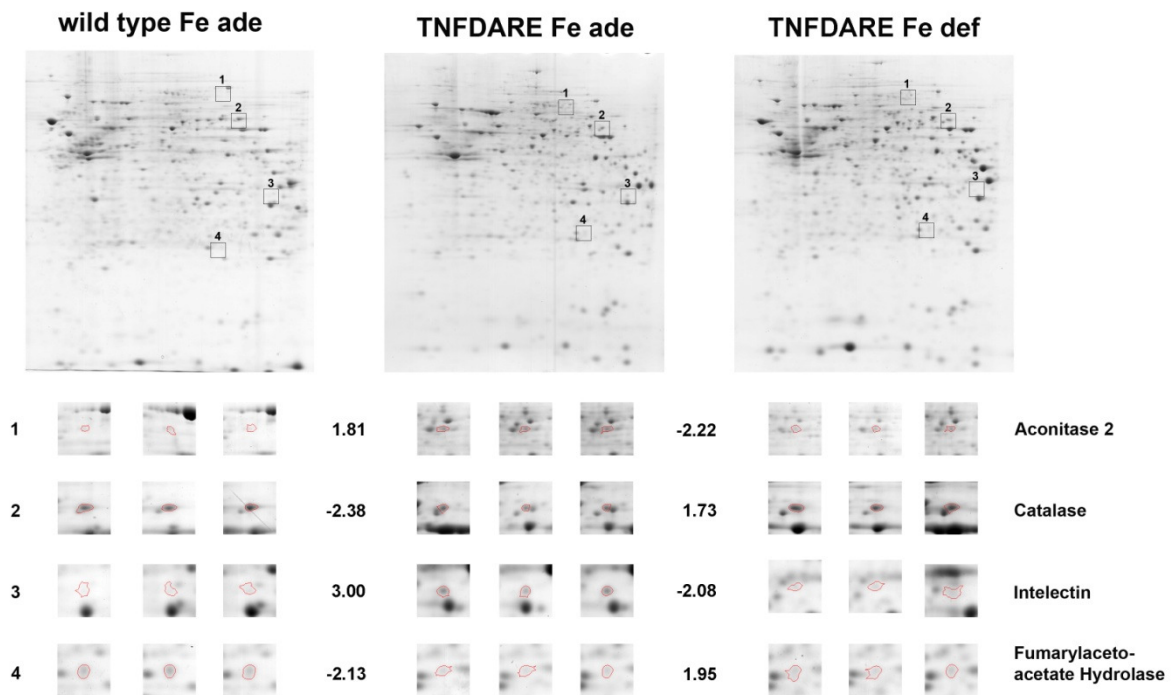


**Figure 12. Representative Coomassie stained 2D-gels from the overlap between the adequate WT-ARE comparison and the ARE-comparison with similar regulated proteins (upper picture) and contrarily regulated proteins (lower picture).** Native IEC were isolated and purified from small intestine of iron-adequately fed WT and iron-adequately or iron-deficiently fed TNF<sup>ΔARE/WT</sup> mice. 250 μg of total protein was subjected to IEF and 2D-SDS-PAGE. Gels were stained with Coomassie Blue and analyzed by Proteomweaver software. Indicated protein spots were picked and analyzed by MALDI-TOF-MS as described in Materials and Methods. Reference gel from mice (big gel) and the corresponding regions from IEC of single mice (small cut outs) are shown. Given Numbers are the regulation factors between the compared groups.

Interestingly, the 4 remaining proteins are contrary regulated between the 2 comparisons suggesting an effective role in the regulation of intestinal inflammation. Aconitase 2 and intelectin 1 are up-regulated in the ade WT-ARE-comparison and down-regulated in the ARE-comparison whereas Catalase and Fumarylacetoacetate hydrolase (FAH) are down-regulated in the ade WT-ARE-comparison and up-regulated in the ARE-comparison (Figure 12). These 4 proteins are involved in energy metabolism, host defense, oxidative stress and ER stress response whereas all of these mechanisms are associated with chronic intestinal inflammation.

The down-regulation of major anti-oxidative enzymes like catalase suggests disturbances in the maintenance of anti-oxidative defense mechanisms under the conditions of chronic inflammation. Additionally, the up-regulation of intelectin 1 under the condition of chronic inflammation in the ade WT-ARE-comparison and down-regulated under non-inflamed conditions in the ARE-comparison may imply a direct regulation by the iron diet as well as down-regulation of host defense mechanisms. We verified the proteome results for catalase and intelectin 1 by Western blot analysis (Figure 13) using antiserum for mouse intelectin 1.

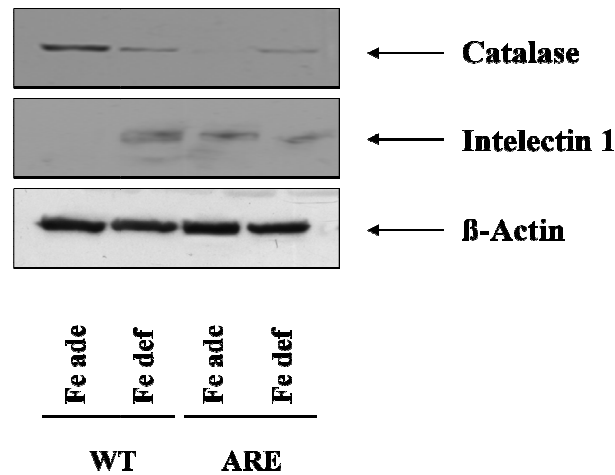


**Figure 13. Verification of proteome results for catalase and intelectin 1.** Western blot analysis was performed with 25  $\mu$ g total protein derived from pooled IEC samples from 5 iron-adequately (Fe ade) or iron-deficiently fed (Fe def) WT and 5 iron-adequately or iron-deficiently fed  $\text{TNF}^{\text{ARE/WT}}$  mice, respectively, using immunoreactive catalase and  $\beta$ -actin as well as intelectin antiserum.

#### 4.1.3 Bibliometric analysis of differentially regulated proteins from the ade WT-ARE- and the ARE-comparison

On the basis of literature co-citation from NCBI Pubmed, we generated a protein-protein network tree using the data mining program Bibliosphere software (Genomatix Software, Munich, Germany). Co-citations are based on abstract-level. As shown in Figure 14, the network tree was compiled of 41 highly interrelated proteins from the ade WT-ARE- and the ARE-comparison to access the relations of proteins regulated under the condition and absence of inflammation. Additional 10 proteins remain unconnected to the large network tree (*Acadvl*; *Ckmt1*; *Dak*; *Ech1*; *Eftb*; *Fbp2*; *Pmm2*; *Shmt2*; *Snd1*; *Tpm2*). Abbreviations are given in Table 9.

In all comparisons, we identified 74 differentially regulated proteins whereas 56 are included in the Bibliosphere analysis. Twenty-five % (14 of 56 proteins) of these regulated proteins belong to the mitochondria and 20% (11 of 56 proteins) are involved in catabolic processes for energy production implicating energy homeostasis as an important factor for the regulation of cell homeostasis under the conditions of inflammation. Interestingly, 11 of these 14 mitochondrial proteins are mostly up-regulated in the ARE-comparisons in the absence of inflammation by the iron-deficient diet suggesting this as a possible mechanism to recover normal energy levels in the epithelium.

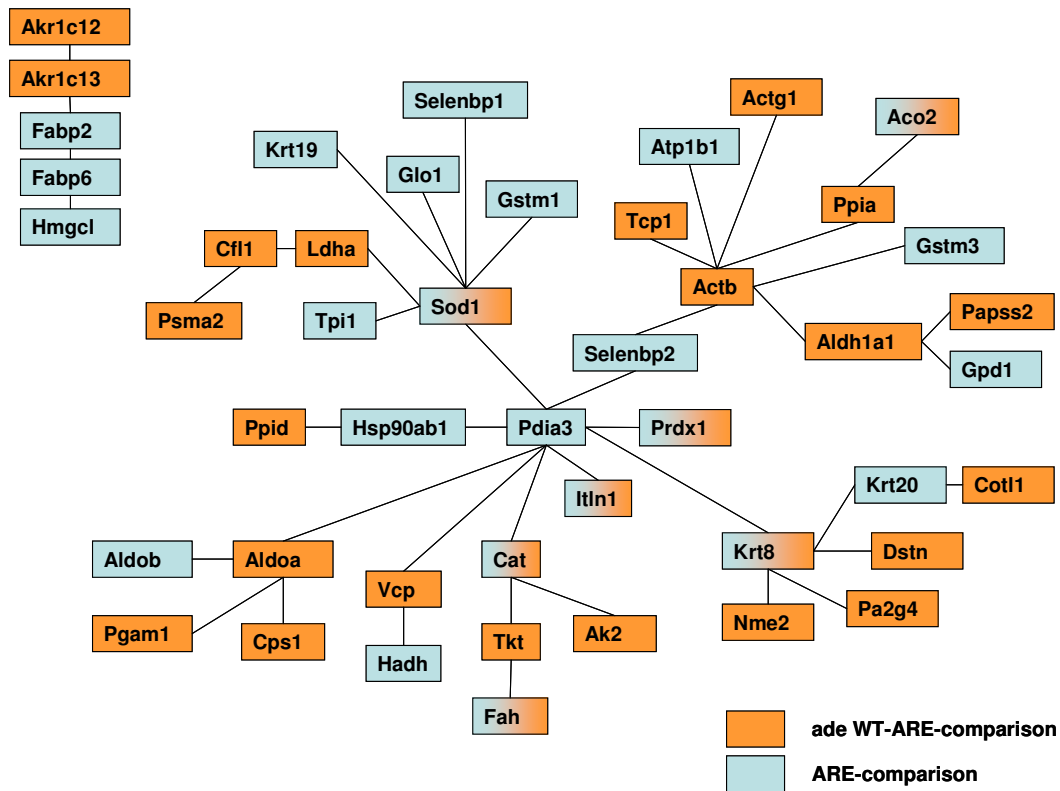


**Figure 14. Bibliometric data analysis of ade WT-ARE-comparison and ARE-comparison.** Bibliometric analysis was performed on the base of literature co-citation from NCBI Pubmed. The data-mining program Bibliosphere software (Genomatix) was used to generate protein-protein network trees from the overlap of the ade WT-ARE-comparison (orange boxes) and the ARE-comparison (blue boxes).

## RESULTS

**Table 9. Abbreviations for Bibliometric data analysis (Figure 14)**

| gene symbol | gene name  | gene symbol | gene name  | gene symbol | gene name   |
|-------------|--|-------------|--|-------------|---|
| Acadvl      | acyl-Coenzyme A dehydrogenase, very long chain                           | Ech1        | enoyl coenzyme A hydratase 1, peroxisomal                    | Ppia        | peptidylprolyl isomerase A                            |
| Ak2         | adenylate kinase 2   | Fabp2       | fatty acid binding protein 2, intestinal                     | Psma2       | proteasome (prosome, macropain) subunit, alpha type 2 |
| Actg1       | actin, gamma, cytoplasmic 1  | Fabp6       | fatty acid binding protein 6, ileal (gastrotropin)           | Prdx1       | peroxiredoxin 1                                       |
| Aldob       | aldolase 2, B isoform  | Fah         | fumarylacetoacetate hydrolase                                | Ppid        | peptidylprolyl isomerase D (cyclophilin D)            |
| Atp1b1      | ATPase, Na <sup>+</sup> /K <sup>+</sup> transporting, beta 1 polypeptide | Fbp2        | fructose bisphosphatase 2                                    | Pdia3       | protein disulfide isomerase associated 3              |
| Akr1c12     | aldo-keto reductase family 1, member C12                                 | Glo1        | glyoxalase 1   | Pgam1       | phosphoglycerate mutase 1                             |
| Aldh1a1     | aldehyde dehydrogenase family 1, subfamily A1                            | Gpd1        | glycerol-3-phosphate dehydrogenase 1 (soluble)               | Pmm2        | phosphomannomutase 2                                  |
| Aldoa       | aldolase 1, A isoform  | Gstm3       | glutathione S-transferase, mu 3                              | Selenbp2    | selenium binding protein 2                            |
| Akr1c13     | aldo-keto reductase family 1, member C13                                 | Gstm1       | glutathione S-transferase, mu 1                              | Selenbp1    | selenium binding protein 1                            |
| Actb        | actin, beta, cytoplasmic   | Hmgcl       | 3-hydroxy-3-methylglutaryl-Coenzyme A lyase                  | Snd1        | staphylococcal nuclease and tudor domain containing 1 |
| Aco2        | aconitase 2, mitochondrial   | Hadh        | hydroxyacyl-Coenzyme A dehydrogenase                         | Sod1        | superoxide dismutase 1, soluble                       |
| Cotl1       | coactosin-like 1 (Dictyostelium)   | Hsp90ab1    | heat shock protein 90kDa alpha (cytosolic), class B member 1 | Shmt2       | serine hydroxymethyltransferase 2 (mitochondrial)     |
| Cat         | catalase   | Itln1       | intelectin 1 (galactofuranose binding)                       | Tkt         | transketolase   |
| Cps1        | carbamoyl-phosphate synthetase 1   | Krt8        | keratin 8  | Tpm2        | tropomyosin 2, beta                                   |
| Ckmt1       | creatine kinase, mitochondrial 1, ubiquitous                             | Krt19       | keratin 19   | Tcp1        | t-complex protein 1                                   |
| Cfl1        | cofilin 1, non-muscle  | Krt20       | keratin 20   | Tpi1        | triosephosphate isomerase 1                           |
| Ldha        | lactate dehydrogenase A  | Nme2        | non-metastatic cells 2, protein (NM23B) expressed in         | Vcp         | valosin containing protein                            |
| Dstn        | destrin  | Papss2      | 3'-phosphoadenosine 5'-phosphosulfate synthase 2             |             |   |
| Etfb        | electron transferring flavoprotein, beta polypeptide                     | Pa2g4       | proliferation-associated 2G4                                 |             |   |

#### 4.1.4 Up-regulation of proteins involved in inflammation, cell stress responses and apoptosis by the iron-adequate diet

Since the proteome analysis revealed differentially regulated proteins involved in inflammation and stress responses, we performed Western blot analysis for verification. We detected phosphorylation of RelA, proofing the activation of NF- $\kappa$ B and supporting histological results. Furthermore, severely inflamed, iron-adequately fed mice showed enhanced expression for proteins involved in ER stress pathways including up-regulated grp-78 expression, phosphorylation of eiF2 $\alpha$  as well as enhanced expression of the valosin containing protein (VCP) as part of the ER-associated degradation (ERAD) complex (Figure 15). The induction of HIF-1 $\alpha$  may be due to the activation of the ER stress-associated PERK pathway which could result in the activation of target genes like HIFs to induce oxidative defense mechanisms. Whereas TNF is able to down-regulate HO-1 expression in peripheral blood mononuclear cells derived from rheumatoid arthritis patients [187], TNF might also be able to down-regulate HO-1 expression in IEC in an animal model developing polyarthritis. In addition to the induction of ER stress response mechanisms, we detected enhanced protein expression of apoptosis-related cleaved caspase 3 (cc3) in severely inflamed, iron-adequately fed TNF<sup>ARE/WT</sup> mice. Clearly contrasting, the iron-deficiently fed TNF<sup>ARE/WT</sup> mice showed absence of inflammation, oxidative and ER stress responses as well as apoptosis in IEC.

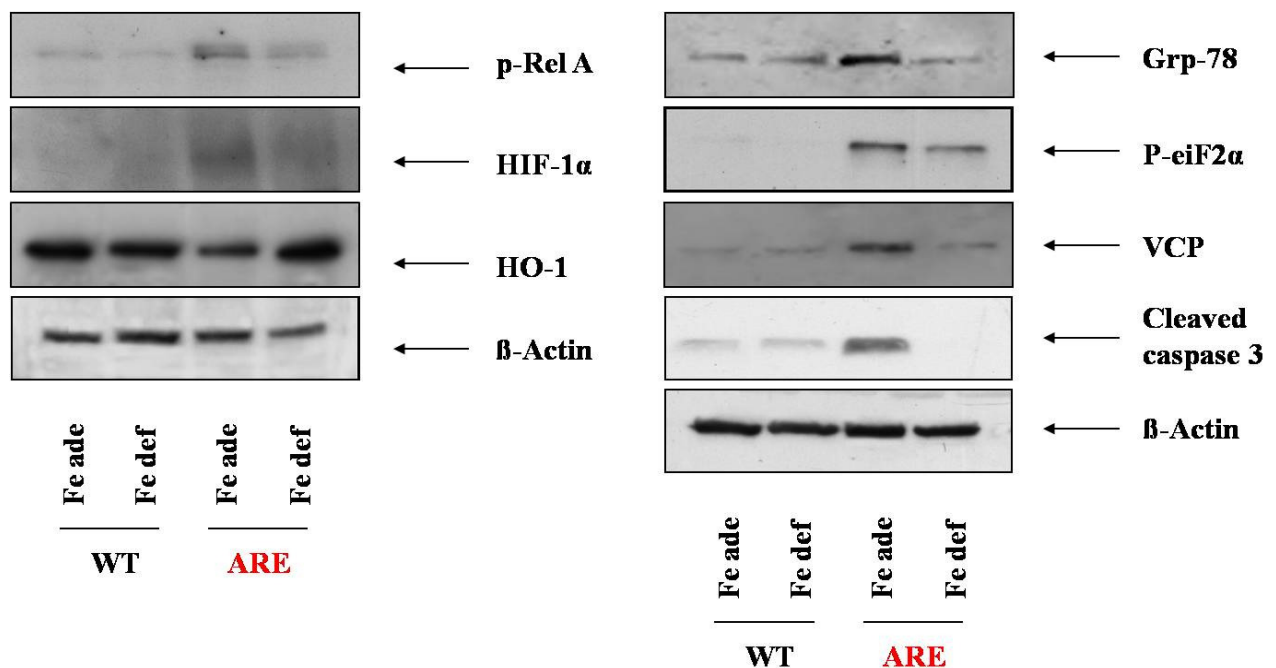


**Figure 15. Enhanced expression of proteins involved in inflammation, oxidative and ER-stress as well as apoptosis by the iron-adequate diet.** Western blot analysis was performed with 25  $\mu$ g total protein derived from pooled IEC samples from 5 iron-adequately (Fe ade) or iron-deficiently fed (Fe def) WT or TNF<sup>ARE/WT</sup> mice, respectively, using immunoreactive p-RelA, HIF-1 $\alpha$ , HO-1, grp-78, p-eiF2 $\alpha$ , VCP, cc3 and  $\beta$ -actin.

## RESULTS

---

Prolonged or unresolved ER stress may lead to apoptosis in the intestinal epithelium. We performed immunofluorescence staining for grp-78 as well as TUNEL-staining for pro-apoptotic processes to visualize Western blot results. Grp-78 immunohistochemical labelling of paraffin-embedded distal ileal sections of inflamed, iron-adequately fed TNF<sup>ΔARE/WT</sup> mice revealed tremendous expression of this major ER-chaperone (brown colour) (Figure 16, upper picture). To visualize cell death, we performed TUNEL staining by labelling fragmented DNA, a characteristic sign of apoptotic cells. Appearance of brown coloured cells in distal ileal sections illustrated massive cell death in the iron-adequately fed TNF<sup>ΔARE/WT</sup> mice. The grp-78 and TUNEL labelled tissue sections showed induction of ER stress and apoptosis (white arrows) particularly in crypt regions (Figure 16). This observation was absent in the iron-deficiently fed TNF<sup>ΔARE/WT</sup> group.

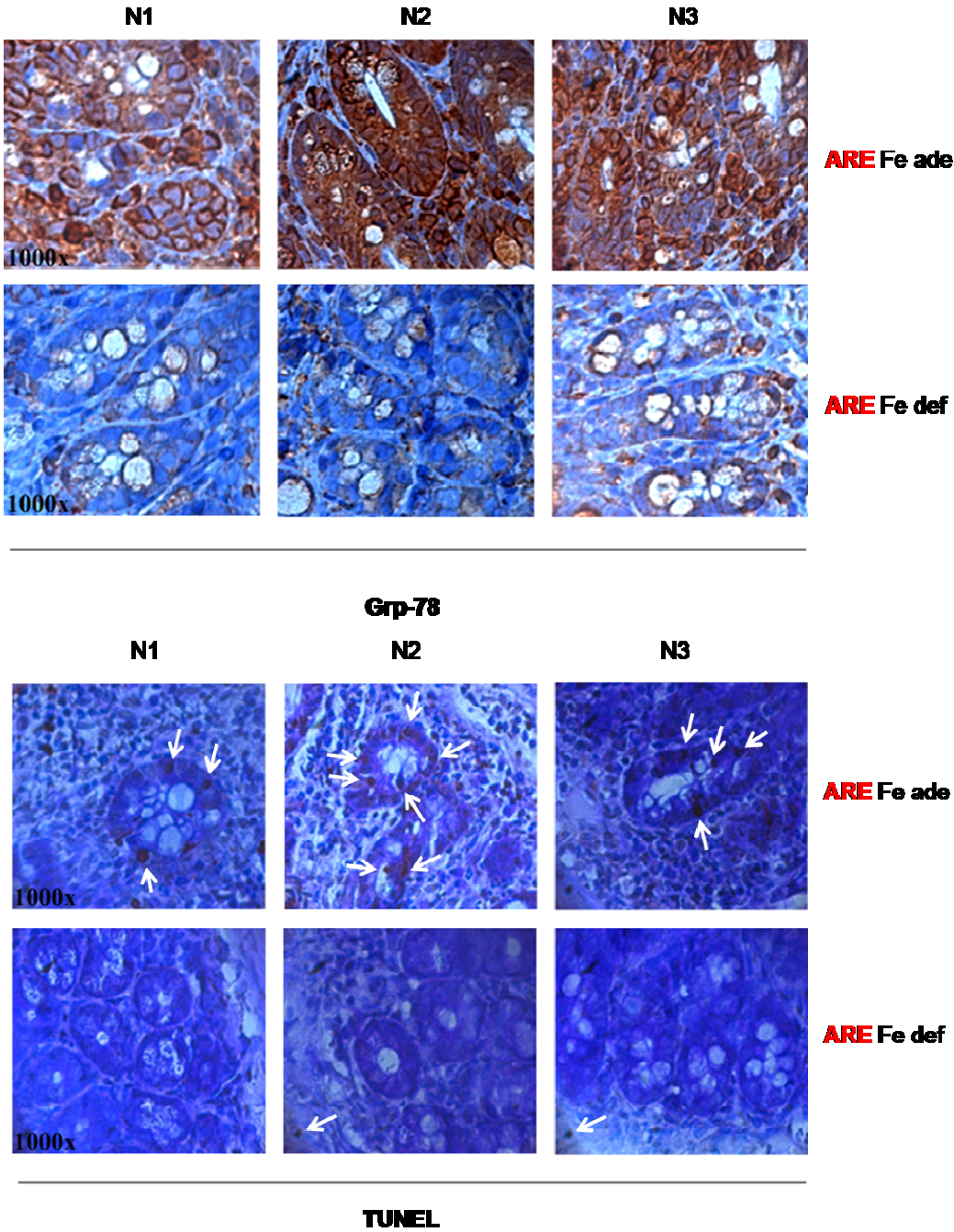
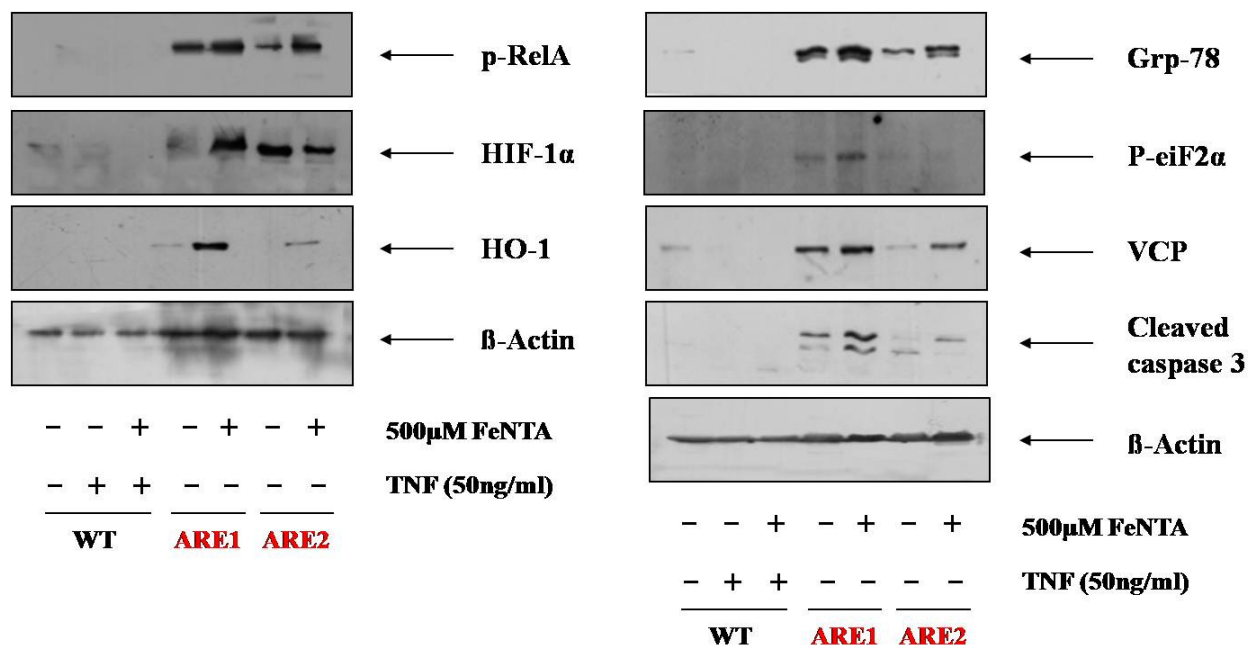


Figure 16. Grp-78 immuno- and TUNEL-staining of distal ileum segments of  $TNF^{\Delta ARE/WT}$  mice. Immunohistochemical analysis of *grp-78* expression (upper picture) and TUNEL staining (lower picture, white arrows) in paraffin-embedded ileal tissue segments visualising appearance especially in crypt regions.

#### 4.1.5 Iron-mediated up-regulation of proteins involved in inflammation, cell stress responses and apoptosis *ex vivo* and *in vitro*

Since the iron-deficient diet inhibited intestinal inflammation and the proteome as well as the Western blot analysis clearly revealed the involvement of proteins participating in different cell stress pathways, we investigated the specific effect of iron on protein expression in additional performed organ and cell culture experiments. Distal ileum segments of WT and TNF<sup>ΔARE/WT</sup> mice were cultivated for 24 hours in the presence or absence of 500μM FeNTA and/or TNF (50ng/ml) in the medium. Western blot analysis revealed phosphorylation of pro-inflammatory RelA after iron stimulation. Furthermore, the iron stimulation lead to enhanced expression of oxidative stress-related (HIF-1α, HO-1) and ER stress-related proteins (grp-78, p-eiF2α, VCP) as well as pro-apoptotic processes (cc3) in TNF<sup>ΔARE/WT</sup> mice but not WT mice (Figure 17).



**Figure 17. Iron-mediated induction of pro-inflammatory, oxidative and ER stress as well as pro-apoptotic protein expression in total tissue.** Western blot analysis was performed with 25 μg total protein derived from total tissue of distal ileum from WT and TNF<sup>ΔARE/WT</sup> mice (24h cultivation) with or without 500μM FeNTA in the medium, using immunoreactive p-RelA, HIF-1α, HO-1(left panel) and grp-78, p-eiF2α, VCP, cc3 as well as β-actin (right panel).

To elucidate the effects of iron in specific on IEC, we performed additional iron stimulation experiments in the murine small IEC line Mode-K. The iron stimulation (500μM FeNTA) triggered fast induction (1h) of pro-inflammatory p-Rel A, HIF-1α and HO-1 as well as ER stress-associated grp-78, p-eiF2α and VCP. At the late time point (3h) iron stimulation causes induction of pro-apoptotic cc3 (Figure 18).

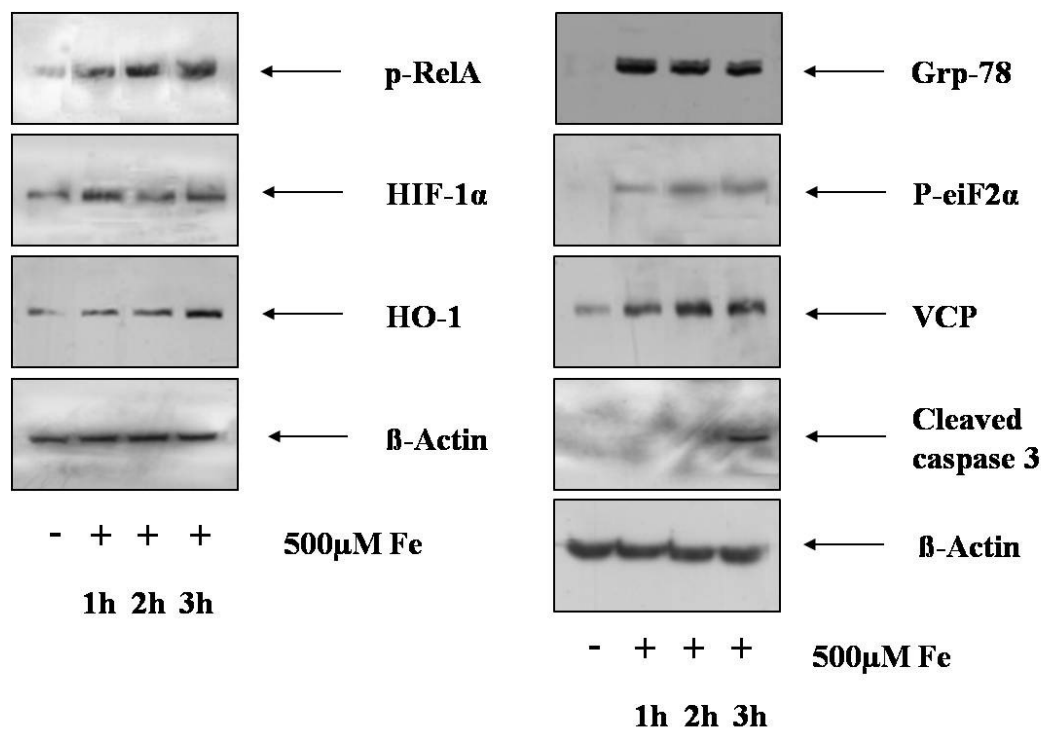


**Figure 18. Iron-mediated induction of pro-inflammatory, oxidative and ER stress as well as pro-apoptotic protein expression in Mode-K cells.** Western blot analysis was performed with 25  $\mu$ g total protein derived from Mode-K cells with or without 500 $\mu$ M FeNTA for 1, 2 and 3 hours in the medium, using immunoreactive p-RelA, HIF-1 $\alpha$ , HO-1(left panel) and grp-78, p-eiF2 $\alpha$ , VCP, cc3 as well as  $\beta$ -actin (right panel).

Iron stimulation (500 $\mu$ M FeNTA) of Mode-K cells lead to a 19-fold increase of HO-1 mRNA expression after 3h of stimulation and a 6.5-fold increase of grp-78 mRNA expression after 6h of stimulation (data not shown). HIF-1 $\alpha$ , p-RelA, p-eiF2 $\alpha$  and cc3 mRNA expression could not be performed because of posttranscriptional and posttranslational regulation.

Since oxidative stress is a known trigger for ER stress response signalling, we investigated the involvement of ROS in iron-induced ER stress. Therefore, Mode-K cells were pre-incubated with the ROS-inhibitor N-acetyl-L-cysteine (NAC) for 24h where indicated and/or stimulated with 500 $\mu$ M FeNTA for 3h to measure ROS-formation. Figure 19 shows ROS induction after iron stimulation with a 50% decrease after 24h of pre-incubation with NAC in the higher concentration (5mM). Western blot analysis of grp-78 protein expression revealed no differences in presence or absence of the ROS inhibitor, suggesting partly ROS-independent iron-mediated induction of ER stress (Figure 19).

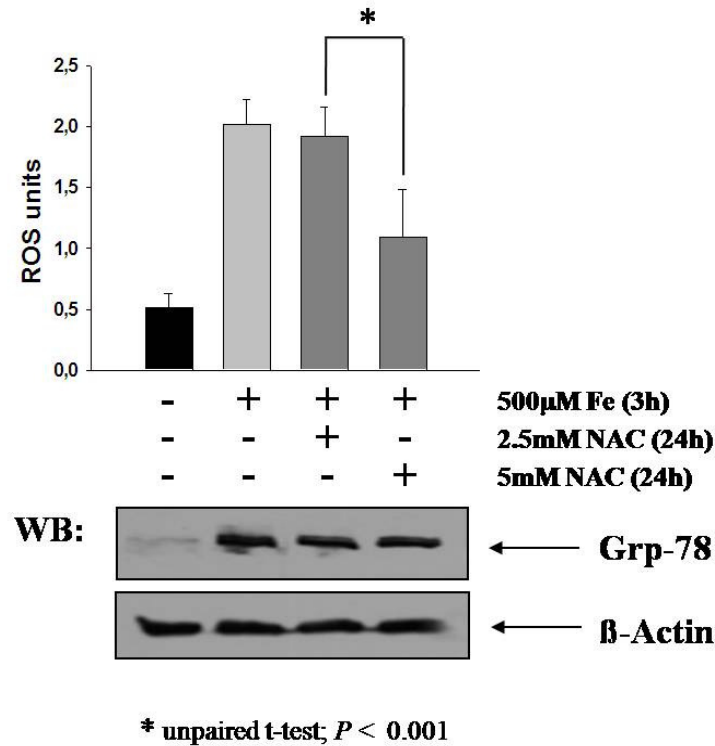


**Figure 19. Partly ROS-independent iron-mediated induction of grp-78 protein expression.** Mode-K cells were pre-incubated with the ROS-inhibitor N-acetyl-L-cysteine (NAC) in different concentrations for 24h and/or stimulated with FeNTA for 3h (bar chart). Western blot analysis of grp-78 protein expression in Mode-K cells after NAC incubation and/or iron stimulation

To further evaluate the iron-mediated ER stress response signalling, we next performed CHIP analysis for three relevant transcription factors involved in the induction of grp-78 mRNA transcription. Mode-K cells were stimulated with 500 μmol FeNTA, TNF (10ng/ml) or both to determine additive effects for 6h, followed by immunoprecipitation for NRF2, XBP-1 and ATF6. Figure 20 illustrates recruitment of NRF2 and XBP-1 but not ATF6 to the grp-78 promoter after iron stimulation. This finding clearly indicates specific iron-mediated mechanisms for the induction of ER stress responses in IEC.

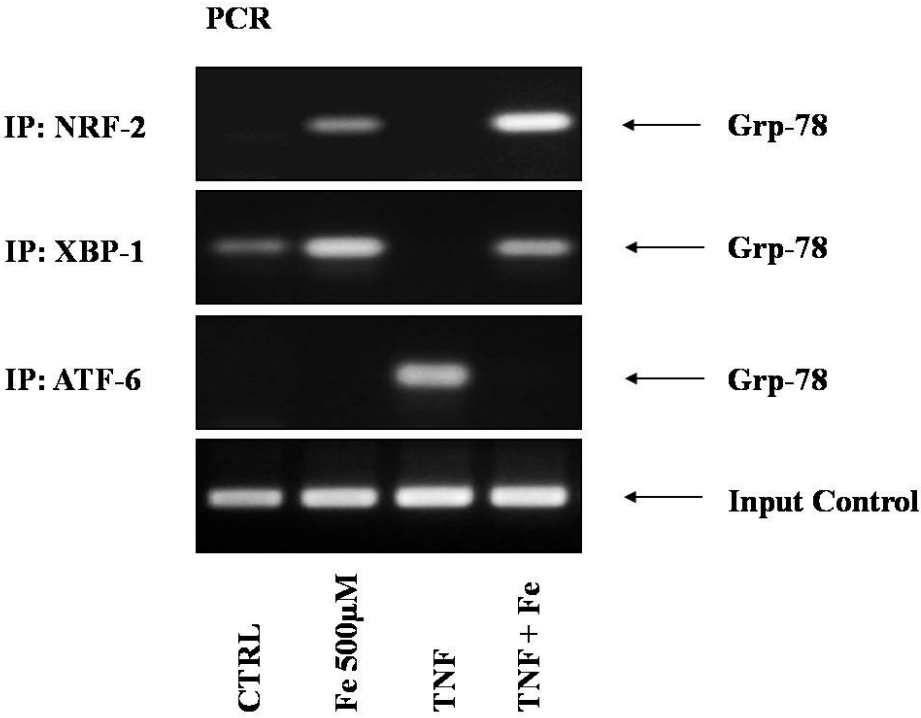


**Figure 20. ChIP analysis in Mode-K cells after iron stimulation.** Mode-K cells were stimulated with 500µM FeNTA and/or TNF (10ng/ml) for 6h. ChIP analysis revealed recruitment of transcription factors XBP-1 and NRF2, but not ATF6 to the grp-78 promoter after iron stimulation.

## 4.2 Effects of short-term reduction of dietary iron in existing ileitis

In contrast to healthy WT mice,  $TNF^{\Delta ARE/WT}$  mice showed increasing tissue pathology with age [176]. Based on the observation that the reduction of dietary iron prevents the development of experimental ileitis in the genetically susceptible host, we next investigated the effect of iron-deficient feeding on an already developed ileitis.  $TNF^{\Delta ARE/WT}$  mice (N = 5 in each group) at the age of 17 weeks were transferred from the iron-adequate diet to an iron-deficient diet for additional 4 weeks (short-term feeding experiment; Figure 21).

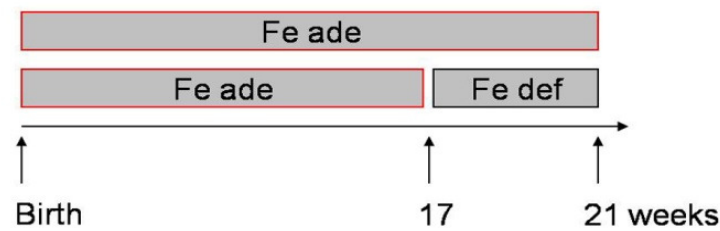


**Figure 21. Overview of short-term feeding experiment.**

Histological examination (score 0-12) of distal ileum segments revealed a significant reduction of the pathological score from  $7.15 \pm 0.38$  in the iron-adequate group to  $3.90 \pm 1.3$  in the  $TNF^{\Delta ARE/WT}$  group receiving an iron-deficient diet (Figure 22, bar chart). Representative H&E stained tissue sections from the ileum confirmed the marked reduction of infiltrating immune cells (Figure 22, pictures).

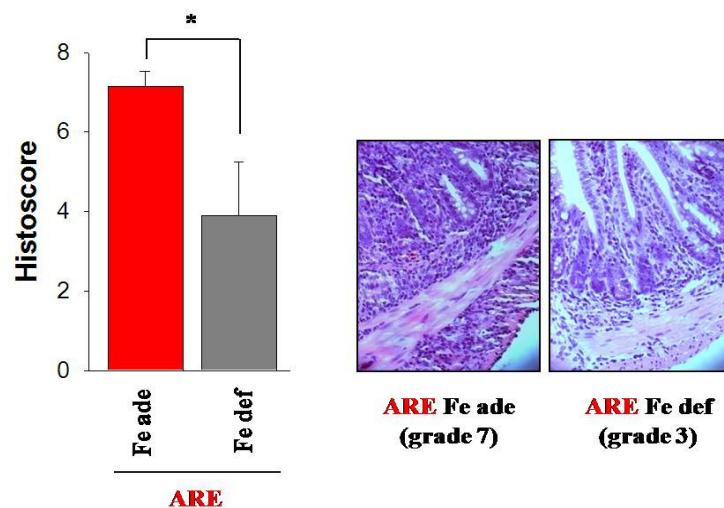


**Figure 22. Histology of the short-term feeding experiment.** Histological analysis of iron-adequately or iron-deficiently fed  $TNF^{\Delta ARE/WT}$  mice (bar chart) and representative H&E-staining of ileal segments from both  $TNF^{\Delta ARE/WT}$  groups (pictures).

Short-term feeding of an iron-deficient diet did not significantly alter hepatic iron storage (Fe ade:  $80.19 \pm 9.38$ ; Fe def:  $53.33 \pm 22.86$ ).

### 4.3 Effects of systemic iron repletion on chronic ileitis: focus on the epithelium

The inhibition of ileitis by a reduction of dietary iron provides therapeutic options for the treatment of CD, but may lead to the development of anemia. Systemic iron repletion in IBD patient with iron-deficiency anemia is an accepted therapeutic approach. To further evaluate the role of iron after systemic application, we next treated iron-deficiently fed  $TNF^{\Delta ARE/WT}$  mice with weekly intraperitoneal injections of 90 $\mu$ mol FeNTA solutions (iron-injection/iron-repletion) parallel to the respective control groups applying 0.9% sodium chloride (NaCL) solution as sham-injections (injection experiment; Figure 23). Calculated on the basis of iron bioavailability, we first assessed an initial dose finding study for the systemic iron application. Due to known toxic effects at higher concentrations, the amount of 90 $\mu$ mol FeNTA was chosen for further experiments.



**Figure 23. Overview of injection experiment.**

The weekly applied injections were adjusted to body weight, starting at the age of 7 weeks. Histological examination (score 0-12) of the distal ileum showed the absence of inflammation (Figure 24) in the iron-deficiently fed, sham-injected  $TNF^{\Delta ARE/WT}$  group ( $1.54 \pm 0.25$ ) as well as in the iron-deficiently fed, iron-repleted  $TNF^{\Delta ARE/WT}$  group ( $1.67 \pm 0.20$ ). This was in complete contrast to severely inflamed iron-adequately fed, sham-injected  $TNF^{\Delta ARE/WT}$  mice ( $7.00 \pm 0.63$ ), clearly demonstrating a critical role for dietary but not parenteral iron in the development of chronic ileitis. Representative tissue sections illustrate the degree of inflammation in the three treatment groups with the special emphasis on the marked reduction of infiltrating immune cells and a normal villus-crypt-structure in the iron-deficiently fed as well as iron-repleted group (Figure 24).

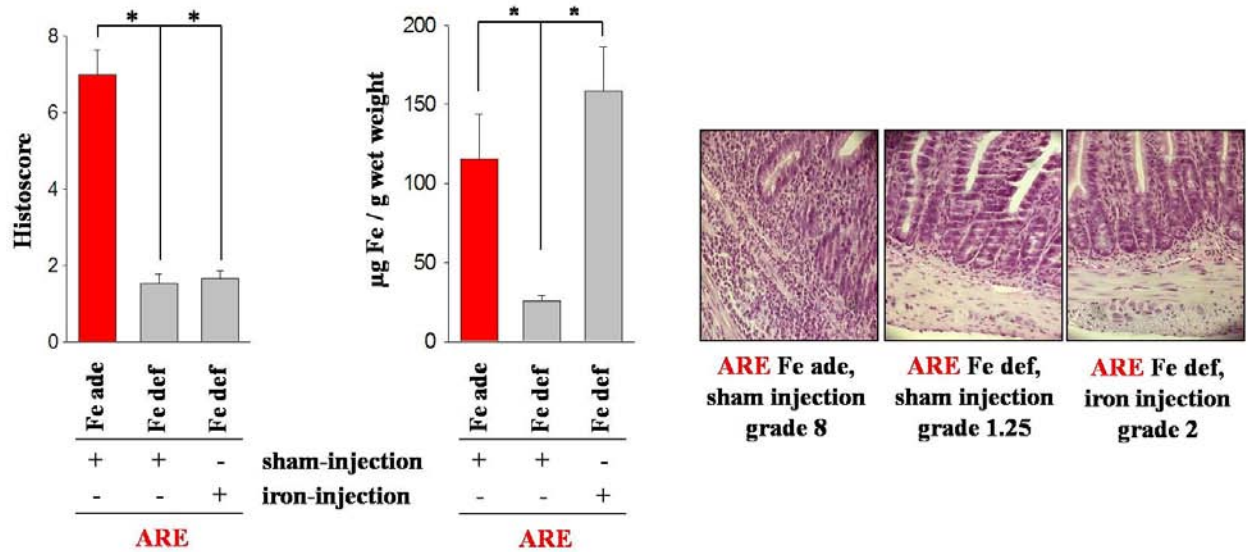


**Figure 24. Histology and hepatic non-heme measurement of the injection experiment.** Histological analysis of iron-adequately or iron-deficiently fed  $TNF^{\Delta ARE/WT}$  mice which received weekly applied sham- or iron injections, respectively (bar chart) and representative H&E-staining of ileal segments from all  $TNF^{\Delta ARE/WT}$  treatment groups (pictures). Non-heme iron content were photometrically determined in liver section of iron-adequately or iron-deficiently fed  $TNF^{\Delta ARE/WT}$  mice which received weekly applied sham- or iron-injections.

As also shown in Figure 24, iron-repletion of iron-deficiently fed mice with  $90\mu\text{mol FeNTA}$  ( $158.61 \pm 27.36$ ) was completely sufficient to restore hepatic non-heme iron content compared to level of the iron-adequate diet ( $115.55 \pm 28.04$ ). Consistent with the previous experiments by Schümann et al., the iron-deficiently fed, sham-injected  $TNF^{\Delta ARE/WT}$  mice revealed significantly reduced hepatic non-heme iron content ( $25.82 \pm 3.43$ ).

#### 4.3.1 Iron repletion maintained down-regulated ER stress and apoptosis-associated protein expression in IEC

To evaluate the role of systemic iron on ER stress responses in IEC, Western blot analysis was performed with  $25\mu\text{g}$  total protein derived from pooled IEC samples from iron-adequately fed, sham-injected, iron-deficiently fed, sham-injected as well as iron-deficiently fed, iron-injected  $TNF^{\Delta ARE/WT}$  mice, respectively. Purity of IEC isolation was confirmed by the absence of  $CD3^+$  T-cell contamination (Figure 25, left panel). Protein expression levels of  $\text{grp-78}$ ,  $\text{p-eiF2}\alpha$ ,  $\text{VCP}$  and  $\text{cc3}$  showed absence of ER stress and apoptosis in iron-deficiently fed  $TNF^{\Delta ARE/WT}$  mice compared to iron-adequately fed  $TNF^{\Delta ARE/WT}$  mice (Figure 25, right panel) confirming Western blot results from the feeding experiment. Most importantly, the iron-repletion maintained the down-regulation of ER stress responses in ileal IEC. The slight regain of apoptosis in the iron-repleted group might be explainable by the up-regulation of the TfR. The TfR is responsible for the basolateral iron up-take. As we were able to show that iron is a strong inducer of ER stress and apoptosis in IEC, the up-regulation of the

TfR in the repleted group may lead to enhanced iron levels in IEC than in the iron-deficiently fed, sham-injected group and therefore to a slight induction of apoptosis.

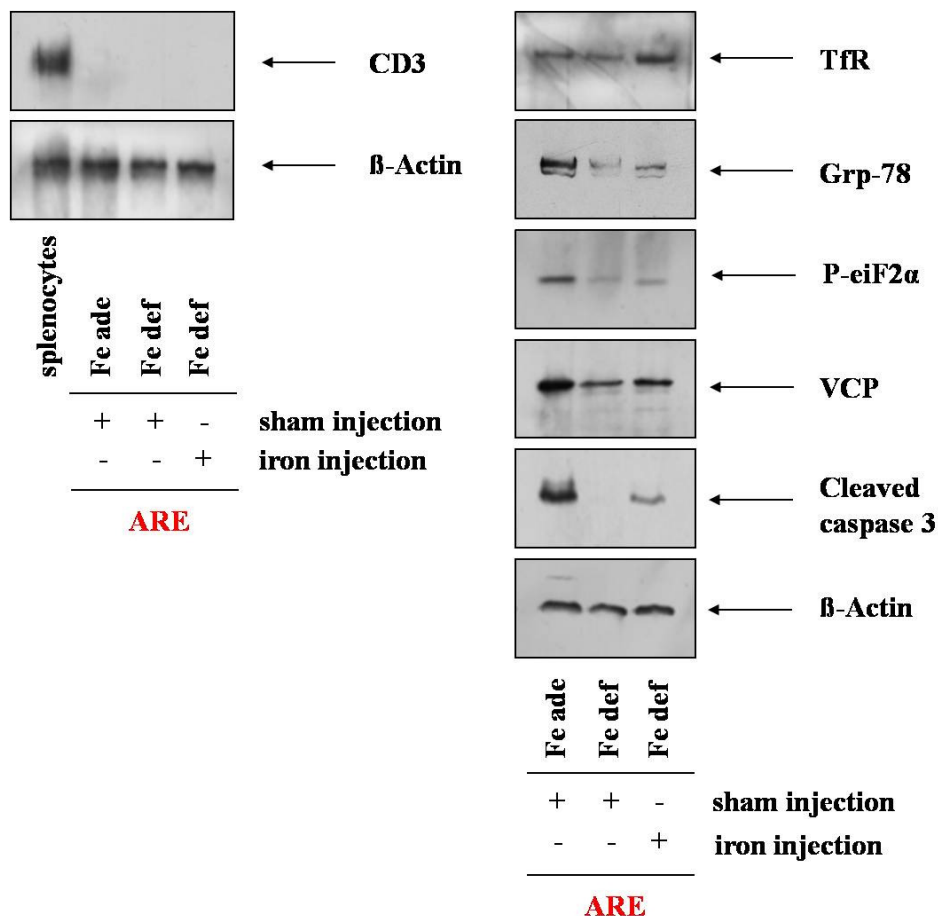


**Figure 25. Purity control of IEC isolation (left panel) and decrease of ER-stress and apoptosis by the reduction of dietary iron (right panel).** Western blot analysis was performed with 25  $\mu$ g total protein derived from splenocytes and pooled IEC samples from 6 iron-adequately (Fe ade) or iron-deficiently fed (Fe def)  $\text{TNF}^{\Delta\text{ARE}/\text{WT}}$  mice which received weekly sham-injections as well as iron-deficiently fed (Fe def)  $\text{TNF}^{\Delta\text{ARE}/\text{WT}}$  mice which received weekly iron-injections using immunoreactive CD-3, grp-78, p-eiF2 $\alpha$ , VCP, cc3 and  $\beta$ -actin.

Immuno- and TUNEL-staining in ileal sections revealed grp-78 expression and pro-apoptotic signals in iron-adequately fed, sham-injected  $\text{TNF}^{\Delta\text{ARE}/\text{WT}}$  mice compared to iron-deficiently fed, sham-injected as well as iron-repleted  $\text{TNF}^{\Delta\text{ARE}/\text{WT}}$  mice (Figure 26). Consistent with the feeding experiment, TUNEL-positive cell appearance was especially detectable in crypt regions of inflamed  $\text{TNF}^{\Delta\text{ARE}/\text{WT}}$  mice.

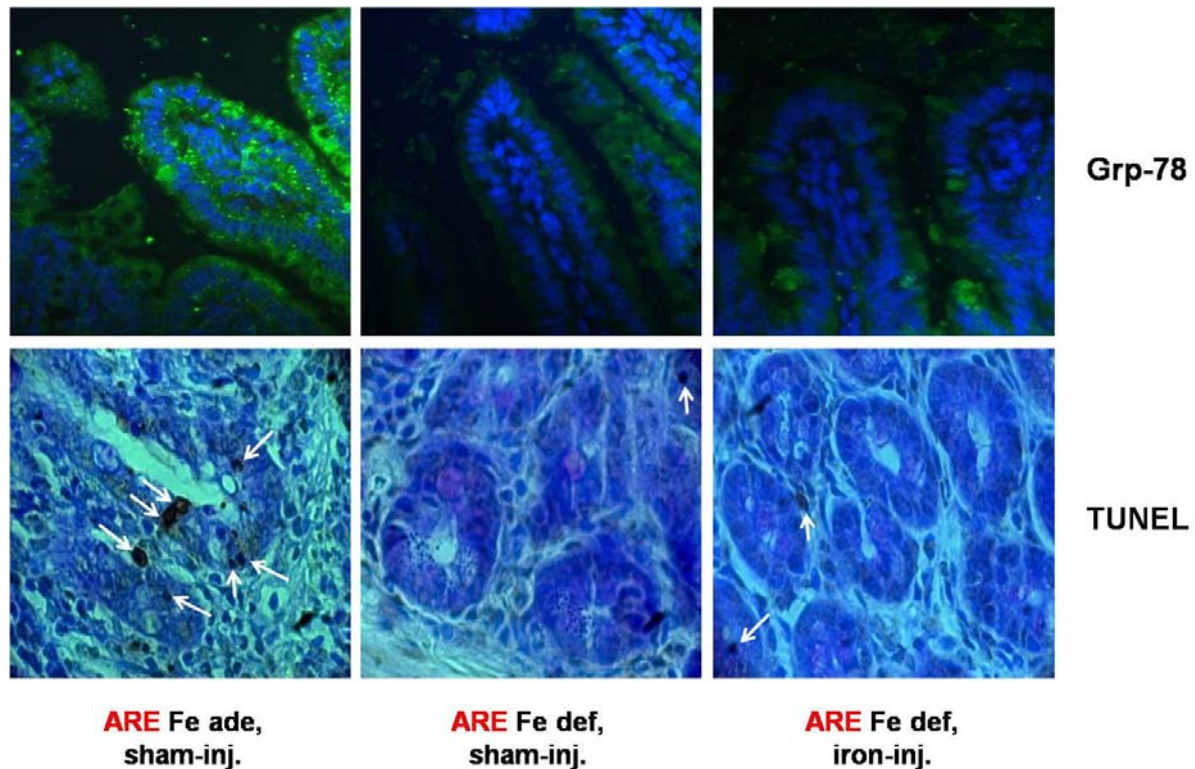


**Figure 26. Immuno- and TUNEL-staining of distal ileum segments of  $TNF^{\Delta ARE/WT}$  mice from the injection experiment.** Immuno- and TUNEL staining was performed from paraffin-embedded ileal tissue segments. High magnification (1000x) of TUNEL-positive cells (white arrows) visualize appearance especially in crypt regions of iron-adequately fed, sham-injected  $TNF^{\Delta ARE/WT}$  in contrast to iron-deficiently, sham-injected as well as iron-injected  $TNF^{\Delta ARE/WT}$  mice.

#### 4.3.2 Ileal explants from the parenteral iron-repletion experiment confirmed the reduction of ER stress and apoptosis

To explore possible differences in protein expression between isolated primary IEC and total tissue, we cultivated distal ileal segments from all mice of the injection experiment (Figure 30). After 24h of cultivation, the tissue was harvested for further Western blot analysis. Similar to the IEC protocol, the tissue samples were pooled and 25 $\mu$ g of total protein was applied to SDS-PAGE.

Ileal tissue explants from iron-deficiently fed, sham-injected as well as the iron-repleted  $TNF^{\Delta ARE/WT}$  mice showed reduced expression of proteins involved in ER stress (grp-78, p-eiF2 $\alpha$  and VCP) and apoptosis (cc3) compared to tissue explants from iron-adequately fed, sham-injected  $TNF^{\Delta ARE/WT}$  mice (Figure 27, left panel). In parallel, we determined the TNF protein secretion in supernatants of the cultivated tissue explants of each group. TNF concentrations were adjusted to total protein concentration. Consistent with the degree of tissue pathology, ELISA analysis revealed significantly elevated levels of TNF in the inflamed iron-adequately fed, sham-injected group (74.10  $\pm$  16.91) compared to the iron-deficient, sham-injected (31.58  $\pm$  15.74) as well as iron-repleted group (35.16  $\pm$  6.01) (Figure 27, graph).

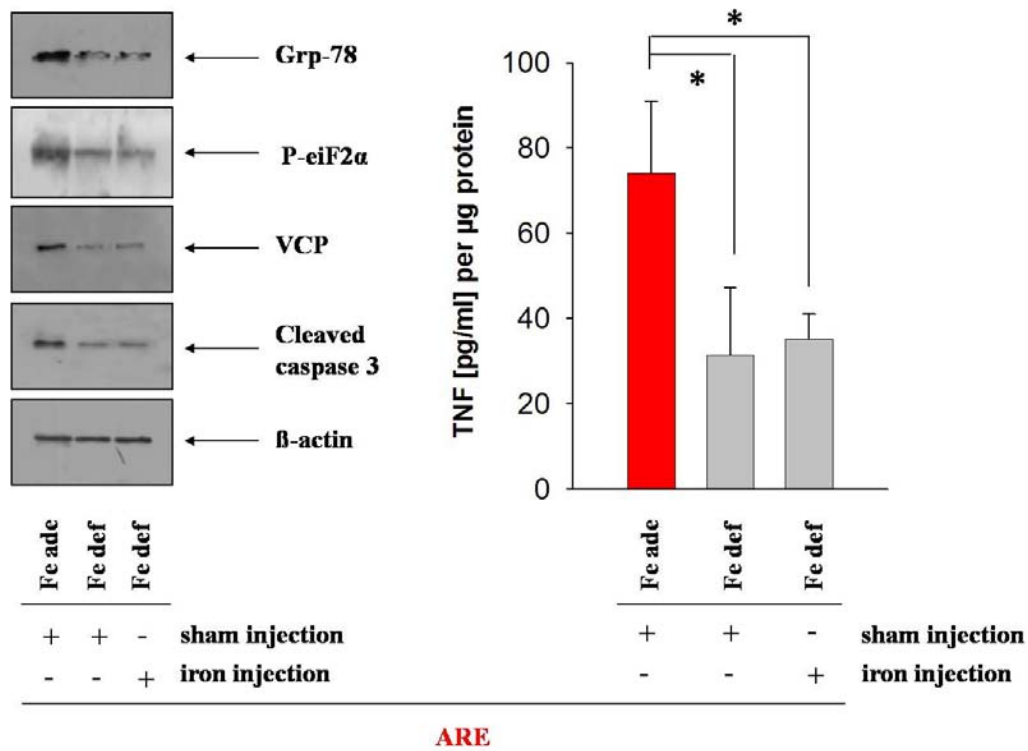


**Figure 27. ER stress protein- and TNF expression of total ileal tissue from  $TNF^{\Delta ARE/WT}$  mice of the injection experiment.** Western blot analysis was performed with 25  $\mu$ g total protein derived from total ileal tissue samples from 6 iron-adequately (Fe ade) or iron-deficiently fed (Fe def)  $TNF^{\Delta ARE/WT}$  mice which received weekly sham-injections as well as iron-deficiently fed (Fe def)  $TNF^{\Delta ARE/WT}$  mice which received weekly iron-injections (left panel). TNF expression was determined in medium of cultivated explants after 24h.

#### 4.4 Effects of systemic iron repletion on chronic ileitis: focus on immune cells and the gut microbiota

We first focused on the intestinal epithelium as directly affected compartment to identify the inflammation-reducing effect of the combined treatment of luminal iron deprivation and systemic iron repletion. Since the results arouse other questions like how the luminal iron deprivation protects the epithelium from ER stress, we next focused on immune cells and bacteria which might influence epithelial cell function. Since immune cells and bacteria need iron for function, growth and survival, the injection experiment was repeated to investigate how the iron-deficient diet in combination with parenteral iron repletion might influence IEL populations and function as well as the gut microbial ecology. The repetition of the experiment also included WT animals.

Confirming the first experiment, histological analysis of the distal ileum showed absence of inflammation (Figure 28) in the iron-deficiently fed, sham-injected  $TNF^{\Delta ARE/WT}$  group ( $1.00 \pm 0.33$ ) as well as in the iron-repleted  $TNF^{\Delta ARE/WT}$  group ( $0.71 \pm 0.23$ ). This was in complete contrast to inflamed iron-adequately fed, sham-injected  $TNF^{\Delta ARE/WT}$  mice ( $4.61 \pm 0.89$ ). WT mice showed absence of inflammation in all groups (iron-adequate:  $0.45 \pm 0.11$ ; iron-deficient:  $0.50 \pm 0.00$ ; iron-repleted:  $0.45 \pm 0.21$ ). Figure 29 illustrates H&E staining of representative paraffin-embedded distal ileal segments from all WT and  $TNF^{\Delta ARE/WT}$  mice receiving the three indicated iron protocols.

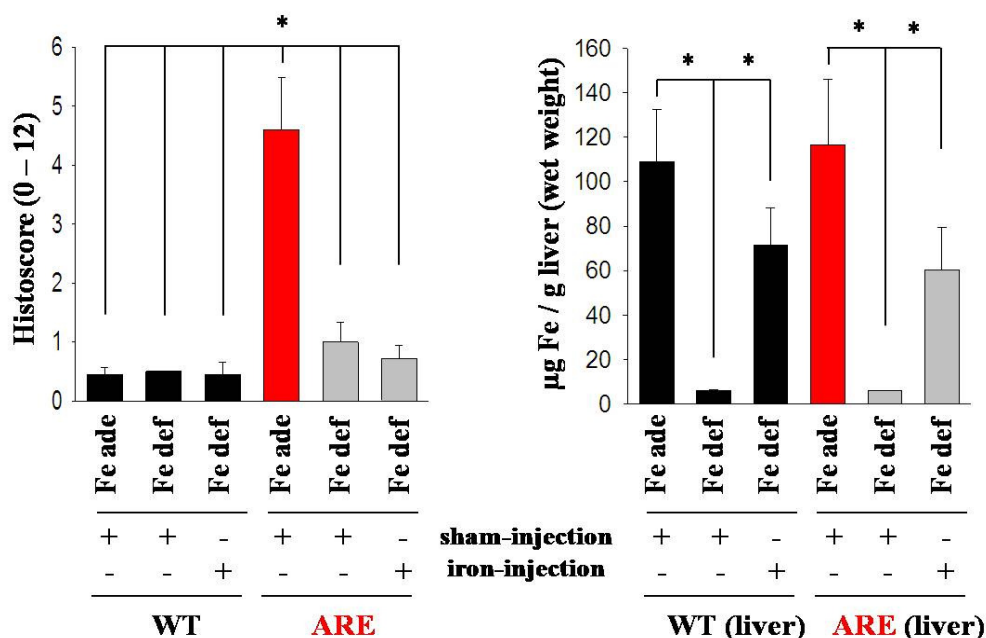


**Figure 28. Histology and hepatic non-heme measurement of the repeated injection experiment.** Histological analysis of iron-adequately or iron-deficiently fed WT and  $TNF^{\Delta ARE/WT}$  mice which received weekly applied sham- or iron injections, respectively (bar chart) with photometrically determined hepatic non-heme content.

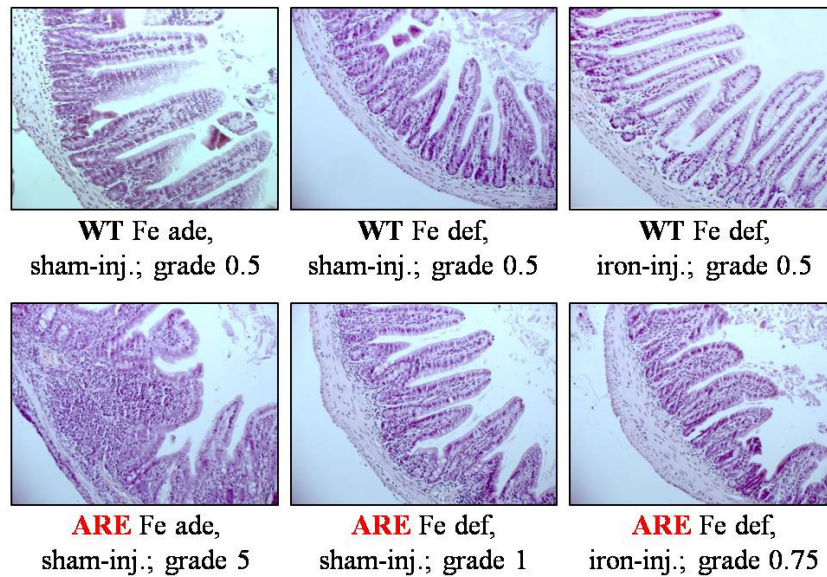


**Figure 29. H&E staining of ileal tissue segments of the repeated injection experiment confirming histology**

As shown in Figure 28, iron-repletion of iron-deficiently fed WT ( $71.66 \pm 16.71$ ) and  $\text{TNF}^{\Delta\text{ARE}/\text{WT}}$  ( $60.17 \pm 19.14$ ) mice lead to a 50% restoration of hepatic non-heme iron content compared to levels of the iron-adequately fed WT ( $109.12 \pm 23.12$ ) and  $\text{TNF}^{\Delta\text{ARE}/\text{WT}}$  ( $116.65 \pm 29.30$ ) mice. The iron-deficiently fed mice revealed significantly reduced hepatic non-heme iron content (WT:  $6.16 \pm 0.51$ ;  $\text{TNF}^{\Delta\text{ARE}/\text{WT}}$ :  $6.04 \pm 0.28$ ). Comparing the results from the first with the second injection experiment, large inter-individual differences in hepatic non-heme iron content are observable, but major iron storage seems to be independent of histology in iron-repleted  $\text{TNF}^{\Delta\text{ARE}/\text{WT}}$  mice.

To evaluate the effect of luminal iron deprivation and systemic repletion on iron blood parameters, Hc and Hb levels were measured. Hc blood levels of iron-deficiently fed  $\text{TNF}^{\Delta\text{ARE}/\text{WT}}$  ( $34.88 \pm 5.06$ ) decreased significantly in comparison to iron-adequately fed  $\text{TNF}^{\Delta\text{ARE}/\text{WT}}$  ( $42.13 \pm 1.73$ ) as well as WT ( $42.40 \pm 2.61$ ) mice (Figure 30). Iron-deficiently fed WT ( $39.20 \pm 5.72$ ) mice showed no significant difference to all other groups pointing to an influence of Hc levels by genotype. Hc levels of iron-repleted  $\text{TNF}^{\Delta\text{ARE}/\text{WT}}$  mice showed no significant differences to all other groups. There were no significant differences for Hb blood levels between all 6 treatment groups detectable (Figure 30). As there are no reference ranges available for Hb and Hc values of mice, only the 3 treatments can be compared without assessing the anemic status.

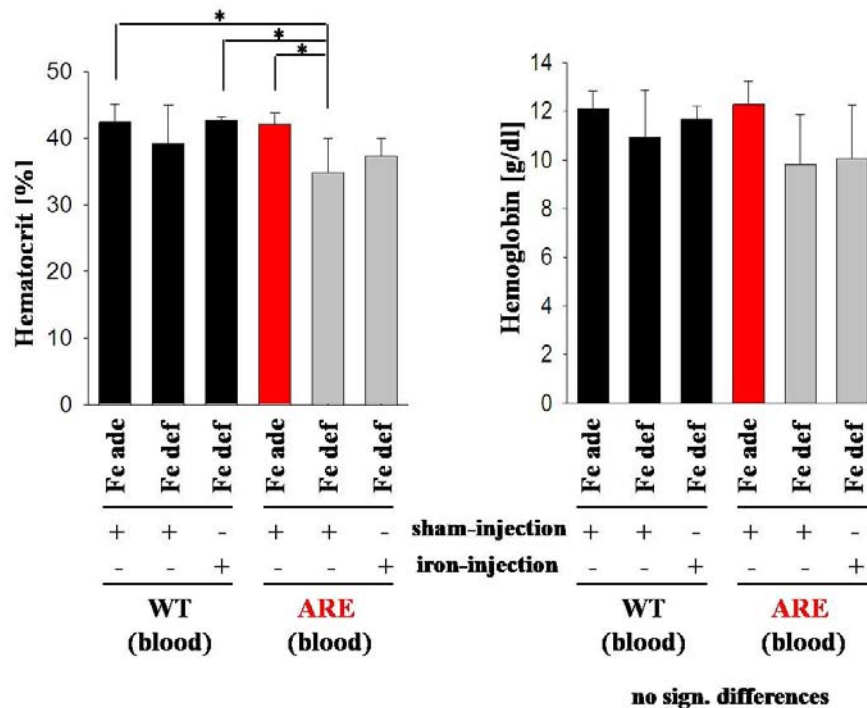


**Figure 30. Hematocrit (Hc) and hemoglobin (Hb) blood levels of all mice from the repeated injection experiment.** Hb blood levels were measured by centrifugation, Hc levels by photometric determination.

#### 4.4.1 Luminal ID and systemic iron repletion did not influence the phenotype of intraepithelial lymphocytes (IEL)

Since the  $TNF^{\Delta ARE/WT}$  mouse model is a T cell-dependent model, we isolated IEL from all mice and performed immunophenotyping by FACS analysis to evaluate the role of luminal or systemic iron on immune cell phenotype.  $CD8^+$  T cells constitute the main phenotype resident in the small intestinal epithelium and  $CD8\alpha\beta^+$  are the major effector cells in the  $TNF^{\Delta ARE/WT}$  model. Therefore, we separated  $CD3^+CD8^+$  T cells into  $CD3^+CD8\alpha\alpha^+$  and  $CD3^+CD8\alpha\beta^+$  from pooled IEL (N = 5 per group) using a cell sorter.

In WT mice, we detected a significant increase in  $CD4^+$  T cells in iron-deficiently fed WT mice compared to iron-adequately fed WT mice and a significant decrease if we compare  $CD4^+$  T cell numbers of iron-repleted WT with iron-deficiently fed WT mice. Furthermore, we detected a significant decrease of  $CD3^+CD8\alpha\alpha^+$  as well as a significant increase in  $CD3^+CD8\alpha\beta^+$  T cells when comparing the iron-adequately fed group with the iron-deficiently fed group (Figure 31). These changes in IEL numbers seem to have no effect as histology scores are equal in the non-susceptible WT host receiving the three indicated iron protocols.

Consistent with Apostolaki et al., we confirmed the loss of  $CD8\alpha\alpha^+$  and the increase in  $CD8\alpha\beta^+$  when comparing WT (92.0% / 7.8%) to  $TNF^{\Delta ARE/WT}$  mice (76.4% / 22.6%). Importantly, the iron deficient diet as well as the iron repletion in  $TNF^{\Delta ARE/WT}$  mice had no effect on the  $CD8\alpha\alpha^+$  /  $CD8\alpha\beta^+$  ration

## RESULTS

supporting that the absence of histology under luminal iron deprivation is not due to changes in effector T cell numbers.

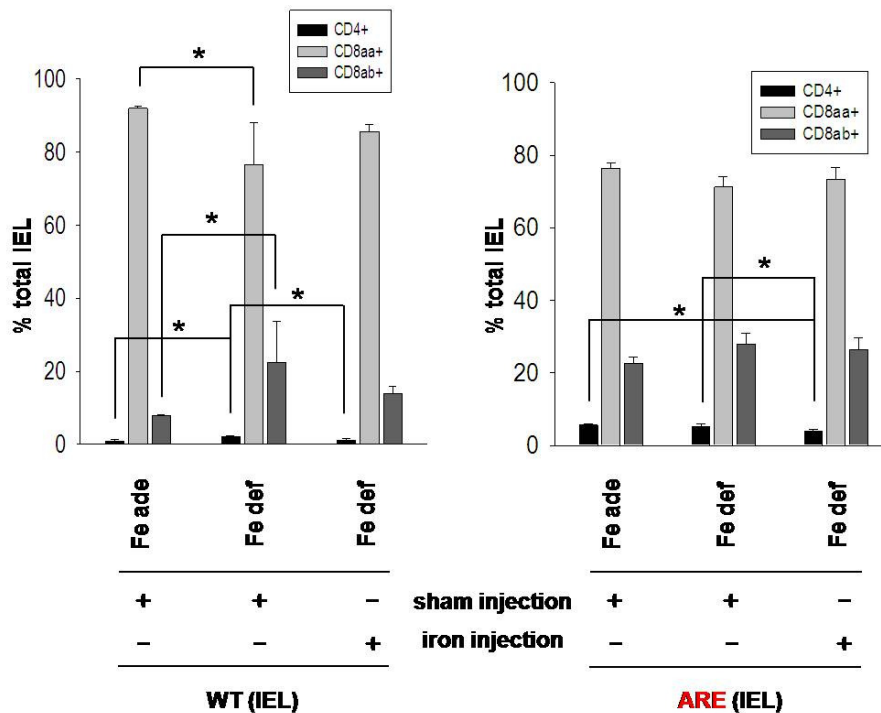


**Figure 31. Percent ratio of CD4<sup>+</sup>, CD8αα<sup>+</sup> and CD8αβ<sup>+</sup> IEL of WT and TNF<sup>ΔARE/WT</sup> mice of the injection experiment. IEL were isolated and subpopulation were phenotyped using FACS analysis.**

Whereas T cell numbers in TNF<sup>ΔARE/WT</sup> mice were not affected, we further elucidated the role of luminal iron deprivation and systemic iron repletion on T cell reactivity determining CD25 and CD69 expression levels in CD4<sup>+</sup>, CD8αα<sup>+</sup> and CD8αβ<sup>+</sup> IEL. There was a significant increase in CD25 positive CD8αα<sup>+</sup> IEL comparing the iron-deficiently and iron-repleted TNF<sup>ΔARE/WT</sup> mice with the iron-adequately fed TNF<sup>ΔARE/WT</sup> group (Figure 32). Only in the iron-deficiently fed group, a significant increase in CD25 positive CD4<sup>+</sup> IEL was observable, but if this points to an increase in regulatory T cell phenotype by the iron-deficient diet has to be elucidated. In the iron-repleted group, we detected a higher percentage of CD25 positive CD8αβ<sup>+</sup> IEL compared to the iron-adequately fed group. Increasing percentage of CD69 positive CD4<sup>+</sup>, CD8αα<sup>+</sup> and CD8αβ<sup>+</sup> IEL was found for the iron-deficiently as well as the iron-repleted TNF<sup>ΔARE/WT</sup> mice when compared to the iron-adequately fed group pointing to an even higher activated status of all three T cell subpopulations by a luminal iron deprivation (Figure 39).

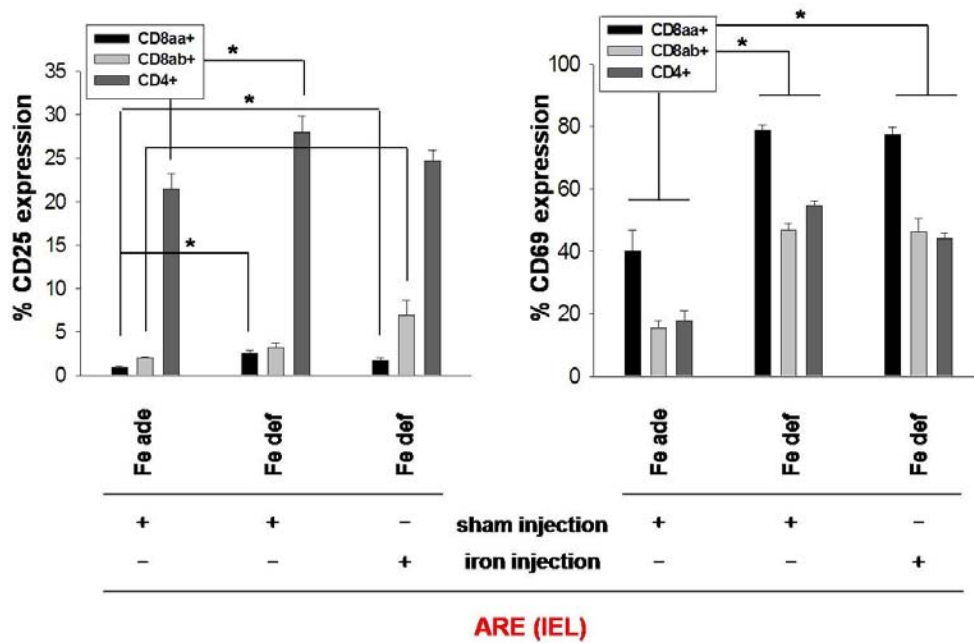


**Figure 32.** CD25 and CD69 expression of CD4<sup>+</sup>, CD8aa<sup>+</sup> und CD8ab<sup>+</sup> IEL from all TNF<sup>ΔARE/WT</sup> mice of the injection experiment. IEL were isolated and subpopulation were separated by FACS staining.

We next pooled mRNA of effector CD8ab<sup>+</sup> T cells from each group of TNF<sup>ΔARE/WT</sup> mice of the injection experiment to test T cell cytotoxicity, but GrzmB mRNA levels of CD8ab<sup>+</sup> T cells from iron-deficiently as well as iron-repleted TNF<sup>ΔARE/WT</sup> mice showed no differences compared to the GrzmB mRNA levels of CD8ab<sup>+</sup> T cells from the inflamed, iron-adequately fed TNF<sup>ΔARE/WT</sup> mice (data not shown). Iron-repletion seems to restore iron content in T cells as mRNA levels for TfR decrease (1.4-fold decrease) in contrast to a 5.2-fold increase under the iron-deficient diet when compared to TfR mRNA levels of CD8ab<sup>+</sup> T cells from iron-adequately fed TNF<sup>ΔARE/WT</sup> mice (data not shown).

#### 4.4.1.1 Higher susceptibility towards cytotoxic T cell-induced apoptosis in an ER-stressed epithelium

Since the reduction of luminal iron did not affect cytotoxic CD8ab<sup>+</sup> IEL numbers and cytotoxicity itself in TNF<sup>ΔARE/WT</sup> mice, we wanted to test the effect of cytotoxic T cells on ER stressed and unstressed IEC. Therefore, we performed co-culture experiments with Mode-K cells and CD8ab<sup>+</sup> T cell isolated from mesenteric lymph nodes of TNF<sup>ΔARE/WT</sup> mice. The cytotoxic T cells were activated by the stimulation with CD3<sup>+</sup>CD28<sup>+</sup> microbeads. Before co-culturing, Mode-K cells were pre-incubated for 24 h with BrdU which incorporates into the DNA. After induction of apoptosis, BrdU-labeled DNA fragments can be measured photometrically in the co-culture supernatant. In addition, Mode-K cells were treated for 6 h with the ER stressor Tunicamycin (Tm; 0.5μM) where indicated.

## RESULTS

As shown in Figure 33A (lower panel), pre-treatment of Mode-K cells with Tm before co-culturing with activated T cells led to increased apoptosis by determination of DNA fragmentation in comparison to non-stressed Mode-K cells over all time points. In addition, the activation of CD8 $\alpha\beta^+$  T cell led to increased levels of cytolytic GrzmB (Figure 33A middle panel) as well as IFN- $\gamma$  (Figure 33A upper panel). Figure 33B illustrates Mode-K cell monolayers under the above described conditions, clearly visualizing the increased cell death rate of Tm sensitized epithelial cells co-cultured with activated CD8 $\alpha\beta^+$  T cells. This experiment demonstrates that the induction of ER stress in the intestinal epithelium may lead to a higher susceptibility towards cytotoxic T cell-induced apoptosis.

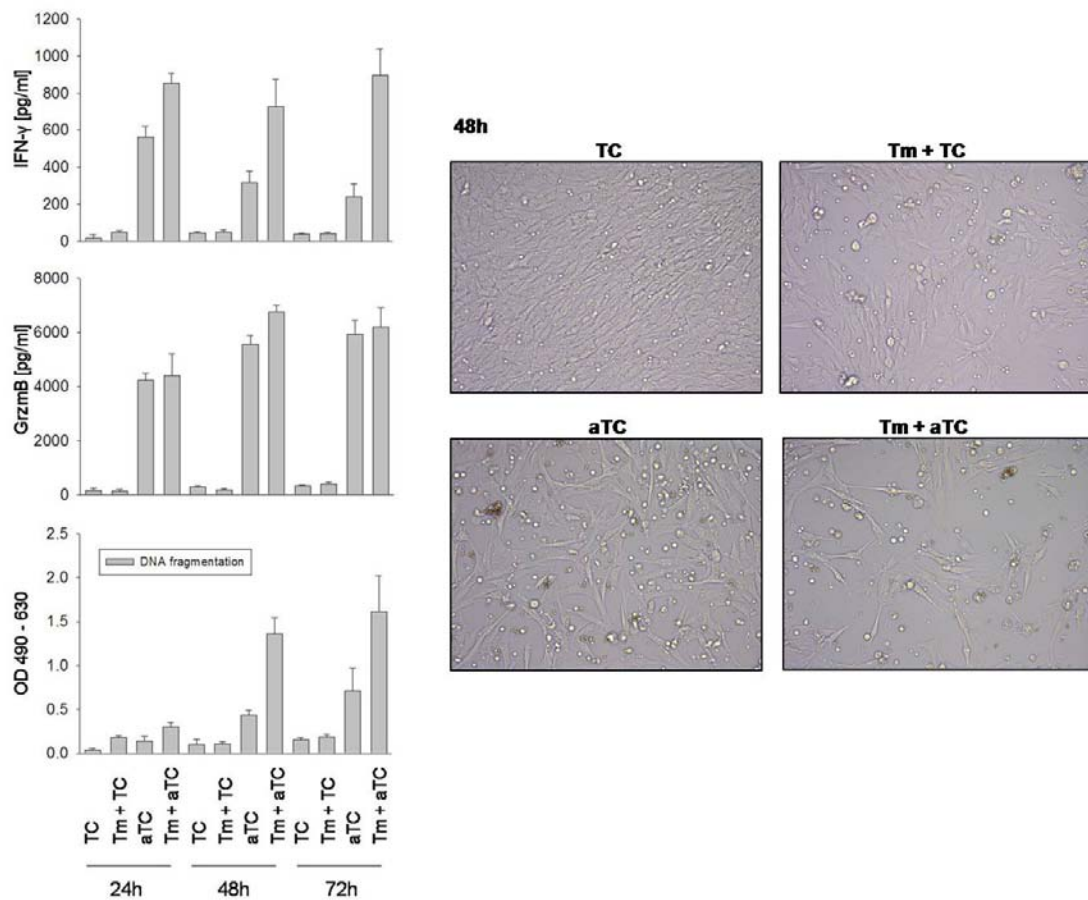


**Figure 33A + B. Co-culture experiment of cytotoxic CD8 $\alpha\beta^+$  T cells with Mode-K cells.** CD3 $^+$ /CD28 $^+$  activated or non-activated CD8 $\alpha\beta^+$  T cells from mesenteric lymph nodes of TNF $^{\Delta ARE/WT}$  mice were co-culture with Mode-K cells pre-treated with Tm were indicated. Pre-treatment with Tm lead to a higher susceptibility towards cytotoxic T cell-induced apoptosis compared to an unstressed epithelium.

#### 4.4.2 Luminal iron rather than the inflammatory host response affect the gut microbiota

Bacteria are a likely contributor to the pathogenesis of human IBD, and they have been suggested to be one factor that drives ER stress in the intestinal epithelium [188]. As bacteria have stringent requirements for iron, we hypothesized that the iron-deficient diet would alter the gut microbiota as described in a previous study [183]. To evaluate this effect, a comprehensive analysis of the cecal microbiota in all six groups of mice was performed by pyrosequencing of 16S rRNA tags at the Department of Food Science and Technology from the University of Nebraska.

##### 4.4.2.1 Iron-deficient diet induces significant alterations of the gut microbiota

We performed a comprehensive analysis of the cecal microbiota by pyrosequencing of 16S rRNA tags in WT and  $TNF^{\Delta ARE/WT}$  mice on an iron-adequate, an iron-deficient diet, and on an iron-deficient diet in combination with systemic iron repletion (N = 5 per group). We obtained a total of 132,938 sequences after quality control with an average of 4431 sequences per animal. Analysis of these sequence pools revealed significant differences in microbial community composition between groups of animals, while the total microbial diversity (Shannon's diversity index) and the number of total operational taxonomic units (OTUs) were not significantly affected by the treatments. Figure 34 shows the score plot of the principal component analysis (PCA) based on the normalized abundance of the dominant bacterial groups at the genus taxonomic level with color code according to iron treatment using principal components PC1 (explained 33% of the variation) and PC2 (explained 11% of the variation). The score plot shows major clustering of samples according to iron treatment and not to host inflammatory response, indicating that the iron-deficient diet led to most of the alterations in the microbial population regardless of systemic iron repletion.

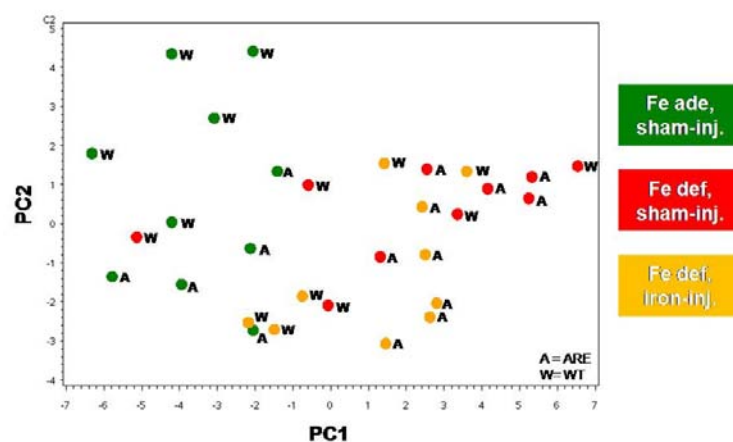


Figure 34. Score plot of the PCA analysis based on the proportions of the dominant bacterial groups at the genus taxonomic level as identified by the RDP classifier, colored by treatment.

The analysis revealed that 8 bacterial families, 9 bacterial genera (Table 10), and 46 Operational Taxonomic Units (OTUs) (Table 11) were significantly ( $p < 0.01$ ) affected by luminal iron deprivation. For most taxa, intraperitoneal injection of iron had no detectable effect. Among others, the genera *Bifidobacterium* ( $p = 0.0018$ ), *Clostridium* ( $p = 0.0017$ ), *Succinivibrio* ( $p = 0.0027$ ), and *Turicibacter* ( $p = 0.0020$ ) were significantly increased in iron-deficiently fed mice, while the genera *Desulfovibrio* ( $p < 0.0001$ ) and *Bacteroides* ( $p < 0.0001$ ) were significantly decreased. Only 1 phylum, 2 families, 2 genera (Table 12), and 29 OTUs (Table 13) showed significant differences ( $p < 0.01$ ) in abundance in WT and TNF<sup>ΔARE/WT</sup> mice. Among others, TNF<sup>ΔARE/WT</sup> mice had an overall decrease in the phylum Proteobacteria ( $p = 0.0024$ ) and the genus *Helicobacter* ( $p = 0.0016$ ) and a significant increase in *Peptostreptococcaceae Insertae Sedis* ( $p = 0.0025$ ). One genus, *Dorea*, (Table 14), and 13 OTUs (Table 15) were affected by an interaction between treatment and host-mediated inflammation.

#### **4.4.2.2 Highly significant associations between members of the gut microbiota and inflammation**

To identify bacterial populations that might contribute to inflammation in TNF<sup>ΔARE/WT</sup> mice and to evaluate the effects on luminal iron deprivation in this context, histology scores of individual mice were correlated to all bacterial taxa and OTUs. This analysis revealed remarkable associations between bacterial groups and inflammation (Table 10-15). Taxa showing high correlation between abundance and inflammation were *Succinivibrio* ( $p < 0.0001$ ,  $r = -0.85$ ) (Figure 35), *Turicibacter* ( $p = 0.0009$ ,  $r = -0.77$ ) (Figure 36), *Desulfovibrio* ( $p = 0.0014$ ,  $r = 0.75$ ) (Figure 37) and *Bifidobacterium* ( $p = 0.011$ ,  $r = -0.64$ ) (Figure 38). All of these taxa were also significantly affected by luminal iron. A significant association was also detected for *Bacteroides* ( $p = 0.0007$ ,  $r = 0.77$ ). OTU 1476, which belongs to this genus and is distantly related to *Bacteroides stercoris*, showed remarkably high correlations with host inflammation ( $p < 0.0001$ ,  $r = -0.91$ ) (Figure 39). In conclusion, the analysis of the gut microbiota revealed a significant impact of luminal iron on gut microbiota composition with high associations between ileitis and bacterial populations, suggesting that the protective effect of luminal iron deprivation on both inflammation and ER stress-associated apoptosis could be conferred, at least in part, by a modulation of the gut microbiota.

## RESULTS

**Table 10. Bacterial taxa affected by iron treatment**

| Bacterial taxa                        | Percent abundance of bacterial group [mean ± SD] for the different treatments |                           |                      |                           |                      |                           | P- Value for factorial ANOVA           |  |  | Correlations of bacterial taxa with histology scores |                    |
|---------------------------------------|---|---------------------------|----------------------|---------------------------|----------------------|---------------------------|--|--|--|--|--------------------|
|                                       | WT Fe ade, sham-inj.  | TNFΔARE Fe ade, sham-inj. | WT Fe def, sham-inj. | TNFΔARE Fe def, sham-inj. | WT Fe def, iron-inj. | TNFΔARE Fe def, iron-inj. | Fe ade, sham-inj. vs Fe def, sham-inj. | Fe ade, sham-inj. vs Fe def, iron-inj. | Fe def, sham-inj. vs Fe def, iron-inj. | R  | P-value            |
| Family level                          |   |                           |                      |                           |                      |                           |  |  |  |  |                    |
| Bifidobacteriaceae                    | 0.04 ± 0.05   | 0.03 ± 0.03               | 4.41 ± 5.27          | 3.95 ± 2.43               | 3.41 ± 4.76          | 3.52 ± 3.18               | <b>0.0029</b>                          | <b>0.0116</b>                          | > 0.01                                 | -0.6339  | 0.0112             |
| Rikenellaceae                         | 1.92 ± 2.39   | 3.69 ± 4.54               | 0.27 ± 0.15          | 0.32 ± 0.10               | 0.82 ± 0.65          | 0.40 ± 0.11               | <b>0.0061</b>                          | <b>0.0337</b>                          | > 0.01                                 | 0.5486   | 0.0343             |
| Unclassified Desulfovibrionales       | 0.11 ± 0.03   | 0.11 ± 0.08               | 0.49 ± 0.34          | 1.11 ± 0.87               | 1.12 ± 1.47          | 1.19 ± 0.98               | <b>0.0157</b>                          | <b>0.0025</b>                          | > 0.01                                 | -0.5826  | 0.0227             |
| Bacteroidaceae                        | 4.02 ± 2.56   | 5.36 ± 3.27               | 0.87 ± 0.69          | 0.24 ± 0.09               | 3.55 ± 1.93          | 0.84 ± 0.47               | <b>&lt; 0.0001</b>                     | <b>0.0048</b>                          | <b>0.0083</b>                          | 0.7734   | <b>0.0007</b>      |
| Desulfovibrionaceae                   | 3.87 ± 1.37   | 2.49 ± 1.27               | 0.79 ± 0.53          | 1.03 ± 1.01               | 1.63 ± 0.41          | 0.87 ± 0.37               | <b>&lt; 0.0001</b>                     | <b>0.0001</b>                          | > 0.01                                 | 0.7306   | <b>0.0020</b>      |
| Lactobacillaceae                      | 1.17 ± 2.21   | 1.55 ± 2.00               | 2.98 ± 3.06          | 4.49 ± 2.14               | 0.33 ± 0.53          | 0.73 ± 0.56               | <b>0.0270</b>                          | > 0.01                                 | <b>0.0047</b>                          | -0.1917  | 0.4937             |
| Erysipelotrichaceae                   | 6.68 ± 7.64   | 12.04 ± 9.94              | 17.04 ± 14.18        | 27.51 ± 9.57              | 19.61 ± 7.07         | 29.02 ± 4.01              | <b>0.0093</b>                          | <b>0.0019</b>                          | > 0.01                                 | -0.7491  | <b>0.0013</b>      |
| Lachnospiraceae                       | 40.09 ± 8.82  | 24.67 ± 7.96              | 22.02 ± 11.89        | 15.34 ± 5.88              | 24.21 ± 5.60         | 17.75 ± 4.87              | <b>0.0022</b>                          | <b>0.0167</b>                          | > 0.01                                 | 0.5632   | 0.0288             |
| Succinivibrionaceae                   | 0.75 ± 0.30   | 0.56 ± 0.31               | 1.73 ± 1.13          | 1.56 ± 0.40               | 1.00 ± 0.69          | 1.61 ± 0.51               | <b>0.0032</b>                          | <b>0.0438</b>                          | > 0.01                                 | -0.8440  | <b>&lt; 0.0001</b> |
| Genus level                           |   |                           |                      |                           |                      |                           |  |  |  |  |                    |
| Unclassified Prevotellaceae           | 1.88 ± 0.96   | 1.87 ± 1.12               | 2.99 ± 1.53          | 3.44 ± 0.66               | 2.79 ± 1.15          | 3.56 ± 0.50               | <b>0.0147</b>                          | <b>0.0160</b>                          | > 0.01                                 | -0.7947  | <b>0.0004</b>      |
| <i>Bifidobacterium</i>                | 0.01 ± 0.01   | 0.02 ± 0.01               | 3.86 ± 4.62          | 3.31 ± 2.81               | 2.76 ± 3.89          | 2.77 ± 2.43               | <b>0.0022</b>                          | <b>0.0120</b>                          | > 0.01                                 | -0.6373  | 0.0106             |
| <i>Lactobacillus</i>                  | 1.16 ± 2.19   | 1.50 ± 1.93               | 2.91 ± 3.00          | 4.40 ± 2.14               | 0.32 ± 0.54          | 0.71 ± 0.54               | <b>0.0277</b>                          | <b>0.0044</b>                          | > 0.01                                 | -0.1917  | 0.4937             |
| <i>Clostridium</i>                    | 0.08 ± 0.05   | 0.11 ± 0.11               | 0.21 ± 0.12          | 0.28 ± 0.07               | 0.21 ± 0.13          | 0.30 ± 0.11               | <b>0.0052</b>                          | <b>0.0037</b>                          | > 0.01                                 | -0.7128  | <b>0.0029</b>      |
| <i>Succinivibrio</i>                  | 0.72 ± 0.30   | 0.54 ± 0.29               | 1.71 ± 1.11          | 1.50 ± 0.39               | 0.92 ± 0.56          | 1.53 ± 0.47               | <b>0.0021</b>                          | <b>0.0487</b>                          | > 0.01                                 | -0.8495  | <b>&lt; 0.0001</b> |
| Unclassified Erysipelotrichaceae      | 2.30 ± 2.78   | 3.56 ± 2.68               | 5.12 ± 4.01          | 9.93 ± 3.70               | 8.05 ± 3.48          | 12.32 ± 1.35              | <b>0.0067</b>                          | <b>&lt; 0.0001</b>                     | > 0.01                                 | -0.8349  | <b>0.0001</b>      |
| <i>Turicibacter</i>                   | 0.18 ± 0.13   | 0.17 ± 0.08               | 0.36 ± 0.14          | 0.51 ± 0.16               | 0.27 ± 0.19          | 0.50 ± 0.18               | <b>0.0022</b>                          | <b>0.0162</b>                          | > 0.01                                 | -0.7656  | <b>0.0009</b>      |
| <i>Bacteroides</i>                    | 4.02 ± 2.56   | 5.36 ± 3.27               | 0.87 ± 0.69          | 0.24 ± 0.09               | 3.54 ± 1.93          | 0.84 ± 0.47               | <b>&lt; 0.0001</b>                     | <b>0.0047</b>                          | <b>0.0085</b>                          | 0.7734   | <b>0.0007</b>      |
| <i>Dorea*</i>                         | 2.59 ± 1.39   | 0.14 ± 0.13               | 0.32 ± 0.26          | 0.42 ± 0.33               | 0.17 ± 0.17          | 0.22 ± 0.24               | > 0.01                                 | <b>0.0046</b>                          | > 0.01                                 | -0.3674  | 0.1780             |
| <i>Lachnospiraceae Insertae Sedis</i> | 7.19 ± 2.68   | 2.95 ± 0.65               | 2.82 ± 1.53          | 2.12 ± 0.35               | 3.28 ± 1.16          | 2.38 ± 0.47               | <b>0.0005</b>                          | <b>0.0043</b>                          | > 0.01                                 | 0.5458   | 0.0353             |
| <i>Desulfovibrio</i>                  | 2.19 ± 1.11   | 1.69 ± 0.84               | 0.30 ± 0.22          | 0.44 ± 0.56               | 0.66 ± 0.32          | 0.37 ± 0.26               | <b>&lt; 0.0001</b>                     | <b>&lt; 0.0001</b>                     | > 0.01                                 | 0.0747   | <b>0.0014</b>      |

\*These bacterial groups showed statistically significant interactions between iron treatment and genotype.

## RESULTS

**Table 11. OTUs affected by iron treatment**

| Highest match in RDP database (type strain)                                   | Sequence similarity score to closest type strain <sup>1</sup> | Percent abundance of bacterial group [mean ± SD] for the different treatments |                           |                      |                           |                      |                           | P-values                               |  |  | Correlation parameters of bacterial taxa with histology scores |                    |
|---|---|---|---------------------------|----------------------|---------------------------|----------------------|---------------------------|--|--|--|--|--------------------|
|   |   | WT Fe ade, sham-inj.  | TNFΔARE Fe ade, sham-inj. | WT Fe def, sham-inj. | TNFΔARE Fe def, sham-inj. | WT Fe def, iron-inj. | TNFΔARE Fe def, iron-inj. | Fe ade, sham-inj. vs Fe def, sham-inj. | Fe ade, sham-inj. vs Fe def, iron-inj. | Fe def, sham-inj. vs Fe def, iron-inj. | R  | P-value            |
| <i>Allobaculum stercoricanis</i> (T) DSM 13633                                | 0.484   | 1.301 ± 1.364   | 1.344 ± 1.206             | 2.258 ± 1.162        | 4.448 ± 2.770             | 5.255 ± 3.333        | 8.807 ± 1.545             | <b>0.0327</b>                          | <b>&lt; 0.0001</b>                     | <b>0.0149</b>                          | -0.7288  | <b>0.0021</b>      |
| <i>Lactobacillus johnsonii</i> (T); ATCC 33200 (T).                           | 0.969   | 1.045 ± 2.284   | 1.482 ± 2.016             | 2.934 ± 3.348        | 4.061 ± 2.348             | 0.012 ± 0.028        | 0.658 ± 0.711             | > 0.01                                 | > 0.01                                 | <b>0.0070</b>                          | -0.1469  | 0.6013             |
| <i>Desulfovibrio desulfuricans</i> subsp. <i>desulfuricans</i> (T); ATCC29577 | 0.726   | 3.673 ± 0.606   | 2.851 ± 0.509             | 0.729 ± 0.940        | 1.152 ± 0.734             | 1.152 ± 0.734        | 0.606 ± 0.422             | <b>&lt; 0.0001</b>                     | <b>&lt; 0.0001</b>                     | > 0.01                                 | 0.7430   | <b>0.0015</b>      |
| <i>Clostridium oroticum</i> (T); M59109*                                      | 0.805   | 5.447 ± 3.306   | 0.050 ± 0.069             | 0.375 ± 0.316        | 0.347 ± 0.428             | 0.012 ± 0.017        | 0.136 ± 0.234             | <b>0.0277</b>                          | <b>0.0005</b>                          | > 0.01                                 | -0.3498  | 0.2013             |
| <i>Clostridium xylanolyticum</i> (T); ATCC 4963*                              | 0.813   | 4.545 ± 3.624   | 1.209 ± 0.745             | 0.000 ± 0.000        | 0.000 ± 0.000             | 0.000 ± 0.000        | 0.000 ± 0.000             | <b>0.0008</b>                          | <b>0.0008</b>                          | > 0.01                                 | 0.8509   | <b>&lt; 0.0001</b> |
| <i>Bacteroides dorei</i> (T); JCM 13471                                       | 0.729   | 1.143 ± 0.602   | 2.039 ± 1.695             | 0.220 ± 0.226        | 0.016 ± 0.022             | 1.047 ± 0.949        | 0.177 ± 0.190             | <b>0.0018</b>                          | <b>0.0395</b>                          | > 0.01                                 | 0.6888   | <b>0.0045</b>      |
| <i>Succinivibrio dextrinosolvens</i> (T); DSM 3072                            | 0.805   | 0.184 ± 0.110   | 0.245 ± 0.161             | 0.698 ± 0.444        | 0.566 ± 0.201             | 0.389 ± 0.221        | 0.723 ± 0.371             | <b>0.0070</b>                          | <b>0.0290</b>                          | > 0.01                                 | -0.6690  | <b>0.0064</b>      |
| <i>Bacteroides dorei</i> (T); JCM 13471                                       | 0.760   | 0.844 ± 0.379   | 1.374 ± 1.293             | 0.158 ± 0.170        | 0.014 ± 0.019             | 0.741 ± 0.780        | 0.126 ± 0.127             | <b>&lt; 0.0001</b>                     | <b>0.0129</b>                          | > 0.01                                 | 0.6483   | <b>0.0090</b>      |
| <i>Clostridium orbiscindens</i> (T); DSM 6740                                 | 0.685   | 0.333 ± 0.307   | 0.160 ± 0.250             | 0.869 ± 1.016        | 0.760 ± 0.355             | 0.081 ± 0.052        | 0.035 ± 0.064             | <b>0.0318</b>                          | > 0.01                                 | <b>0.0039</b>                          | -0.3047  | 0.2695             |
| <i>Clostridium orbiscindens</i> (T); DSM 6740*                                | 0.662   | 1.059 ± 0.366   | 0.421 ± 0.275             | 0.207 ± 0.197        | 0.769 ± 0.142             | 0.420 ± 0.199        | 0.308 ± 0.188             | <b>&lt; 0.0001</b>                     | <b>0.0002</b>                          | > 0.01                                 | 0.6086   | 0.0161             |
| <i>Succinivibrio dextrinosolvens</i> (T); DSM 3072                            | 0.812   | 0.187 ± 0.182   | 0.123 ± 0.103             | 0.438 ± 0.319        | 0.460 ± 0.165             | 0.244 ± 0.165        | 0.387 ± 0.093             | <b>0.0044</b>                          | > 0.01                                 | > 0.01                                 | -0.7974  | <b>0.0004</b>      |
| <i>Parabacteroides distasonis</i> (T); M86695                                 | 0.598   | 0.114 ± 0.097   | 0.062 ± 0.071             | 0.171 ± 0.160        | 0.454 ± 0.269             | 0.397 ± 0.298        | 0.629 ± 0.265             | > 0.01                                 | <b>0.0005</b>                          | > 0.01                                 | -0.7494  | <b>0.0013</b>      |
| <i>Marinilabilia salmonicolor</i> (T); M62422                                 | 0.536   | 0.079 ± 0.123   | 0.035 ± 0.058             | 0.368 ± 0.228        | 0.380 ± 0.178             | 0.426 ± 0.415        | 0.391 ± 0.102             | <b>0.0015</b>                          | <b>0.0029</b>                          | > 0.01                                 | -0.8171  | <b>0.0002</b>      |
| <i>Desulfovibrio desulfuricans</i> subsp. <i>desulfuricans</i> (T); ATCC29577 | 0.606   | 0.000 ± 0.000   | 0.000 ± 0.000             | 0.231 ± 0.190        | 0.346 ± 0.423             | 0.538 ± 0.780        | 0.622 ± 0.624             | <b>0.0056</b>                          | <b>0.0001</b>                          | > 0.01                                 | -0.5154  | 0.0493             |
| <i>Turicibacter sanguinis</i> (T); AF349724                                   | 0.894   | 0.158 ± 0.157   | 0.120 ± 0.063             | 0.284 ± 0.100        | 0.384 ± 0.123             | 0.207 ± 0.167        | 0.412 ± 0.132             | <b>0.0065</b>                          | <b>0.0242</b>                          | > 0.01                                 | 0.7572   | <b>0.0011</b>      |
| <i>Bacteroides eggerthii</i> (T); L16485*                                     | 0.712   | 0.448 ± 0.701   | 0.430 ± 0.402             | 0.030 ± 0.034        | 0.009 ± 0.012             | 0.848 ± 0.369        | 0.020 ± 0.032             | <b>0.0021</b>                          | > 0.01                                 | <b>0.0064</b>                          | 0.7715   | <b>0.0008</b>      |
| <i>Allobaculum stercoricanis</i> (T); type strain: DSM 13633*                 | 0.515   | 0.000 ± 0.000   | 0.000 ± 0.000             | 0.024 ± 0.023        | 0.030 ± 0.042             | 0.000 ± 0.000        | 1.452 ± 1.632             | > 0.01                                 | <b>0.0036</b>                          | <b>0.0250</b>                          | -0.3288  | 0.2314             |
| <i>Bacteroides capillosus</i> (T); ATCC 29799                                 | 0.614   | 0.041 ± 0.065   | 0.160 ± 0.066             | 0.117 ± 0.154        | 0.303 ± 0.157             | 0.399 ± 0.497        | 0.495 ± 0.213             | > 0.01                                 | <b>0.0060</b>                          | > 0.01                                 | -0.5932  | 0.0198             |
| <i>Clostridium oroticum</i> (T); M59109                                       | 0.760   | 1.572 ± 0.881   | 0.027 ± 0.060             | 0.116 ± 0.085        | 0.076 ± 0.037             | 0.019 ± 0.031        | 0.072 ± 0.103             | <b>0.0283</b>                          | <b>0.0010</b>                          | > 0.01                                 | -0.4056  | 0.1336             |
| <i>Allobaculum stercoricanis</i> (T); DSM 13633 (T).*                         | 0.494   | 0.146 ± 0.192   | 0.050 ± 0.064             | 0.181 ± 0.158        | 0.237 ± 0.118             | 0.222 ± 0.100        | 0.566 ± 0.163             | > 0.01                                 | <b>0.0002</b>                          | > 0.01                                 | -0.7037  | <b>0.0034</b>      |
| <i>Clostridium lituseburense</i> (T); M59107*                                 | 0.885   | 0.107 ± 0.083   | 0.085 ± 0.061             | 0.156 ± 0.090        | 0.481 ± 0.154             | 0.249 ± 0.163        | 0.215 ± 0.112             | <b>0.0013</b>                          | <b>0.0206</b>                          | > 0.01                                 | -0.6560  | <b>0.0079</b>      |
| <i>Allobaculum stercoricanis</i> (T); DSM 13633 (T).                          | 0.491   | 0.052 ± 0.088   | 0.066 ± 0.053             | 0.150 ± 0.068        | 0.268 ± 0.158             | 0.261 ± 0.219        | 0.513 ± 0.233             | <b>0.0176</b>                          | <b>0.0004</b>                          | > 0.01                                 | -0.6645  | <b>0.0069</b>      |
| <i>Bacteroides dorei</i> (T); JCM 13471                                       | 0.697   | 0.287 ± 0.164   | 0.813 ± 0.755             | 0.077 ± 0.094        | 0.000 ± 0.000             | 0.329 ± 0.288        | 0.058 ± 0.079             | <b>0.0001</b>                          | <b>0.0215</b>                          | > 0.01                                 | 0.6406   | 0.0101             |
| <i>Clostridium oroticum</i> (T); M59109*                                      | 0.746   | 1.231 ± 0.748   | 0.014 ± 0.019             | 0.124 ± 0.129        | 0.064 ± 0.058             | 0.005 ± 0.012        | 0.046 ± 0.067             | <b>0.0025</b>                          | <b>0.0007</b>                          | > 0.01                                 | -0.3527  | 0.1973             |
| <i>Allobaculum stercoricanis</i> (T); DSM 13633 (T).                          | 0.486   | 0.077 ± 0.100   | 0.132 ± 0.136             | 0.183 ± 0.159        | 0.181 ± 0.108             | 0.258 ± 0.150        | 0.421 ± 0.181             | > 0.01                                 | <b>0.0038</b>                          | > 0.01                                 | -0.4793  | 0.0706             |
| <i>Allobaculum stercoricanis</i> (T); type strain: DSM 13633                  | 0.480   | 0.076 ± 0.142   | 0.079 ± 0.081             | 0.080 ± 0.096        | 0.272 ± 0.096             | 0.264 ± 0.213        | 0.487 ± 0.078             | > 0.01                                 | <b>0.0009</b>                          | <b>0.0245</b>                          | -0.6624  | <b>0.0071</b>      |
| <i>Allobaculum stercoricanis</i> (T); DSM 13633 (T)                           | 0.471   | 0.057 ± 0.127   | 0.060 ± 0.055             | 0.105 ± 0.061        | 0.168 ± 0.052             | 0.292 ± 0.073        | 0.519 ± 0.219             | <b>0.0102</b>                          | <b>&lt; 0.0001</b>                     | <b>0.0008</b>                          | -0.6052  | 0.0168             |
| <i>Allobaculum stercoricanis</i> (T); type strain: DSM 13633                  | 0.482   | 0.087 ± 0.142   | 0.067 ± 0.042             | 0.093 ± 0.093        | 0.229 ± 0.081             | 0.343 ± 0.347        | 0.375 ± 0.169             | > 0.01                                 | <b>0.0016</b>                          | > 0.01                                 | -0.7068  | <b>0.0032</b>      |
| <i>Clostridium lituseburense</i> (T); M59107                                  | 0.888   | 0.022 ± 0.033   | 0.178 ± 0.092             | 0.121 ± 0.034        | 0.268 ± 0.205             | 0.259 ± 0.188        | 0.258 ± 0.201             | > 0.01                                 | <b>0.0098</b>                          | > 0.01                                 | -0.3000  | 0.2773             |
| <i>Desulfitobacterium metallireducens</i> (T); AF297871                       | 0.443   | 0.545 ± 0.274   | 0.170 ± 0.128             | 0.159 ± 0.147        | 0.029 ± 0.029             | 0.119 ± 0.110        | 0.125 ± 0.091             | <b>0.0030</b>                          | > 0.01                                 | > 0.01                                 | 0.4450   | 0.0965             |
| <i>Allobaculum stercoricanis</i> (T); DSM 13633 (T).                          | 0.487   | 0.044 ± 0.071   | 0.014 ± 0.020             | 0.076 ± 0.082        | 0.174 ± 0.173             | 0.307 ± 0.174        | 0.323 ± 0.102             | <b>0.0311</b>                          | <b>&lt; 0.0001</b>                     | <b>0.0041</b>                          | -0.6775  | <b>0.0055</b>      |
| <i>Blautia hydrogenotrophica</i> (T); S5a36                                   | 0.496   | 0.552 ± 0.170   | 0.090 ± 0.092             | 0.116 ± 0.166        | 0.005 ± 0.010             | 0.269 ± 0.231        | 0.042 ± 0.045             | <b>0.0006</b>                          | > 0.01                                 | > 0.01                                 | 0.4554   | 0.0880             |

## RESULTS

|   |       |               |               |               |               |               |               |                 |                 |               |         |                 |
|---|-------|---------------|---------------|---------------|---------------|---------------|---------------|-----------------|-----------------|---------------|---------|-----------------|
| Faecalibacterium prausnitzii (T); ATCC 27768*                 | 0.879 | 0.070 ± 0.078 | 0.067 ± 0.082 | 0.080 ± 0.064 | 0.362 ± 0.137 | 0.163 ± 0.028 | 0.148 ± 0.086 | <b>0.0015</b>   | > 0.01          | > 0.01        | -0.5749 | 0.0250          |
| Verrucomicrobium spinosum (T); DSM 4136T                      | 0.442 | 0.060 ± 0.056 | 0.087 ± 0.057 | 0.119 ± 0.058 | 0.210 ± 0.147 | 0.160 ± 0.131 | 0.231 ± 0.240 | <b>0.0024</b>   | > 0.01          | > 0.01        | -0.4001 | 0.1395          |
| Desulfovibrio desulfuricans subsp. desulfuricans (T); Essex 6 | 0.598 | 0.000 ± 0.000 | 0.000 ± 0.000 | 0.163 ± 0.185 | 0.224 ± 0.219 | 0.321 ± 0.481 | 0.196 ± 0.107 | <b>0.0062</b>   | <b>0.0015</b>   | > 0.01        | -0.5678 | 0.0272          |
| Alistipes shahii (T); WAL 8301*                               | 0.714 | 0.147 ± 0.213 | 0.702 ± 0.557 | 0.030 ± 0.029 | 0.011 ± 0.016 | 0.123 ± 0.129 | 0.010 ± 0.014 | <b>0.0016</b>   | <b>0.0096</b>   | > 0.01        | 0.7849  | <b>0.0005</b>   |
| Bacillus funiculus (T); NAF001                                | 0.374 | 0.499 ± 0.552 | 0.331 ± 0.219 | 0.061 ± 0.054 | 0.033 ± 0.033 | 0.125 ± 0.263 | 0.010 ± 0.022 | <b>0.0067</b>   | <b>0.0020</b>   | > 0.01        | 0.1783  | <b>0.0026</b>   |
| Prevotella salivae (T); JCM 12084                             | 0.629 | 0.045 ± 0.044 | 0.064 ± 0.049 | 0.160 ± 0.148 | 0.258 ± 0.211 | 0.136 ± 0.091 | 0.083 ± 0.034 | <b>0.0042</b>   | > 0.01          | > 0.01        | -0.3489 | 0.2024          |
| Allobaculum stercoricanis (T); type strain: DSM 13633*        | 0.486 | 0.047 ± 0.051 | 0.032 ± 0.021 | 0.089 ± 0.052 | 0.139 ± 0.091 | 0.103 ± 0.061 | 0.309 ± 0.133 | > 0.01          | <b>0.0002</b>   | <b>0.0342</b> | -0.6706 | <b>0.0062</b>   |
| Blautia hydrogenotrophica (T); S5a36; X95624*                 | 0.705 | 0.553 ± 0.315 | 0.047 ± 0.057 | 0.061 ± 0.098 | 0.013 ± 0.030 | 0.121 ± 0.127 | 0.028 ± 0.033 | <b>0.0008</b>   | <b>0.0210</b>   | > 0.01        | 0.2509  | 0.3671          |
| Eubacterium ruminantium (T); GA195                            | 0.597 | 0.000 ± 0.000 | 0.036 ± 0.049 | 0.411 ± 0.572 | 0.188 ± 0.218 | 0.066 ± 0.101 | 0.000 ± 0.000 | <b>0.0061</b>   | > 0.01          | <b>0.0095</b> | -0.1940 | 0.4884          |
| Eubacterium rectale (T); L34627                               | 0.821 | 0.035 ± 0.036 | 0.026 ± 0.026 | 0.082 ± 0.083 | 0.129 ± 0.139 | 0.110 ± 0.127 | 0.262 ± 0.161 | > 0.01          | <b>0.0100</b>   | > 0.01        | -0.5151 | 0.0494          |
| Acetanaerobacterium elongatum (T); Z7*                        | 0.517 | 0.602 ± 0.518 | 0.136 ± 0.194 | 0.016 ± 0.035 | 0.027 ± 0.021 | 0.013 ± 0.018 | 0.086 ± 0.096 | <b>0.0067</b>   | <b>0.0129</b>   | > 0.01        | 0.3312  | 0.2278          |
| Allobaculum stercoricanis (T); type strain: DSM 13633         | 0.488 | 0.054 ± 0.107 | 0.052 ± 0.045 | 0.081 ± 0.077 | 0.122 ± 0.086 | 0.180 ± 0.095 | 0.172 ± 0.048 | > 0.01          | <b>0.0057</b>   | > 0.01        | -0.6647 | <b>0.0069</b>   |
| Bacteroides stercoris (T); ATCC 43183 (T).                    | 0.657 | 0.321 ± 0.412 | 0.258 ± 0.096 | 0.026 ± 0.032 | 0.005 ± 0.010 | 0.026 ± 0.041 | 0.007 ± 0.015 | < <b>0.0001</b> | < <b>0.0001</b> | > 0.01        | 0.9111  | < <b>0.0001</b> |
| Clostridium xylanolyticum (T); ATCC 4963                      | 0.758 | 0.494 ± 0.451 | 0.146 ± 0.157 | 0.000 ± 0.000 | 0.000 ± 0.000 | 0.000 ± 0.000 | 0.000 ± 0.000 | < <b>0.0001</b> | < <b>0.0001</b> | > 0.01        | 0.7265  | <b>0.0022</b>   |

\*These bacterial groups showed statistically significant interactions between iron treatment and genotype.

<sup>1</sup>Obtained with the SeqMatch tool of RDP.

**Table 12. Bacterial taxa affected by host genotype.**

| Bacterial taxa                             | Percent abundance of bacterial group [mean ± SD] for the different treatments |                           |                      |                           |                      |                           | <i>P</i> -value for factorial ANOVA | Correlations of bacterial taxa with histology scores |                 |
|--|---|---------------------------|----------------------|---------------------------|----------------------|---------------------------|-------------------------------------|--|-----------------|
|  | WT Fe ade, sham-inj.  | TNFΔARE Fe ade, sham-inj. | WT Fe def, sham-inj. | TNFΔARE Fe def, sham-inj. | WT Fe def, iron-inj. | TNFΔARE Fe def, iron-inj. |                                     | R  | <i>P</i> -value |
| Phylum level                               |   |                           |                      |                           |                      |                           |                                     |  |                 |
| Proteobacteria                             | 10.26 ± 3.69  | 5.14 ± 2.15               | 6.34 ± 3.02          | 5.08 ± 2.23               | 6.24 ± 1.32          | 4.87 ± 2.28               | <b>0.0024</b>                       | 0.0228   | 0.9356          |
| Family level                               |   |                           |                      |                           |                      |                           |                                     |  |                 |
| Helicobacteraceae                          | 4.60 ± 4.69   | 0.56 ± 0.61               | 2.93 ± 2.58          | 0.69 ± 0.50               | 2.06 ± 1.44          | 0.78 ± 0.96               | <b>0.0019</b>                       | -0.1184  | 0.6743          |
| Peptosreptococcaceae                       | 0.20 ± 0.24   | 1.35 ± 1.08               | 0.43 ± 0.17          | 0.82 ± 0.32               | 0.75 ± 0.22          | 1.00 ± 0.71               | <b>0.0023</b>                       | 0.2095   | 0.4536          |
| Genus level                                |   |                           |                      |                           |                      |                           |                                     |  |                 |
| <i>Helicobacter</i>                        | 4.27 ± 4.39   | 0.50 ± 0.58               | 2.70 ± 2.37          | 0.60 ± 0.44               | 1.87 ± 1.30          | 0.71 ± 0.87               | <b>0.0016</b>                       | -0.1190  | 0.6727          |
| <i>Peptosreptococcaceae Insertae Sedis</i> | 0.18 ± 0.20   | 1.28 ± 1.03               | 0.40 ± 0.16          | 0.75 ± 0.29               | 0.71 ± 0.19          | 0.94 ± 0.66               | <b>0.0025</b>                       | 0.2181   | 0.4349          |

## RESULTS

**Table 13. OTUs affected by genotype.**

| Highest match in RDP database (type strain)                   | Sequence similarity score to closest type strain <sup>1</sup> | Percent abundance of bacterial group [mean ± SD] for the different treatments |                           |                      |                           |                      |                           | <i>P</i> -value for factorial ANOVA | Correlations of bacterial taxa with histology scores |                 |
|---|---|---|---------------------------|----------------------|---------------------------|----------------------|---------------------------|-------------------------------------|--|-----------------|
|   |   | WT Fe ade, sham-inj.  | TNFΔARE Fe ade, sham-inj. | WT Fe def, sham-inj. | TNFΔARE Fe def, sham-inj. | WT Fe def, iron-inj. | TNFΔARE Fe def, iron-inj. |                                     | <i>R</i>   | <i>P</i> -value |
| <i>Helicobacter ganmani</i> (T); CMRI H02                     | 0.916   | 2.984 ± 3.193   | 0.313 ± 0.388             | 1.802 ± 1.699        | 0.333 ± 0.263             | 1.160 ± 0.903        | 0.499 ± 0.690             | <b>0.0018</b>                       | -0.1269  | 0.6522          |
| <i>Clostridium oroticum</i> (T); M59109*                      | 0.805   | 5.447 ± 3.306   | 0.050 ± 0.069             | 0.375 ± 0.316        | 0.347 ± 0.428             | 0.012 ± 0.017        | 0.136 ± 0.234             | <b>0.0027</b>                       | -0.3498  | 0.2013          |
| <i>Clostridium orbiscindens</i> (T); DSM 6740*                | 0.662   | 1.059 ± 0.366   | 0.421 ± 0.275             | 0.207 ± 0.197        | 0.769 ± 0.142             | 0.420 ± 0.199        | 0.308 ± 0.188             | <b>0.0028</b>                       | 0.6086   | 0.0161          |
| <i>Bacteroides eggerthii</i> (T); L16485*                     | 0.712   | 0.448 ± 0.701   | 0.430 ± 0.402             | 0.030 ± 0.034        | 0.009 ± 0.012             | 0.848 ± 0.369        | 0.020 ± 0.032             | <b>0.0093</b>                       | 0.7715   | <b>0.0008</b>   |
| <i>Allobaculum stercoricanis</i> (T); type strain: DSM 13633* | 0.515   | 0.000 ± 0.000   | 0.000 ± 0.000             | 0.024 ± 0.023        | 0.030 ± 0.042             | 0.000 ± 0.000        | 1.452 ± 1.632             | <b>0.0072</b>                       | -0.3288  | 0.2314          |
| <i>Bacteroides capillosus</i> (T); ATCC 29799                 | 0.614   | 0.041 ± 0.065   | 0.160 ± 0.066             | 0.117 ± 0.154        | 0.303 ± 0.157             | 0.399 ± 0.497        | 0.495 ± 0.213             | <b>0.0088</b>                       | -5932  | 0.0198          |
| <i>Clostridium oroticum</i> (T); M59109*                      | 0.760   | 1.572 ± 0.881   | 0.027 ± 0.060             | 0.116 ± 0.085        | 0.076 ± 0.037             | 0.019 ± 0.031        | 0.072 ± 0.103             | <b>0.0013</b>                       | -0.4056  | 0.1336          |
| <i>Clostridium oroticum</i> (T); M59109*                      | 0.746   | 1.231 ± 0.748   | 0.014 ± 0.019             | 0.124 ± 0.129        | 0.064 ± 0.058             | 0.005 ± 0.012        | 0.046 ± 0.067             | <b>0.0014</b>                       | -0.3527  | 0.1973          |
| <i>Helicobacter ganmani</i> (T); CMRI H02                     | 0.932   | 0.390 ± 0.380   | 0.041 ± 0.057             | 0.372 ± 0.361        | 0.065 ± 0.065             | 0.242 ± 0.167        | 0.080 ± 0.123             | <b>0.0027</b>                       | -0.2054  | 0.4627          |
| <i>Blautia hydrogenotrophica</i> (T); S5a36                   | 0.496   | 0.552 ± 0.170   | 0.090 ± 0.092             | 0.116 ± 0.166        | 0.005 ± 0.010             | 0.269 ± 0.231        | 0.042 ± 0.045             | <b>&lt; 0.0001</b>                  | 0.4554   | 0.0880          |
| <i>Faecalibacterium prausnitzii</i> (T); ATCC 27768*          | 0.879   | 0.070 ± 0.078   | 0.067 ± 0.082             | 0.080 ± 0.064        | 0.362 ± 0.137             | 0.163 ± 0.028        | 0.148 ± 0.086             | <b>0.0092</b>                       | -0.5749  | 0.0250          |
| <i>Helicobacter ganmani</i> (T); CMRI H02                     | 0.958   | 0.362 ± 0.366   | 0.035 ± 0.060             | 0.240 ± 0.310        | 0.042 ± 0.046             | 0.168 ± 0.116        | 0.054 ± 0.050             | <b>0.0046</b>                       | -0.0973  | 0.7302          |
| <i>Allobaculum stercoricanis</i> (T); type strain: DSM 13633* | 0.486   | 0.047 ± 0.051   | 0.032 ± 0.021             | 0.089 ± 0.052        | 0.139 ± 0.091             | 0.103 ± 0.061        | 0.309 ± 0.133             | <b>0.0086</b>                       | -0.6706  | <b>0.0062</b>   |
| <i>Blautia hydrogenotrophica</i> (T); S5a36; X95624*          | 0.705   | 0.553 ± 0.315   | 0.047 ± 0.057             | 0.061 ± 0.098        | 0.013 ± 0.030             | 0.121 ± 0.127        | 0.028 ± 0.033             | <b>0.0004</b>                       | 0.2509   | 0.3671          |
| <i>Helicobacter ganmani</i> (T); CMRI H02                     | 0.791   | 0.240 ± 0.256   | 0.042 ± 0.075             | 0.237 ± 0.202        | 0.028 ± 0.052             | 0.146 ± 0.139        | 0.073 ± 0.093             | <b>0.0091</b>                       | -0.06707   | 0.8123          |
| <i>Clostridium symbiosum</i> (T); M59112                      | 0.715   | 0.299 ± 0.608   | 0.000 ± 0.000             | 0.276 ± 0.378        | 0.012 ± 0.027             | 0.055 ± 0.105        | 0.000 ± 0.000             | <b>0.0091</b>                       | -0.2051  | 0.4633          |
| <i>Parabacteroides distasonis</i> (T); M86695*                | 0.724   | 0.597 ± 0.613   | 0.000 ± 0.000             | 0.000 ± 0.000        | 0.000 ± 0.000             | 0.078 ± 0.134        | 0.015 ± 0.022             | <b>0.0057</b>                       | -0.3185  | 0.2472          |

\*These bacterial groups showed statistically significant interactions between iron treatment and genotype.

<sup>1</sup>Obtained with the SeqMatch tool of RDP.

## RESULTS

**Table 14. Bacterial taxa affected by the interaction of iron treatment and genotype**

| Bacterial taxa | Percent abundance of bacterial group [mean ± SD] for the different treatments |                           |                      |                           |                      |                           | Interaction treatment genotype | Correlations of bacterial taxa with histology scores |                 |
|----------------|---|---------------------------|----------------------|---------------------------|----------------------|---------------------------|--------------------------------|--|-----------------|
|                | WT Fe ade, sham-inj.  | TNFΔARE Fe ade, sham-inj. | WT Fe def, sham-inj. | TNFΔARE Fe def, sham-inj. | WT Fe def, iron-inj. | TNFΔARE Fe def, iron-inj. | <i>P</i> -value                | <i>R</i>   | <i>P</i> -value |
| Genus level    |   |                           |                      |                           |                      |                           |                                |  |                 |
| <i>Dorea</i>   | 2.59 ± 1.39   | 0.14 ± 0.13               | 0.32 ± 0.26          | 0.42 ± 0.33               | 0.17 ± 0.17          | 0.22 ± 0.24               | <b>0.0003<sup>a</sup></b>      | -0.3674  | 0.178           |

<sup>a</sup> The significant difference was within the Fe ade, sham-inj.

**Table 15. Bacterial taxa affected by the interaction of iron treatment and genotype.**

| Closest related type strain                                  | Sequence similarity score to closest type strain <sup>1</sup> | Percent abundance of bacterial group [mean ± SD] for the different treatments |                           |                      |                           |                      |                           | Correlation parameters of bacterial taxa with histology scores |          |                 |
|--|---|---|---------------------------|----------------------|---------------------------|----------------------|---------------------------|--|----------|-----------------|
|  |   | WT Fe ade, sham-inj.  | TNFΔARE Fe ade, sham-inj. | WT Fe def, sham-inj. | TNFΔARE Fe def, sham-inj. | WT Fe def, iron-inj. | TNFΔARE Fe def, iron-inj. | <i>P</i> -value  | <i>R</i> | <i>P</i> -value |
| <i>Clostridium oroticum</i> (T); M59109                      | 0.805   | 5.447 ± 3.306   | 0.050 ± 0.069             | 0.375 ± 0.316        | 0.347 ± 0.428             | 0.012 ± 0.017        | 0.136 ± 0.234             | <b>&lt; 0.0001<sup>a</sup></b>                                 | -0.3498  | 0.2013          |
| <i>Bacteroides eggerthii</i> (T); L16485                     | 0.712   | 0.448 ± 0.701   | 0.430 ± 0.402             | 0.030 ± 0.034        | 0.009 ± 0.012             | 0.848 ± 0.369        | 0.020 ± 0.032             | <b>0.0020<sup>c</sup></b>                                      | 0.7715   | <b>0.0008</b>   |
| <i>Allobaculum stercoricanis</i> (T); type strain: DSM 13633 | 0.515   | 0.000 ± 0.000   | 0.000 ± 0.000             | 0.024 ± 0.023        | 0.030 ± 0.042             | 0.000 ± 0.000        | 1.452 ± 1.632             | <b>0.0013<sup>c</sup></b>                                      | -0.3288  | 0.2314          |
| <i>Clostridium oroticum</i> (T); M59109                      | 0.760   | 1.572 ± 0.881   | 0.027 ± 0.060             | 0.116 ± 0.085        | 0.076 ± 0.037             | 0.019 ± 0.031        | 0.072 ± 0.103             | <b>&lt; 0.0001<sup>a</sup></b>                                 | -0.4056  | 0.1336          |
| <i>Clostridium oroticum</i> (T); M59109                      | 0.748   | 0.037 ± 0.035   | 0.476 ± 0.360             | 0.356 ± 0.319        | 0.060 ± 0.088             | 0.381 ± 0.340        | 0.298 ± 0.236             | <b>0.0078<sup>a</sup></b>                                      | 0.4233   | 0.1140          |
| <i>Allobaculum stercoricanis</i> (T); DSM 13633 (T).         | 0.494   | 0.146 ± 0.192   | 0.050 ± 0.064             | 0.181 ± 0.158        | 0.237 ± 0.118             | 0.222 ± 0.100        | 0.566 ± 0.163             | <b>0.0057<sup>c</sup></b>                                      | -0.7037  | <b>0.0034</b>   |
| <i>Clostridium lituseburense</i> (T); M59107                 | 0.885   | 0.107 ± 0.083   | 0.085 ± 0.061             | 0.156 ± 0.090        | 0.481 ± 0.154             | 0.249 ± 0.163        | 0.215 ± 0.112             | <b>0.0098<sup>b</sup></b>                                      | -0.6560  | <b>0.0079</b>   |
| <i>Clostridium oroticum</i> (T); M59109                      | 0.746   | 1.231 ± 0.748   | 0.014 ± 0.019             | 0.124 ± 0.129        | 0.064 ± 0.058             | 0.005 ± 0.012        | 0.046 ± 0.067             | <b>0.0002<sup>a</sup></b>                                      | -0.3527  | 0.1973          |
| <i>Allobaculum stercoricanis</i> (T); type strain: DSM 13633 | 0.504   | 0.000 ± 0.000   | 0.000 ± 0.000             | 0.010 ± 0.014        | 0.031 ± 0.041             | 0.000 ± 0.000        | 1.036 ± 1.210             | <b>0.0097<sup>b</sup></b>                                      | -0.3217  | 0.2423          |
| <i>Faecalibacterium prausnitzii</i> (T); ATCC 27768          | 0.879   | 0.070 ± 0.078   | 0.067 ± 0.082             | 0.080 ± 0.064        | 0.362 ± 0.137             | 0.163 ± 0.028        | 0.148 ± 0.086             | <b>0.0008<sup>b</sup></b>                                      | -0.5749  | 0.0250          |
| <i>Alistipes shahii</i> (T); WAL 8301                        | 0.714   | 0.147 ± 0.213   | 0.702 ± 0.557             | 0.030 ± 0.029        | 0.011 ± 0.016             | 0.123 ± 0.129        | 0.010 ± 0.014             | <b>0.0057<sup>a</sup></b>                                      | 0.7849   | <b>0.0005</b>   |
| <i>Parabacteroides distasonis</i> (T); M86695                | 0.763   | 0.024 ± 0.055   | 0.215 ± 0.208             | 0.082 ± 0.085        | 0.068 ± 0.096             | 0.223 ± 0.179        | 0.016 ± 0.036             | <b>0.0010<sup>ac</sup></b>                                     | 0.5017   | 0.0567          |
| <i>Parabacteroides distasonis</i> (T); M86695                | 0.724   | 0.597 ± 0.613   | 0.000 ± 0.000             | 0.000 ± 0.000        | 0.000 ± 0.000             | 0.078 ± 0.134        | 0.015 ± 0.022             | <b>0.0065<sup>a</sup></b>                                      | -0.3185  | 0.2472          |

<sup>a</sup> The significant difference was within the Fe def, iron-inj.

<sup>b</sup> The significant difference was within the Fe ade, sham-inj.

<sup>c</sup> The significant difference was within the Fe ade, iron-inj.

<sup>1</sup> Obtained with the SeqMatch tool of RDP.

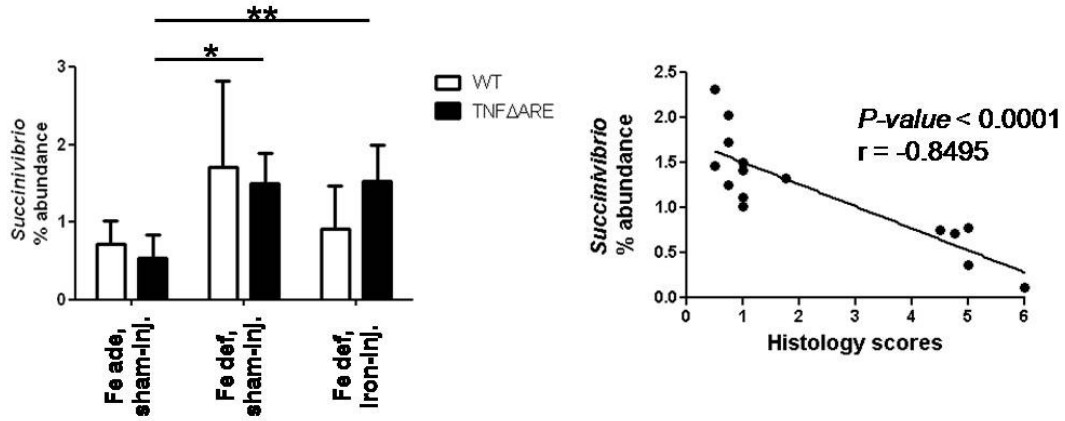


Figure 35. Proportions and correlation with histology score of TNF <sup>$\Delta$ ARE/WT</sup> mice of the genus *Succinivibrio*.

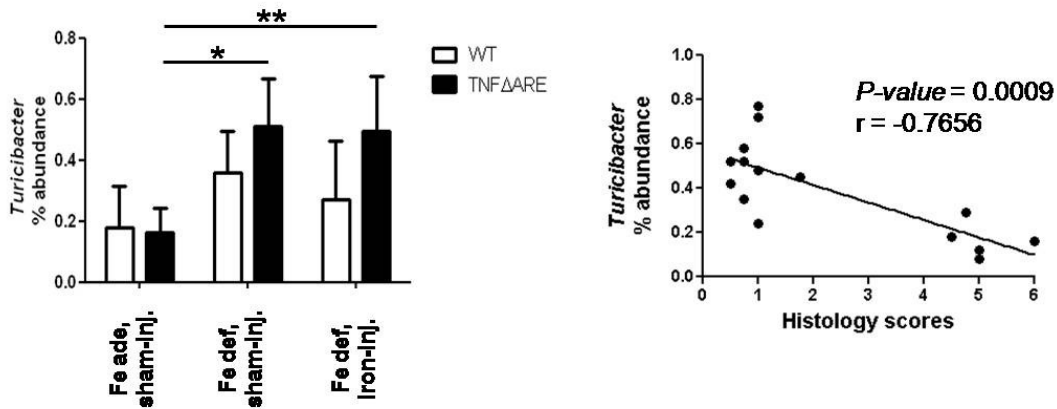


Figure 36. Proportions and correlation with histology score of TNF <sup>$\Delta$ ARE/WT</sup> mice of the genus *Turicibacter*.

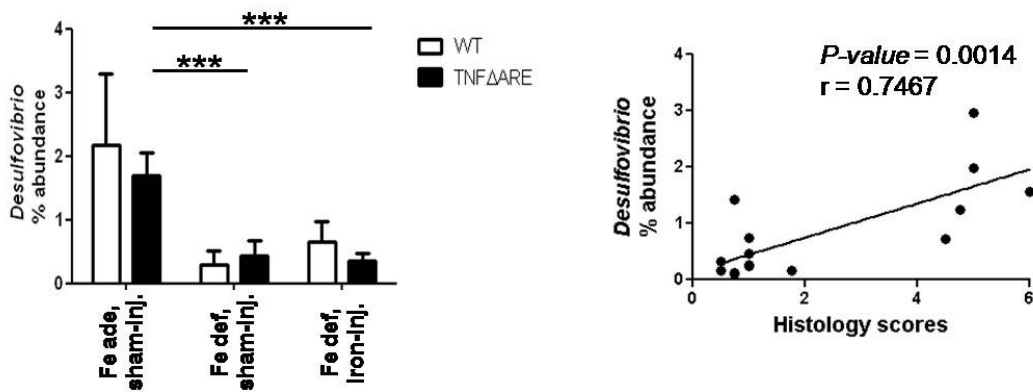


Figure 37. Proportions and correlation with histology score of TNF <sup>$\Delta$ ARE/WT</sup> mice of the genus *Desulfovibrio*.

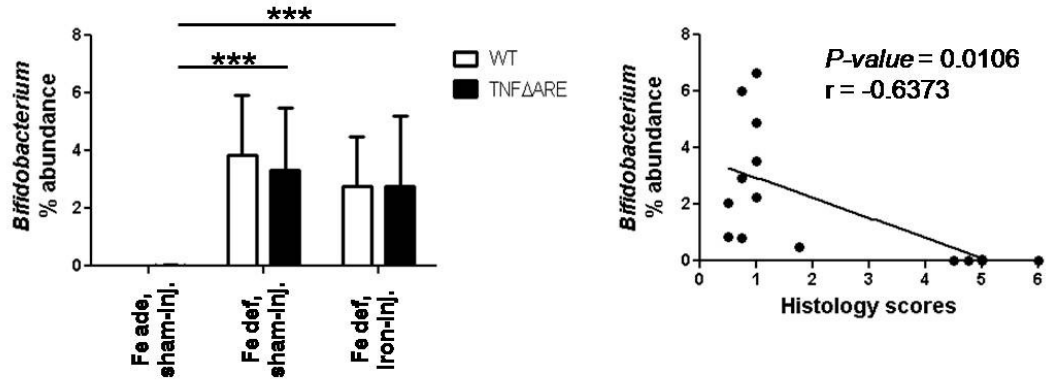


Figure 38. Proportions and correlation with histology score of TNF $\Delta$ ARE/WT mice of the genus *Bifidobacterium*.

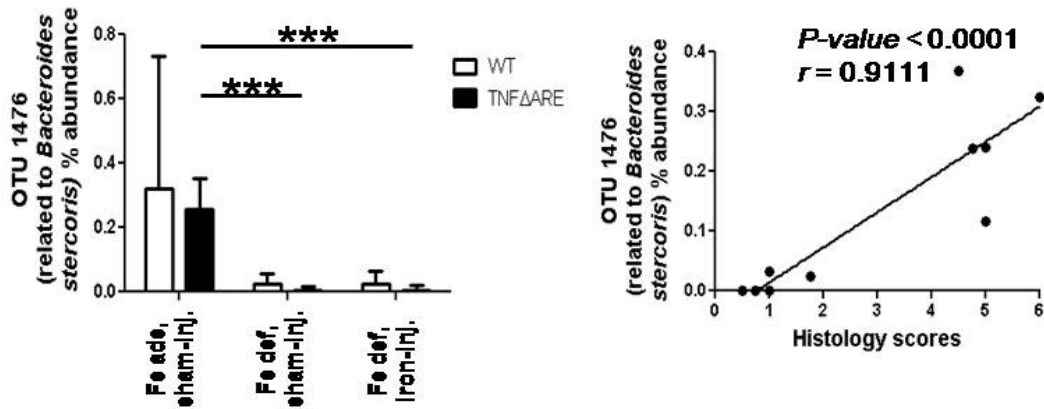


Figure 39. Proportions and correlation with histology score of TNF $\Delta$ ARE/WT mice of the OTU 1476 (distantly related to *Bacteroides stercoris*)

## 5 DISCUSSION

The aim of the present thesis was to investigate the role of iron as an environmental factor for the development of chronic ileitis in the  $\text{TNF}^{\Delta\text{ARE}/\text{WT}}$  mouse model. The findings clearly demonstrated that luminal, but not systemic iron contributes to the pathogenesis of chronic ileitis. The protective effect mediated by the iron-deficient diet implicated significant changes in the gut microbiome which importantly correlated with the histology score for specific bacterial groups. Furthermore, luminal iron deprivation affected regulation of proteins involved in energy metabolism, host defense and stress responses. In specific, the iron-deficient diet inhibited the induction of ER stress and apoptosis in the intestinal epithelium. This correlated with the results of *ex vivo* and *in vitro* experiments where iron was shown to be an inducer of ER stress and apoptosis in total ileal tissue and an IEC cell line. Most importantly, systemic iron repletion maintained the protective effect of the iron deficient diet. The systemic iron application did not reverse the iron-deficient diet mediated changes in the gut microbiome as well as down-regulation of ER stress and apoptosis in the epithelium.

### 5.1 Effects of an iron-deficient diet on the ileal IEC proteome of WT and $\text{TNF}^{\Delta\text{ARE}/\text{WT}}$ mice

In this part of the work, we characterized the protein expression profile in primary intestinal epithelial cells from the ileum of WT and  $\text{TNF}^{\Delta\text{ARE}/\text{WT}}$  mice fed with an iron-adequate and an iron-deficient diet. Histological analysis revealed severe inflammation of the distal ileum in the  $\text{TNF}^{\Delta\text{ARE}/\text{WT}}$  mice fed with the iron-adequate diet and the absence of ileitis in the iron-deficiently fed  $\text{TNF}^{\Delta\text{ARE}/\text{WT}}$  mice. In total, we identified 74 target proteins in primary IEC with significantly altered steady-state expression levels using 2D-gelelectrophoresis and peptide mass fingerprint via MALDI-TOF MS. Considering the fact that dietary ID dramatically altered the susceptibility of  $\text{TNF}^{\Delta\text{ARE}/\text{WT}}$  mice to develop chronic ileitis, we specifically analyzed the ade WT-ARE-comparison under inflamed conditions and the ARE-comparison under non-inflamed conditions. Interestingly, we identified 9 (Dak, cytokeratin 8, fructose-1.6-bisphosphatase, peroxiredoxin 1, superoxide dismutase, aconitase 2, catalase, intelectin 1, FAH) significantly regulated proteins overlapping between the two comparisons. Four of these proteins including aconitase 2, catalase, intelectin and FAH are contrary regulated between the ade WT-ARE-comparison and the ARE-comparison, suggesting an important effect of the iron-deficient diet on the expression of these proteins and therefore in the pathogenesis of chronic intestinal inflammation. Aconitase 2 and intelectin are up-regulated in the ade WT-ARE-comparison and down-regulated in the ARE-comparison, whereas catalase and FAH are down-regulated in the ade WT-ARE-comparison and up-regulated in the ARE-comparison. All 4 proteins are involved in pathways discussed in the pathogenesis of chronic intestinal inflammation including energy homeostasis, host defense, oxidative and ER stress responses [189].

Iron regulatory proteins (IRP) are key iron sensors to control cellular iron metabolism in vertebrates through iron-response element (IRE)-dependent post-transcriptional control. In iron-deficient cells, IRPs bind with high affinity to IREs resulting in the inhibition of mRNAs with 5'IREs and the stabilization of mRNAs containing 3'IREs [190-192]. The aconitase 2 (mitochondrial aconitase) contains a 5'IRE and an active  $[\text{Fe}_4\text{S}_4]^{2+}$  cluster [193, 194]. Interestingly, the cytosolic aconitase (aconitase 1), also containing an  $[\text{Fe}_4\text{S}_4]^{2+}$  cluster, is an IRE-binding protein which may regulate translation of mitochondrial aconitase mRNA [195]. Because of the down-regulation in the ARE-comparison as well as in the WT-comparison under the iron-deficient diet, we may conclude that its expression is controlled by the iron status of the cell leading to a down-regulation under iron-deficient conditions. Aconitase 2 is a mitochondrial enzyme playing a role in the citrate cycle for energy production.

It has been suggested that chronic intestinal inflammation represents an energy-deficiency disease with alterations in the oxidative metabolism of epithelial cells [196, 197]. Several enzymes participating in the glucose metabolism are up-regulated in the ade WT-ARE-comparison as well as in the ARE-comparison but only Dak is overlapping between the 2 comparisons. Proteins in the pathway to form dihydroxyacetone phosphate, including Dak, triosephosphate isomerase, fructose-bisphosphate aldolase B, glycerol-3-phosphate dehydrogenase and the triosephosphate isomerase required to convert dihydroxyacetone phosphate to glyceraldehyd-3-phosphate, are up-regulated in non-inflamed, iron-deficiently fed  $\text{TNF}^{\Delta\text{ARE}/\text{WT}}$  mice. Additionally, we identified mitochondrial creatine kinase and major enzymes of the  $\beta$ -oxidation as well as lysine catabolism such as enoyl coenzyme A hydratase 1, hydroxyacyl-coenzyme A dehydrogenase and HMG-CoA synthase as up-regulated in the ARE-comparison. The HMG-CoA synthase revealed a substantial induction with a regulation factor of 12.87 in the proteome analysis. This enhanced expression of proteins involved in glucose metabolism,  $\beta$ -oxidation and other pathways of energy production in the non-inflamed, iron-deficiently fed  $\text{TNF}^{\Delta\text{ARE}/\text{WT}}$  group support the hypothesis that the failure to maintain energy homeostasis is a critical factor in the pathogenesis of chronic intestinal inflammation. Although proteins that belong to pathways for energy production (Dak, aconitase 2, phosphoglycerate mutase 1, adenylate kinase and transketolase) are also up-regulated in the ade WT-ARE-comparison, these compensatory mechanisms seem to be insufficient to counteract the loss of energy under conditions of chronic inflammation. The  $\beta$ -oxidation might have specific importance as this pathway seems to be preferentially regulated under non-inflamed conditions whereas under inflamed conditions, proteins of the glycolysis are up-regulated but not for the  $\beta$ -oxidation.

Excessive ROS production is an accompanying effect of intestinal inflammation leading to tissue injury and impaired intestinal barrier function [198-200]. Therefore the mucosa contains an anti-oxidative defense system to counteract ROS accumulation. It has been shown that IBD-patients have decreased anti-oxidative defense mechanisms, a higher susceptibility to oxidative tissue damage and therefore an impaired epithelial layer integrity [144, 201].

Superoxide dismutase as well as catalase are major enzymes of the anti-oxidative defense mechanism catalyzing the decomposition of hydrogen peroxide to water and/or oxygen [202-204]. Both enzymes are heme-containing enzymes with ferrous iron in the center of the protoporphyrin IX ring [205]. Once iron has been transported into the mitochondrion it can be inserted into enzymes that belong to different metabolic pathways including heme biosynthesis [206] and [Fe-S] cluster formation [207]. Because of the down-regulation of aconitase 2 containing an active  $[\text{Fe}_4\text{S}_4]^{2+}$  cluster and the up-regulation of above mentioned heme-containing enzymes, heme biosynthesis seems to be preferred and therefore important to maintain cell homeostasis under the iron-deficient diet.

Catalase is a high-efficient enzyme for the degradation of  $\text{H}_2\text{O}_2$ , mainly expressed in cytoplasm, peroxisomes and in mitochondria [208]. Interestingly, an overexpression of catalase in MCF-7 (human breast adenocarcinoma cell line) cells resulted in improved elimination of intracellular ROS, decreased  $\text{H}_2\text{O}_2$ -mediated cytotoxicity, increased cell viability and impaired TNF induced NF- $\kappa$ B activation [209]. Consistent with these experimental findings, the up-regulation of catalase under luminal iron deprivation seems to have protective functions in primary IEC. In contrast to the ARE-comparison, the loss of catalase protein expression in the iron-adequately fed  $\text{TNF}^{\Delta\text{ARE}/\text{WT}}$  group may cause increased  $\text{H}_2\text{O}_2$  accumulation. Enhanced oxidative stress may affect barrier function and tissue integrity leading to the manifestation of chronic intestinal inflammation. Even the up-regulation of the anti-oxidative protein superoxide dismutase and peroxiredoxin 1 seems to be not effective in counteracting the loss of catalase.

Intelectin-1 is the human intestinal lactoferrin receptor located in the brush border membrane of Paneth and goblet cells with its ligand lactoferrin (Lf) playing a role in the innate immune response, antimicrobial activity and iron homeostasis [210]. It has been shown that intracellular iron depletion using an iron chelator resulted in up-regulation of the human lactoferrin receptor in HT-29 cells, supporting a function of intelectin in iron absorption [211]. Since human and mouse intelectin (mITLN) share 84.9% amino acid identity [212], mITLN could be involved in iron metabolism. However, our results rather indicate an ineffectiveness of iron depletion on mITLN-expression likely because of the down-regulation of mITLN under the iron-deficient diet. In the intestinal epithelium, bovine Lf (bLf) can induce the synthesis of pro-inflammatory cytokine interleukin-18 which by itself affects the expression of other pro-inflammatory cytokines including IFN- $\gamma$  in T- or NK-cells and TNF in human blood cells [213, 214]. An obvious but not proven interaction between bLf and the mITLN may be the enhanced production of pro-inflammatory cytokines. The up-regulation of mITLN in the ade WT-ARE-comparison could therefore worsen the situation of chronic intestinal inflammation and point to an imbalance between pro- and anti-inflammatory cytokine regulation at the IEC level. Down-regulation of mITLN in the iron-deficiently fed  $\text{TNF}^{\Delta\text{ARE}/\text{WT}}$  group may counteract inflammatory processes rather than interact in iron homeostasis.

Finally, we are focussing on FAH, a protein involved in the pathogenesis of hereditary tyrosenemia I (HTI), a serious disease of the tyrosine degradation pathway. FAH is responsible for the hydrolysis of

fumarylacetoacetate (FAA). The accumulation of FAA as it appears in HTI can lead to chromosomal instability, cell cycle arrest and apoptosis because of its mutagenic and cytotoxic properties [215-218]. Bergeron et al. showed that treatment of Chinese hamster lung cells with FAA resulted in the onset of ER stress mechanisms including the induction of the major ER chaperone grp78 and phosphorylation of eiF2 $\alpha$  as well as induction of pro-apoptotic CHOP and caspase-12 activation [219]. Liver tissue sections of FAH knock-out mice that develop the HTI phenotype after treatment with 2-(2-nitro-4-trifluoromethylbenzoyl)-1,3 cyclohexanedione also showed increased expression levels of grp78 and p-eiF2 $\alpha$  as well as induction of apoptosis. RNAi against the homolog of FAH in *C. elegans* produced a lethal phenotype with massive intestinal damage due to the induction of oxidative and ER stress responses [220]. Down-regulation of this enzyme as it appears in the ade WT-ARE-comparison could lead to the accumulation of FAA and as a consequence to the induction of ER stress. Additionally to the down-regulation of FAH, we found an up-regulation of the peptidyl-prolyl isomerase (PPI) A and D, also known as cyclophilins, playing a role in the acceleration of protein folding [221, 222]. An up-regulation of these enzymes could be an indicator for an accelerated protein folding machinery under inflammatory conditions. In conclusion, the failure to maintain energy levels, to abolish oxidative stress as well as maintain ER homeostasis may lead to stress-induced pathologies including IBD.

## **5.2 Luminal iron as environmental factor in the pathogenesis of CD-like ileitis**

We clearly demonstrated that an iron-deficient diet prevented the onset of severe ileitis. This long-term feeding protocol was accompanied by the depletion of non-heme iron stores in liver and spleen as well as significant lower Hc and Hb levels in blood. However, the application of an iron-deficient diet for 4 weeks in existing ileitis significantly reduced ileal histopathology, although hepatic iron stores were not significantly affected. Most importantly, iron repletion by weekly intraperitoneal iron injections maintained the protective effect of the iron-deficient diet, suggesting a critical role for dietary but not systemic iron in the pathogenesis of chronic ileitis in the genetically susceptible host. Bacterial composition was most dramatically influenced by luminal iron deprivation and to a lesser extent influenced by the host inflammatory response as well as systemic iron repletion. The iron-deficient diet as well as the iron repletion in the long-term prevention experiment had no influence on IEL phenotype of effector CD8 $\alpha\beta^+$  T cells but interestingly, co-culture experiments revealed a higher susceptibility of ER-stressed IEC towards cytotoxic T cell-induced apoptosis. Considering the emerging role of cellular stress mechanisms in the pathogenesis of IBD, we clearly demonstrated that the reduction of tissue pathology by iron-deficient feeding (long-term) as well as in the iron repletion situation was associated with reduced ER stress response mechanisms and apoptosis at the epithelial cell level. Iron-deficiently fed TNF<sup>ARE/WT</sup> mice almost completely lack ER stress responses and pro-apoptotic mechanisms in the epithelium. Consistent with the observation that iron triggers ER stress-

associated mechanisms in epithelial cell lines already at early time points, the induction of pro-apoptotic responses seemed to be a consequence of prolonged ER stress signalling in the epithelium. ChIP analysis of iron-stimulated Mode-K cells indicated recruitment of NRF2 and XBP-1, but not ATF6 to the grp-78 promoter suggesting iron as an inducer of specific ER stress signalling pathways.

Recent studies indicate that ER stress responses at the epithelial cell level play an important role in the pathogenesis of IBD (reviewed in [223]). In the present study, Western blot analysis of IEC from the long-term feeding and the injection experiment clearly showed induction of ER stress associated protein expression in the inflamed, iron-adequately fed TNF<sup>ΔARE/WT</sup> mice. This activation of ER stress and apoptosis occurred especially in crypt regions. Proliferation and differentiation of cells, building the intestinal epithelium, occurs in the crypt regions harbouring the stem cells [24]. Absence of activated ER stress responses and apoptotic processes in crypts on the iron-deficient diet may therefore have an important role on the development of a normal villus-crypt axis and epithelial barrier. The level of ER stress activation may help the IEC to cope with the stress situation and lead to adaptation rather than apoptosis.

The relation between iron and ER stress is discussed in the context of haptoglobin degradation in C57BL/6 mice [128], hereditary hemochromatosis [224, 225] and chronic hepatitis C infection [226], but to our knowledge, there are no studies published discussing the specific relation between iron-induced ER stress and IBD. *In vitro*, Nunez et al. showed up-regulation of calreticulin, as a molecular chaperone, in Caco-2 cells by iron-induced oxidative stress [227], linking oxidative stress to ER stress. In contrast, our *in vitro* results in Mode-K cells clearly demonstrated iron as potential inducer of ER stress associated grp-78 expression mainly independent of ROS formation.

The ability of free iron to produce ROS via the Fenton reaction can lead to oxidative stress and consecutive tissue damage. *In vitro* studies revealed effects of iron application on alteration of tight junction permeability, cell proliferation, caspase 3-activity and DNA damage [21, 228-230]. Regarding the enhanced caspase-3 activity in CaCo-2 cells, we showed the induction of cc3 protein expression in Mode-K cells suggesting iron as potential inducer of apoptosis in IEC. Correspondingly, iron chelation in the human retinal pigment epithelial cell line ARPE-19 showed to be protective against cell death [231].

Besides the pro-apoptotic property of iron on IEC, LPS-induced augmentation of paracellular permeability is enhanced by co-administration of iron-ascorbate in Caco-2 cells [232]. CD is associated with the loss of the intestinal barrier function [233-235], likely mediated through defects in the epithelial cell integrity. It has been shown that Th1 cytokines like INF- $\gamma$  or TNF which are symptomatic in CD contribute to the increase in intestinal permeability [236]. The down-regulation of TNF protein expression in total ileal tissue cultures of the iron-deficiently fed, sham-injected as well as iron-injected TNF<sup>ΔARE/WT</sup> mice may be protective against decreased intestinal permeability. In the context of increased epithelial permeability, bacterial translocation was demonstrated in CD patients

[237, 238]. Iron is essential for the host as well as commensal bacteria and pathogens. Hence, iron chelation during infection is a major defense mechanism of the host [239]. Accordingly, it has been shown that ID is to some extent protective against infections [240, 241].

The bacterial gut microbiota differs between healthy humans and IBD patients [242], and bacterial translocation and an increased microbial colonization of the mucosal surface is implemented in the pathogenesis of CD [237, 238]. Clearly, bacteria might drive ER stress and apoptosis, and iron deprivation might induce both compositional and functional changes within the gut microbiota that reduce bacterial exposure to the epithelium. Accordingly, our study revealed major alterations in microbial composition by the iron-deficient diet, while host genotype, inflammatory response, and systemic iron application had a minor effect. Furthermore, we found a highly significant association between bacterial groups affected by low luminal iron and inflammation. The highest correlations were found for *Succinivibrio*, *Bacteroides*, *Turicibacter*, *Desulfovibrio*, *Bifidobacterium* and OTU related to *Bacteroides stercoris*. Interestingly, *Desulfovibrio* spp., which decreased through luminal iron deprivation, produce toxic sulphides which have been suggested to contribute to pathogenesis in IBD. Florian et al. showed a higher abundance of *Desulfovibrio* in UC patients [243] whereas other groups reported decreased bifidobacterial faecal concentrations in CD patients [244, 245]. Interestingly, *Desulfovibrio* spp., has been found to be increased whereas *Bifidobacterium* ssp. was decreased in IBD cats [246]. *Bacteroides*, *Bifidobacteria*, *Prevotella* and *Clostridium* are also often discussed in context of IBD [247]. The iron-deficient diet did induce a significant increase in the abundance of bifidobacteria which are often used as probiotics and have shown to prevent inflammation in murine models of IBD [248]. Furthermore, the most striking association ( $r > 0.9$ ) between a bacterial group and inflammation was detected for OUT 1476 of the genus *Bacteroides*. Interestingly, this genus has clearly been associated with colitis in HLA-B27 transgenic rats (53). Therefore, the significant differences in the gut microbiota in animals on an iron-deficient diet may be important by itself because they may constitute a protective mechanism. In addition, decreased iron availability in the gut is also likely to affect both functionality and pathogenicity of the microbes. Foster et al. demonstrated increased bacterial invasion and survival of *Salmonella enteritidis* in Caco-2 cells with elevated iron status [249]. Administration of iron transferrin or iron alone enhanced the severity of infections, prolonged bacteraemia and increased bacterial colony forming units [250]. Although our analysis was not able to detect such functional differences and although the precise mechanism by which luminal iron deprivation may induce local tolerance in  $\text{TNF}^{\Delta\text{ARE}/\text{WT}}$  mice remains to be elucidated, the significant associations between bacterial populations and inflammation as detected in our study strongly suggest the bacteria as an important link between iron administration and alleviation of ileitis.

The  $\text{TNF}^{\Delta\text{ARE}/\text{WT}}$  mouse model is a  $\text{CD8}^+$  T cell-dependent model for Crohn's like IBD [178]. The TNF-driven CD phenotype in this animal model is characterized by a marked reduction of  $\text{CD8}\alpha\alpha$ -expressing IEL and increased presence of  $\text{CD8}\alpha\beta$  IEL as a newly identified effector T lymphocyte

fraction. Neither long-term luminal iron deprivation nor iron repletion affected the CD8 $\alpha\alpha^+$ /CD8 $\alpha\beta^+$  ratio, suggesting IEL independent mechanisms to support a tissue protective effect. Since ER stress sensitized the epithelium to cytotoxic T cell-induced apoptosis as shown by the co-culture experiments, the absence of ER stress in IEC rather than direct effects on IEL itself may be a protective mechanism mediated by the iron-deficient diet.

Iron supplementation may become ultimately necessary for the treatment of anemia as one of the most frequent complications in IBD. Based on our results, we speculate that an oral iron supplementation strategy may lead to an exacerbation of intestinal inflammation. In these experiments, ferrous sulfate was used as iron source in the diet. Since ferrous sulfate is used in oral preparations and is also recommended for food fortification by the WHO, this iron compound is of importance and may be critical for IBD patients. In healthy volunteers, oral supplementation with ferrous sulfate increased the production of free radicals in faeces [149]. There is clear evidence for a negative effect of oral iron supplementation on inflammation in different animal models (reviewed in [251]). In addition, Erichsen et al. showed an increased Crohn's disease activity index (CDAI) after the administration of oral ferrous fumarate compared to intravenous applied iron sucrose [252]. In DSS-induced colitis, systemic iron supplementation replenished iron stores without enhancing intestinal inflammation and colon carcinogenesis in contrast to an iron-enriched diet [253]. Although FeNTA is not applicable in human therapy, it resembles an iron-(III)-complex as other intravenous iron preparation and these compounds have become nowadays safe [254, 255] and seems to be more effective than oral supplementation [256].

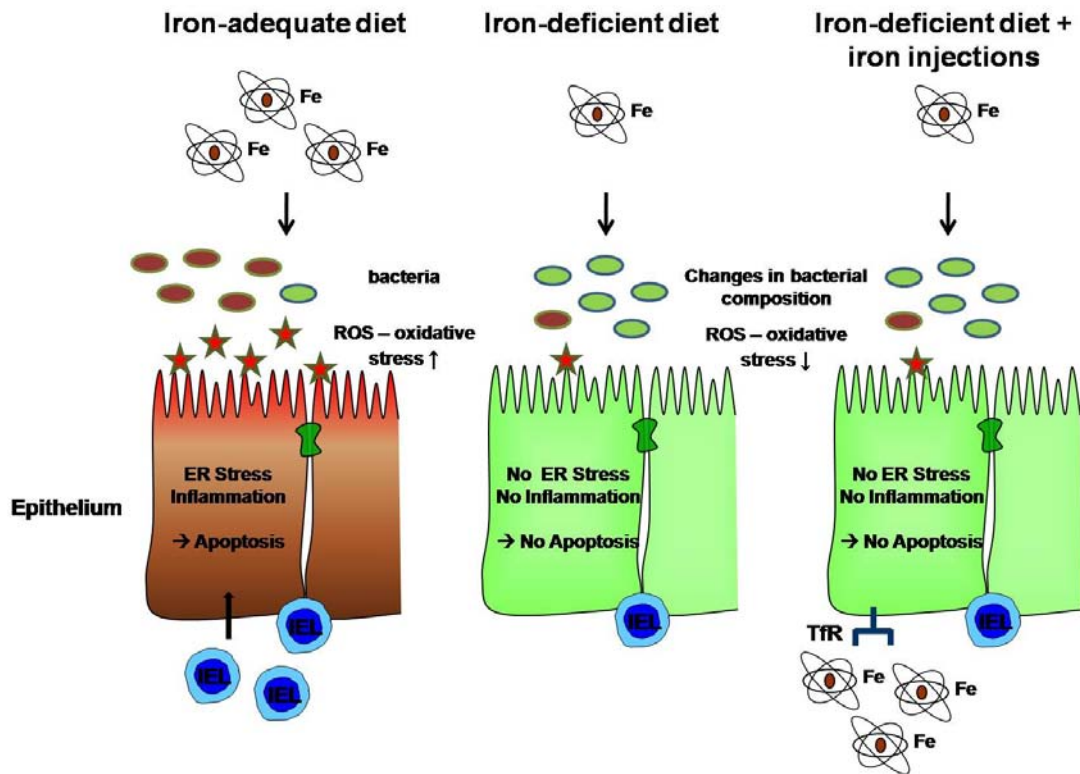


Figure 40. Summarizing overview of results.

This study presents for the first time a direct association between luminal iron as dietary factor and the pathogenesis of chronic ileitis in an animal model for ileal CD. The iron-deficient diet and most importantly, the combination with parenteral iron repletion was successful to maintain IEC homeostasis through mechanisms that target changes in the gut microbiota as well as ER-associated stress responses and apoptosis in the intestinal epithelium (Figure 41). These data may offer a new possibility for the simultaneous treatment of chronic intestinal inflammation and anemia in CD patients through modulation of the patients' iron status.

### 5.3 Outlook

Further experiments may include animal models for colitis, to elucidate the role of iron in the second major form of IBD. As iron is also discussed in cancer, an iron-deficient diet may also have protective effects on carcinogenesis.

Additionally, the pro-inflammatory potential of different dietary iron compounds should be tested, since in this animal trial, we only investigated the effects of iron sulphate as food iron source. Already ongoing studies test different food iron concentrations to investigate the iron-concentration in correlation to the histology grade of the mice.

It may be of thought to test oral application of iron chelators in combination with systemic iron application as this may also be a possible therapeutic approach for a human trial. Iron chelators already have been tested on UC biopsies to decrease ROS and therefore tissue damage. In the  $TNF^{\Delta ARE/WT}$  mice, it would be interesting to measure the oxidative burden at the side of inflammation to investigate the ROS-damaging effect and if the iron-deficient diet also act through the depletion of ROS production.

For the gut microbial ecology part, supplementary studies may imply experiments with single bacterial taxa which have been shown to correlate with the histology score in the present thesis. It would be the best approach to mono-associate germ-free  $TNF^{\Delta ARE/WT}$  mice with the bacterium of interest to elucidate the antigenic potential to drive inflammation, but to our knowledge, there are no germ-free  $TNF^{\Delta ARE/WT}$  mice available at the moment.

Besides iron, other metals and trace elements may also play a direct or indirect role in the pathogenesis of IBD. Copper and zinc could be candidates to have a look for. As osteoporosis and therefore calcium are problematic in IBD patients [257] and  $TNF^{\Delta ARE/WT}$  mice shown impaired expression of intestinal calcium transporters [258], this could also be a target.

## LIST OF FIGURES

|   |    |
|---|----|
| Figure 1. Schematic illustration of the GI tract (left) and cross section of the small intestine (right). .   | 13 |
| Figure 2. Overview of the GALT (modified from Magelhaes 2007 [24] and Haller 2008 [25]).  | 15 |
| Figure 3. Schematic overview of iron absorption, storage and transport in the enterocyte (modified from Gomollón et al. [44]).  | 18 |
| Figure 4. Transferrin-bound iron uptake via the TfR1 (from Anderson and Vulpe [50]).  | 19 |
| Figure 5. Overview of the regulation of systemic iron metabolism (from Vaulont et al. [80]).  | 22 |
| Figure 6. Overview of ER stress pathways.   | 26 |
| Figure 7. Classical pathway of NF-κB activation (from Gloire et al. [154]).   | 32 |
| Figure 8. Experimental setup of the feeding experiment.   | 48 |
| Figure 9. Histology of the feeding experiment.  | 49 |
| Figure 10. Overview of all performed proteome comparisons including numbers of significantly regulated proteins (*).  | 50 |
| Figure 11. Absence of CD3+T-cell contamination as confirmation for IEC purity.  | 51 |
| Figure 12. Representative Coomassie stained 2D-gels from the overlap between the adequate WT-ARE comparison and the ARE-comparison with similar regulated proteins (upper picture) and contrarily regulated proteins (lower picture). | 59 |
| Figure 13. Verification of proteome results for catalase and intelectin 1.  | 60 |
| Figure 14. Bibliometric data analysis of ade WT-ARE-comparison and ARE-comparison.  | 61 |
| Figure 15. Enhanced expression of proteins involved in inflammation, oxidative and ER-stress as well as apoptosis by the iron-adequate diet.  | 63 |
| Figure 16. Grp-78 immuno- and TUNEL-staining of distal ileum segments of TNF <sup>ΔARE/WT</sup> mice.   | 65 |
| Figure 17. Iron-mediated induction of pro-inflammatory, oxidative and ER stress as well as pro-apoptotic protein expression in total tissue.  | 66 |
| Figure 18. Iron-mediated induction of pro-inflammatory, oxidative and ER stress as well as pro-apoptotic protein expression in Mode-K cells.  | 67 |
| Figure 19. Partly ROS-independent iron-mediated induction of grp-78 protein expression.   | 68 |
| Figure 20. ChIP analysis in Mode-K cells after iron stimulation.  | 69 |
| Figure 21. Overview of short-term feeding experiment.   | 70 |
| Figure 22. Histology of the short-term feeding experiment.  | 70 |
| Figure 23. Overview of injection experiment.  | 71 |
| Figure 24. Histology and hepatic non-heme measurement of the injection experiment.  | 72 |
| Figure 25. Purity control of IEC isolation (left panel) and decrease of ER-stress and apoptosis by the reduction of dietary iron (right panel).   | 73 |
| Figure 26. Immuno- and TUNEL-staining of distal ileum segments of TNF <sup>ΔARE/WT</sup> mice from the injection experiment.  | 74 |
| Figure 27. ER stress protein- and TNF expression of total ileal tissue from TNF <sup>ΔARE/WT</sup> mice of the injection experiment.  | 75 |
| Figure 28. Histology and hepatic non-heme measurement of the repeated injection experiment.   | 76 |
| Figure 29. H&E staining of ileal tissue segments of the repeated injection experiment confirming histology  | 77 |
| Figure 30. Hematocrit (Hc) and hemoglobin (Hb) blood levels of all mice from the repeated injection experiment.   | 78 |
| Figure 31. Percental ratio of CD4 <sup>+</sup> , CD8αα <sup>+</sup> and CD8αβ <sup>+</sup> IEL of WT and TNF <sup>ΔARE/WT</sup> mice of the injection experiment.   | 79 |

## LIST OF FIGURES

---

|   |    |
|---|----|
| Figure 32. CD25 and CD69 expression of CD4 <sup>+</sup> , CD8αα <sup>+</sup> und CD8αβ <sup>+</sup> IEL from all TNF <sup>ΔARE/WT</sup> mice of the injection experiment.....                   | 80 |
| Figure 33A + B. Co-culture experiment of cytotoxic CD8αβ <sup>+</sup> T cells with Mode-K cells.....  | 81 |
| Figure 34. Score plot of the PCA analysis based on the proportions of the dominant bacterial groups at the genus taxonomic level as identified by the RDP classifier, colored by treatment..... | 82 |
| Figure 35. Proportions and correlation with histology score of TNF <sup>ΔARE/WT</sup> mice of the genus <i>Succinivibrio</i> .....  | 89 |
| Figure 36. Proportions and correlation with histology score of TNF <sup>ΔARE/WT</sup> mice of the genus <i>Turicibacter</i> .....   | 89 |
| Figure 37. Proportions and correlation with histology score of TNF <sup>ΔARE/WT</sup> mice of the genus <i>Desulfovibrio</i> .....  | 89 |
| Figure 38. Proportions and correlation with histology score of TNF <sup>ΔARE/WT</sup> mice of the genus <i>Bifidobacterium</i> .....  | 90 |
| Figure 39. Proportions and correlation with histology score of TNF <sup>ΔARE/WT</sup> mice of the OTU 1476 (distantly related to <i>Bacteroides stercoris</i> ).....                            | 90 |
| Figure 40. Summarizing overview of results. ....  | 98 |

**LIST OF TABLES**

|  |    |
|--|----|
| Table 1. Degree of ID evaluated by serum ferritin or transferring saturation (from [140]) .....  | 29 |
| Table 2. Preparations for intravenous iron therapy (modified from [160]).....  | 31 |
| Table 3. List of used antibodies.....  | 38 |
| Table 4. List of used primers with sequences (SYBR and UPL) .....  | 42 |
| Table 5. ade WT-ARE-comparison: differentially regulated proteins in IEC from iron-adequately fed TNF <sup>ΔARE/WT</sup> mice compared to iron-adequately fed WT mice .....              | 51 |
| Table 6. ARE-comparison: differentially regulated proteins in IEC from iron-deficiently fed TNF <sup>ΔARE/WT</sup> mice compared to iron-adequately fed TNF <sup>ΔARE/WT</sup> mice..... | 54 |
| Table 7. WT-comparison: differentially regulated proteins in IEC from iron-deficiently fed WT mice compared to iron-adequately fed WT mice.....  | 56 |
| Table 8. def WT-ARE-comparison: differentially regulated proteins in IEC from iron-deficiently fed TNF <sup>ΔARE/WT</sup> mice compared to iron-deficiently fed WT mice.....             | 56 |
| Table 9. Abbreviations for Bibliometric data analysis (Figure 14).....   | 62 |
| Table 10. Bacterial taxa affected by iron treatment .....  | 84 |
| Table 11. OTUs affected by iron treatment.....   | 85 |
| Table 12. Bacterial taxa affected by host genotype.....  | 86 |
| Table 13. OTUs affected by genotype.....   | 87 |
| Table 14. Bacterial taxa affected by the interaction of iron treatment and genotype .....  | 88 |
| Table 15. Bacterial taxa affected by the interaction of iron treatment and genotype.....   | 88 |

## ABBREVIATIONS

|        |  |
|--------|--|
| ABC    | ATP-binding cassette   |
| ACD    | anemia of chronic disease  |
| ACI/D  | anemia of chronic inflammation/disease   |
| APC    | antigen presenting cell  |
| ARE    | antioxidative response elements  |
| ASK1   | apoptosis signal-regulating kinase 1   |
| ATF4   | activating transcription factor 4  |
| ATF6   | activating transcription factor 6  |
| BMP    | bone morphogenetic protein   |
| C/EBP  | cAMP response element-binding transcription factor   |
| CARD   | caspase recruitment domain-containing protein  |
| cc3    | cleaved caspase 3  |
| CD     | Crohn's disease  |
| CHOP   | C/EBP homologues protein   |
| Dak    | dihydroxyacetone kinase  |
| DC     | dendritic cell   |
| DLG5   | discs large homolog 5  |
| DMT-1  | divalent metalloprotein transporter 1  |
| DNBS   | dinitro-benzene-sulphonic acid   |
| DSS    | dextrane sulfate sodium  |
| DyctB  | duodenal cytochrom B   |
| EGCG   | epigallocatechin-gallate   |
| ER     | endoplasmic reticulum  |
| ERAD   | ER-associated degradation complex  |
| ERSE   | ER stress response elements  |
| FAA    | fumarylacetoacetate  |
| FAH    | fumarylacetoacetate hydrolase  |
| FeNTA  | Fe(NO <sub>3</sub> ) <sub>3</sub> -complexed with nitrilotriacetic acid (NTA) in a 1:2 ratio |
| Fe-S   | iron-sulfur  |
| GADD34 | growth-arrest DNA damage gene 34   |

## ABBREVIATIONS

---

|                |                                     |
|----------------|-------------------------------------|
| GALT           | gut-associated lymphoid tissue      |
| GI             | gastrointestinal                    |
| grp-78         | glucose related protein-78          |
| GrzmB          | granzyme B                          |
| h              | hour                                |
| H&E            | hematoxylin and eosin               |
| HAMP           | hepcidin antimicrobial peptide      |
| Hb             | hemoglobin                          |
| Hc             | hematocrit                          |
| HFE            | hemochromatosis (High Iron Fe)      |
| HH             | hereditary hemochromatosis          |
| HIF-1 $\alpha$ | hypoxia-inducible factor-1 $\alpha$ |
| HJV            | hemojuvelin                         |
| HMG-CoA        | hydroxymethylglutaryl-CoA           |
| HO-1           | heme oxygenase-1                    |
| HTI            | hereditary tyrosenemia I            |
| IBD            | inflammatory bowel disease          |
| ICAM-1         | intercellular adhesion molecule-1   |
| ID             | iron deficiency                     |
| IEC            | intestinal epithelial cell          |
| IEL            | intraepithelial lymphocyte          |
| IgA            | immunoglobuline A                   |
| IKK            | inhibitor $\kappa$ B kinase         |
| IL             | interleukin                         |
| IRE            | iron responsive element             |
| IRE1           | inositol-requiring enzyme 1         |
| IRP            | iron regulatory protein             |
| I $\kappa$ B   | inhibitor of $\kappa$ B             |
| k.o.           | knock out                           |
| Lf             | lactoferrin                         |
| LP             | lamina propria                      |

## ABBREVIATIONS

---

|         |  |
|---------|--|
| LPL     | lamina propria lymphocyte                          |
| LPO     | lipide peroxidase                                  |
| LPS     | lipopolysaccharide                                 |
| MAMP    | microbial associated molecular pattern             |
| M cell  | microfold cell                                     |
| MAPKK   | mitogen-activated protein kinase kinase            |
| Mfn     | mitoferrin   |
| MHC     | major histocompatibility complex                   |
| min     | minute   |
| mITLN   | mouse intelectin                                   |
| MLN     | mesenteric lymph node                              |
| MØ      | macrophage   |
| MPO     | myeloperoxidase                                    |
| MT      | metallothionein                                    |
| NAC     | N-Acetylcysteine                                   |
| NADPH   | nicotinamide adenine dinucleotide phosphate        |
| NEMO    | NF-κB essential modulator                          |
| NF-κB   | nuclear factor κB                                  |
| NOD     | nucleotide-binding oligomerization domain          |
| NRAMP-1 | natural resistance-associated macrophage protein-1 |
| NRF2    | nuclear related factor 2                           |
| OCTN    | organic cation transporter                         |
| ON      | over night   |
| PAMP    | pathogen-associated molecular patterns             |
| PCBP1   | poly (rC) binding protein 1                        |
| PERK    | ER kinase-like ER-associated kinase                |
| PP      | Peyer´s Patch                                      |
| PRM     | pattern recognition molecules                      |
| PRR     | pattern recognition receptors                      |
| RAG     | recombinase activating gene-1                      |
| ROI     | reactive oxygen intermediates                      |

## ABBREVIATIONS

---

|              |                                     |
|--------------|-------------------------------------|
| ROS          | reactive oxygen species             |
| sec          | second                              |
| SOD          | superoxide dismutase                |
| TfR          | transferrin receptor                |
| TGF- $\beta$ | transforming growth factor $\beta$  |
| TLR          | toll-like receptor                  |
| Tm           | Tunicamycin                         |
| TNBS         | 2,4,6-trinitrobenzene sulfonic acid |
| TNF          | tumor necrosis factor $\alpha$      |
| TRAF2        | TNF receptor-associated factor 2    |
| UC           | Ulcerative colitis                  |
| UPR          | unfolded protein response           |
| UPRE         | UPR elements                        |
| VCAM-1       | vascular cell adhesion molecule-1   |
| VCP          | valosin containing protein          |
| WHO          | World Health Organisation           |
| XBP1         | X-box protein 1                     |

## REFERENCES

1. Oldenburg B, Koningsberger JC, et al. Iron and inflammatory bowel disease. *Aliment Pharmacol Ther* 2001;15(4):429-38.
2. Cazzola M, Bergamaschi G, et al. Manipulations of cellular iron metabolism for modulating normal and malignant cell proliferation: achievements and prospects. *Blood* 1990;75(10):1903-19.
3. Stein RS. Letter: Iron deficiency and infection. *Lancet* 1974;2(7896):1567.
4. Pakhomov Iu N. [The effect of Zn and Fe deficiency on the immunobiological reactivity of the organism]. *Gig Sanit* 1969;34(12):33-5.
5. Toyokuni S. Iron and carcinogenesis: from Fenton reaction to target genes. *Redox Rep* 2002;7(4):189-97.
6. Stohs SJ, Bagchi D. Oxidative mechanisms in the toxicity of metal ions. *Free Radic Biol Med* 1995;18(2):321-36.
7. Hunt JR, Roughead ZK. Adaptation of iron absorption in men consuming diets with high or low iron bioavailability. *Am J Clin Nutr* 2000;71(1):94-102.
8. Benito P MD. Iron absorption and bioavailability: an update review. *Nutr Res* 1998;18:581-603.
9. Bowman BA, RM R. Present knowledge in nutrition. Washington DC: ILSI Press; 2001.
10. Lopez MA, Martos FC. Iron availability: An updated review. *Int J Food Sci Nutr* 2004;55(8):597-606.
11. Hallberg L, Rossander-Hulthen L, et al. Inhibition of haem-iron absorption in man by calcium. *Br J Nutr* 1993;69(2):533-40.
12. Zimmermann MB, Hurrell RF. Nutritional iron deficiency. *Lancet* 2007;370(9586):511-20.
13. WHO. Guidelines on food fortification with micronutrients. Geneva, Switzerland: World Health Organization; 2006.
14. Friend D. Oral Colon-Specific Drug Delivery; 1992.
15. Savage DC. Microbial ecology of the gastrointestinal tract. *Annu Rev Microbiol* 1977;31:107-33.
16. Sartor RB. Microbial influences in inflammatory bowel diseases. *Gastroenterology* 2008;134(2):577-94.
17. Koster W. ABC transporter-mediated uptake of iron, siderophores, heme and vitamin B12. *Res Microbiol* 2001;152(3-4):291-301.
18. Zarantonelli ML, Szatanik M, et al. Transgenic mice expressing human transferrin as a model for meningococcal infection. *Infect Immun* 2007;75(12):5609-14.
19. Schaible UE, Collins HL, et al. Correction of the iron overload defect in beta-2-microglobulin knockout mice by lactoferrin abolishes their increased susceptibility to tuberculosis. *J Exp Med* 2002;196(11):1507-13.
20. Tompkins GR, O'Dell NL, et al. The effects of dietary ferric iron and iron deprivation on the bacterial composition of the mouse intestine. *Curr Microbiol* 2001;43(1):38-42.
21. Zodi B, Sargazi M, et al. Toxicological effects of iron on intestinal cells. *Cell Biochem Funct* 2004;22(3):143-7.
22. Bernotti S, Seidman E, et al. Inflammatory reaction without endogenous antioxidant response in Caco-2 cells exposed to iron/ascorbate-mediated lipid peroxidation. *Am J Physiol Gastrointest Liver Physiol* 2003;285(5):G898-906.
23. Courtois F, Suc I, et al. Iron-ascorbate alters the efficiency of Caco-2 cells to assemble and secrete lipoproteins. *Am J Physiol Gastrointest Liver Physiol* 2000;279(1):G12-9.
24. Daniele B, D'Agostino L. Proliferation and differentiation of the small intestinal epithelium: from Petri dish to bedside. *Ital J Gastroenterol* 1994;26(9):459-70.
25. Kraehenbuhl JP, Neutra MR. Epithelial M cells: differentiation and function. *Annu Rev Cell Dev Biol* 2000;16:301-32.
26. Walker WA. Development of the intestinal mucosal barrier. *J Pediatr Gastroenterol Nutr* 2002;34 Suppl 1:S33-9.
27. Ouellette AJ, Selsted ME. Paneth cell defensins: endogenous peptide components of intestinal host defense. *Faseb J* 1996;10(11):1280-9.

28. Wang S, Liu J, et al. Individual subtypes of enteroendocrine cells in the mouse small intestine exhibit unique patterns of inositol 1,4,5-trisphosphate receptor expression. *J Histochem Cytochem* 2004;52(1):53-63.
29. Neutra MR. Current concepts in mucosal immunity. V Role of M cells in transepithelial transport of antigens and pathogens to the mucosal immune system. *Am J Physiol* 1998;274(5 Pt 1):G785-91.
30. Carter PB, Collins FM. The route of enteric infection in normal mice. *J Exp Med* 1974;139(5):1189-203.
31. Magalhaes JG, Tattoli I, et al. The intestinal epithelial barrier: how to distinguish between the microbial flora and pathogens. *Semin Immunol* 2007;19(2):106-15.
32. Haller D. Mehr als nur ein Bollwerk - Das Darmepithel als integraler Bestandteil der Barriere und Abwehrfunktion im Darm. *Aktuel Ernähr Med* 2008;33(Supplement 1):S7 - S10.
33. Janeway, editor. Immunologie: Spektrum Akademischer Verlag; 2009.
34. Nagler-Anderson C. Man the barrier! Strategic defences in the intestinal mucosa. *Nat Rev Immunol* 2001;1(1):59-67.
35. Brandtzaeg P. Overview of the mucosal immune system. *Curr Top Microbiol Immunol* 1989;146:13-25.
36. Saldanha-Araujo F, Souza AM. Early effects on T lymphocyte response to iron deficiency in mice. Short communication. *Biol Trace Elem Res* 2009;127(2):95-101.
37. Kuvibidila S BS. Role of Iron in Immunity and Infection. In: P.C. Calder CJFaHSG, editor. Nutrition and Immune Function. London, UK: CABI Publishing; 2002. p. 209-217.
38. Neutra MR, Mantis NJ, et al. Collaboration of epithelial cells with organized mucosal lymphoid tissues. *Nat Immunol* 2001;2(11):1004-9.
39. Niess JH, Brand S, et al. CX3CR1-mediated dendritic cell access to the intestinal lumen and bacterial clearance. *Science* 2005;307(5707):254-8.
40. Framson PE, Cho DH, et al. Polarized expression and function of the costimulatory molecule CD58 on human intestinal epithelial cells. *Gastroenterology* 1999;116(5):1054-62.
41. Toy LS, Yio XY, et al. Defective expression of gp180, a novel CD8 ligand on intestinal epithelial cells, in inflammatory bowel disease. *J Clin Invest* 1997;100(8):2062-71.
42. Hershberg RM, Framson PE, et al. Intestinal epithelial cells use two distinct pathways for HLA class II antigen processing. *J Clin Invest* 1997;100(1):204-15.
43. Campbell NA, Kim HS, et al. The nonclassical class I molecule CD1d associates with the novel CD8 ligand gp180 on intestinal epithelial cells. *J Biol Chem* 1999;274(37):26259-65.
44. Abreu MT, Fukata M, et al. TLR signaling in the gut in health and disease. *J Immunol* 2005;174(8):4453-60.
45. Hisamatsu T, Suzuki M, et al. CARD15/NOD2 functions as an antibacterial factor in human intestinal epithelial cells. *Gastroenterology* 2003;124(4):993-1000.
46. Yang SK, Eckmann L, et al. Differential and regulated expression of C-X-C, C-C, and C-chemokines by human colon epithelial cells. *Gastroenterology* 1997;113(4):1214-23.
47. Campbell KJ, Perkins ND. Regulation of NF-kappaB function. *Biochem Soc Symp* 2006(73):165-80.
48. Tsuji NM, Kosaka A. Oral tolerance: intestinal homeostasis and antigen-specific regulatory T cells. *Trends Immunol* 2008;29(11):532-40.
49. Gomollon F, Gisbert JP. Anemia and digestive diseases: an update for the clinician. *World J Gastroenterol* 2009;15(37):4615-6.
50. Munoz Gomez M, Campos Garriguez A, et al. [Fisiopathology of iron metabolism: diagnostic and therapeutic implications]. *Nefrologia* 2005;25(1):9-19.
51. Oates PS, West AR. Heme in intestinal epithelial cell turnover, differentiation, detoxification, inflammation, carcinogenesis, absorption and motility. *World J Gastroenterol* 2006;12(27):4281-95.
52. Keel SB, Doty RT, et al. A heme export protein is required for red blood cell differentiation and iron homeostasis. *Science* 2008;319(5864):825-8.
53. McKie AT, Marciani P, et al. A novel duodenal iron-regulated transporter, IREG1, implicated in the basolateral transfer of iron to the circulation. *Mol Cell* 2000;5(2):299-309.
54. Wessling-Resnick M. Iron imports. III. Transfer of iron from the mucosa into circulation. *Am J Physiol Gastrointest Liver Physiol* 2006;290(1):G1-6.
55. Anderson GJ, Vulpe CD. Mammalian iron transport. *Cell Mol Life Sci* 2009;66(20):3241-61.

56. Zhang AS, Sheftel AD, et al. The anemia of "haemoglobin-deficit" (hbd/hbd) mice is caused by a defect in transferrin cycling. *Exp Hematol* 2006;34(5):593-8.
57. Kawabata H, Yang R, et al. Molecular cloning of transferrin receptor 2. A new member of the transferrin receptor-like family. *J Biol Chem* 1999;274(30):20826-32.
58. Deaglio S, Capobianco A, et al. Structural, functional, and tissue distribution analysis of human transferrin receptor-2 by murine monoclonal antibodies and a polyclonal antiserum. *Blood* 2002;100(10):3782-9.
59. Gunshin H, Fujiwara Y, et al. Slc11a2 is required for intestinal iron absorption and erythropoiesis but dispensable in placenta and liver. *J Clin Invest* 2005;115(5):1258-66.
60. Wassell J. Haptoglobin: function and polymorphism. *Clin Lab* 2000;46(11-12):547-52.
61. Tolosano E, Altruda F. Hemopexin: structure, function, and regulation. *DNA Cell Biol* 2002;21(4):297-306.
62. Fabriek BO, Dijkstra CD, et al. The macrophage scavenger receptor CD163. *Immunobiology* 2005;210(2-4):153-60.
63. Hvidberg V, Maniecki MB, et al. Identification of the receptor scavenging hemopexin-heme complexes. *Blood* 2005;106(7):2572-9.
64. Kruszewski M. Labile iron pool: the main determinant of cellular response to oxidative stress. *Mutat Res* 2003;531(1-2):81-92.
65. Prohaska JR, Gybina AA. Intracellular copper transport in mammals. *J Nutr* 2004;134(5):1003-6.
66. Shi H, Bencze KZ, et al. A cytosolic iron chaperone that delivers iron to ferritin. *Science* 2008;320(5880):1207-10.
67. Rouault TA, Tong WH. Iron-sulphur cluster biogenesis and mitochondrial iron homeostasis. *Nat Rev Mol Cell Biol* 2005;6(4):345-51.
68. Ajioka RS, Phillips JD, et al. Biosynthesis of heme in mammals. *Biochim Biophys Acta* 2006;1763(7):723-36.
69. Paradkar PN, Zumbrennen KB, et al. Regulation of mitochondrial iron import through differential turnover of mitoferrin 1 and mitoferrin 2. *Mol Cell Biol* 2009;29(4):1007-16.
70. Sheftel AD, Zhang AS, et al. Direct interorganellar transfer of iron from endosome to mitochondrion. *Blood* 2007;110(1):125-32.
71. Pantopoulos K. Iron metabolism and the IRE/IRP regulatory system: an update. *Ann N Y Acad Sci* 2004;1012:1-13.
72. Rouault TA. The role of iron regulatory proteins in mammalian iron homeostasis and disease. *Nat Chem Biol* 2006;2(8):406-14.
73. Ponka P, Beaumont C, et al. Function and regulation of transferrin and ferritin. *Semin Hematol* 1998;35(1):35-54.
74. Gunshin H, Allerson CR, et al. Iron-dependent regulation of the divalent metal ion transporter. *FEBS Lett* 2001;509(2):309-16.
75. Abboud S, Haile DJ. A novel mammalian iron-regulated protein involved in intracellular iron metabolism. *J Biol Chem* 2000;275(26):19906-12.
76. Melefors O, Goossen B, et al. Translational control of 5-aminolevulinic synthase mRNA by iron-responsive elements in erythroid cells. *J Biol Chem* 1993;268(8):5974-8.
77. Weiss G. Modification of iron regulation by the inflammatory response. *Best Pract Res Clin Haematol* 2005;18(2):183-201.
78. Lok CN, Ponka P. Identification of a hypoxia response element in the transferrin receptor gene. *J Biol Chem* 1999;274(34):24147-52.
79. Yeh KY, Yeh M, et al. Dietary iron induces rapid changes in rat intestinal divalent metal transporter expression. *Am J Physiol Gastrointest Liver Physiol* 2000;279(5):G1070-9.
80. Johnson MB, Chen J, et al. Transferrin receptor 2: evidence for ligand-induced stabilization and redirection to a recycling pathway. *Mol Biol Cell* 2007;18(3):743-54.
81. Enns C. Transferrin receptor. In: Molecular and cellular iron transport. New York: Marcel Dekker; 2001. p. 71-94.
82. Nemeth E, Tuttle MS, et al. Hepcidin regulates cellular iron efflux by binding to ferroportin and inducing its internalization. *Science* 2004;306(5704):2090-3.
83. Gunshin H, Starr CN, et al. Cybrd1 (duodenal cytochrome b) is not necessary for dietary iron absorption in mice. *Blood* 2005;106(8):2879-83.

84. Donovan A, Lima CA, et al. The iron exporter ferroportin/Slc40a1 is essential for iron homeostasis. *Cell Metab* 2005;1(3):191-200.
85. Vulont S, Lou DQ, et al. Of mice and men: the iron age. *J Clin Invest* 2005;115(8):2079-82.
86. Fleming RE, Ahmann JR, et al. Targeted mutagenesis of the murine transferrin receptor-2 gene produces hemochromatosis. *Proc Natl Acad Sci U S A* 2002;99(16):10653-8.
87. Bahram S, Gilfillan S, et al. Experimental hemochromatosis due to MHC class I HFE deficiency: immune status and iron metabolism. *Proc Natl Acad Sci U S A* 1999;96(23):13312-7.
88. Andriopoulos B, Jr., Corradini E, et al. BMP6 is a key endogenous regulator of hepcidin expression and iron metabolism. *Nat Genet* 2009;41(4):482-7.
89. Niederkofler V, Salie R, et al. Hemojuvelin is essential for dietary iron sensing, and its mutation leads to severe iron overload. *J Clin Invest* 2005;115(8):2180-6.
90. Huang FW, Pinkus JL, et al. A mouse model of juvenile hemochromatosis. *J Clin Invest* 2005;115(8):2187-91.
91. Millard KN, Frazer DM, et al. Changes in the expression of intestinal iron transport and hepatic regulatory molecules explain the enhanced iron absorption associated with pregnancy in the rat. *Gut* 2004;53(5):655-60.
92. Nicolas G, Chauvet C, et al. The gene encoding the iron regulatory peptide hepcidin is regulated by anemia, hypoxia, and inflammation. *J Clin Invest* 2002;110(7):1037-44.
93. Lee P, Peng H, et al. Regulation of hepcidin transcription by interleukin-1 and interleukin-6. *Proc Natl Acad Sci U S A* 2005;102(6):1906-10.
94. Inamura J, Ikuta K, et al. Upregulation of hepcidin by interleukin-1beta in human hepatoma cell lines. *Hepatol Res* 2005;33(3):198-205.
95. Lakatos PL. Recent trends in the epidemiology of inflammatory bowel diseases: up or down? *World J Gastroenterol* 2006;12(38):6102-8.
96. Fuss IJ. Is the Th1/Th2 paradigm of immune regulation applicable to IBD? *Inflamm Bowel Dis* 2008;14 Suppl 2:S110-2.
97. Baumgart DC, Sandborn WJ. Inflammatory bowel disease: clinical aspects and established and evolving therapies. *Lancet* 2007;369(9573):1641-57.
98. Orholm M, Binder V, et al. Concordance of inflammatory bowel disease among Danish twins. Results of a nationwide study. *Scand J Gastroenterol* 2000;35(10):1075-81.
99. Thompson NP, Driscoll R, et al. Genetics versus environment in inflammatory bowel disease: results of a British twin study. *Bmj* 1996;312(7023):95-6.
100. Tysk C, Lindberg E, et al. Ulcerative colitis and Crohn's disease in an unselected population of monozygotic and dizygotic twins. A study of heritability and the influence of smoking. *Gut* 1988;29(7):990-6.
101. Barrett JC, Hansoul S, et al. Genome-wide association defines more than 30 distinct susceptibility loci for Crohn's disease. *Nat Genet* 2008;40(8):955-62.
102. Welcker K, Martin A, et al. Increased intestinal permeability in patients with inflammatory bowel disease. *Eur J Med Res* 2004;9(10):456-60.
103. Zeissig S, Burgel N, et al. Changes in expression and distribution of claudin 2, 5 and 8 lead to discontinuous tight junctions and barrier dysfunction in active Crohn's disease. *Gut* 2007;56(1):61-72.
104. Martin HM, Campbell BJ, et al. Enhanced *Escherichia coli* adherence and invasion in Crohn's disease and colon cancer. *Gastroenterology* 2004;127(1):80-93.
105. Kraus TA, Toy L, et al. Failure to induce oral tolerance in Crohn's and ulcerative colitis patients: possible genetic risk. *Ann N Y Acad Sci* 2004;1029:225-38.
106. Brown SJ, Mayer L. The immune response in inflammatory bowel disease. *Am J Gastroenterol* 2007;102(9):2058-69.
107. Hooper LV, Wong MH, et al. Molecular analysis of commensal host-microbial relationships in the intestine. *Science* 2001;291(5505):881-4.
108. Gersemann M, Becker S, et al. Differences in goblet cell differentiation between Crohn's disease and ulcerative colitis. *Differentiation* 2009;77(1):84-94.
109. Fellermann K, Stange DE, et al. A chromosome 8 gene-cluster polymorphism with low human beta-defensin 2 gene copy number predisposes to Crohn disease of the colon. *Am J Hum Genet* 2006;79(3):439-48.
110. Wehkamp J, Salzman NH, et al. Reduced Paneth cell alpha-defensins in ileal Crohn's disease. *Proc Natl Acad Sci U S A* 2005;102(50):18129-34.

111. Nuding S, Fellermann K, et al. Reduced mucosal antimicrobial activity in Crohn's disease of the colon. *Gut* 2007;56(9):1240-7.
112. Brandtzaeg P, Carlsen HS, et al. The B-cell system in inflammatory bowel disease. *Adv Exp Med Biol* 2006;579:149-67.
113. Satsangi J, Morecroft J, et al. Genetics of inflammatory bowel disease: scientific and clinical implications. *Best Pract Res Clin Gastroenterol* 2003;17(1):3-18.
114. Doering J, Begue B, et al. Induction of T lymphocyte apoptosis by sulphasalazine in patients with Crohn's disease. *Gut* 2004;53(11):1632-8.
115. Bouma G, Strober W. The immunological and genetic basis of inflammatory bowel disease. *Nat Rev Immunol* 2003;3(7):521-33.
116. Ina K, Itoh J, et al. Resistance of Crohn's disease T cells to multiple apoptotic signals is associated with a Bcl-2/Bax mucosal imbalance. *J Immunol* 1999;163(2):1081-90.
117. Monteleone G, Kumberova A, et al. Blocking Smad7 restores TGF-beta1 signaling in chronic inflammatory bowel disease. *J Clin Invest* 2001;108(4):601-9.
118. Boirivant M, Marini M, et al. Lamina propria T cells in Crohn's disease and other gastrointestinal inflammation show defective CD2 pathway-induced apoptosis. *Gastroenterology* 1999;116(3):557-65.
119. Cong Y, Weaver CT, et al. Bacterial-reactive T regulatory cells inhibit pathogenic immune responses to the enteric flora. *J Immunol* 2002;169(11):6112-9.
120. Hoffmann JC, Pawlowski NN, et al. Animal models of inflammatory bowel disease: an overview. *Pathobiology* 2002;70(3):121-30.
121. Ron D. Translational control in the endoplasmic reticulum stress response. *J Clin Invest* 2002;110(10):1383-8.
122. Szegezdi E, Logue SE, et al. Mediators of endoplasmic reticulum stress-induced apoptosis. *EMBO Rep* 2006;7(9):880-5.
123. Kaneko M, Niinuma Y, et al. Activation signal of nuclear factor-kappa B in response to endoplasmic reticulum stress is transduced via IRE1 and tumor necrosis factor receptor-associated factor 2. *Biol Pharm Bull* 2003;26(7):931-5.
124. Shkoda A, Ruiz PA, et al. Interleukin-10 blocked endoplasmic reticulum stress in intestinal epithelial cells: impact on chronic inflammation. *Gastroenterology* 2007;132(1):190-207.
125. Kaser A, Lee AH, et al. XBP1 links ER stress to intestinal inflammation and confers genetic risk for human inflammatory bowel disease. *Cell* 2008;134(5):743-56.
126. Heazlewood CK, Cook MC, et al. Aberrant mucin assembly in mice causes endoplasmic reticulum stress and spontaneous inflammation resembling ulcerative colitis. *PLoS Med* 2008;5(3):e54.
127. Bertolotti A, Wang X, et al. Increased sensitivity to dextran sodium sulfate colitis in IRE1beta-deficient mice. *J Clin Invest* 2001;107(5):585-93.
128. Faye A, Ramey G, et al. Haptoglobin is degraded by iron in C57BL/6 mice: a possible link with endoplasmic reticulum stress. *Blood Cells Mol Dis* 2007;39(3):229-37.
129. Lou LX, Geng B, et al. Endoplasmic reticulum stress involved in heart and liver injury in iron-loaded rats. *Clin Exp Pharmacol Physiol* 2009;36(7):612-8.
130. de Almeida SF, de Sousa M. The unfolded protein response in hereditary haemochromatosis. *J Cell Mol Med* 2008;12(2):421-34.
131. Sato M, Suzuki S. [Endoplasmic reticulum stress and metallothionein]. *Yakugaku Zasshi* 2007;127(4):703-8.
132. Vecchi C, Montosi G, et al. ER stress controls iron metabolism through induction of hepcidin. *Science* 2009;325(5942):877-80.
133. Perl DP, Fogarty U, et al. Bacterial-metal interactions: the potential role of aluminum and other trace elements in the etiology of Crohn's disease. *Inflamm Bowel Dis* 2004;10(6):881-3.
134. Roy CN, Andrews NC. Anemia of inflammation: the hepcidin link. *Curr Opin Hematol* 2005;12(2):107-11.
135. Semrin G, Fishman DS, et al. Impaired intestinal iron absorption in Crohn's disease correlates with disease activity and markers of inflammation. *Inflamm Bowel Dis* 2006;12(12):1101-6.
136. Blick M, Sherwin SA, et al. Phase I study of recombinant tumor necrosis factor in cancer patients. *Cancer Res* 1987;47(11):2986-9.
137. Vadhan-Raj S, Al-Katib A, et al. Phase I trial of recombinant interferon gamma in cancer patients. *J Clin Oncol* 1986;4(2):137-46.

138. Lomer MC, Kodjabashia K, et al. Intake of dietary iron is low in patients with Crohn's disease: a case-control study. *Br J Nutr* 2004;91(1):141-8.
139. Taffet SL, Das KM. Sulfasalazine. Adverse effects and desensitization. *Dig Dis Sci* 1983;28(9):833-42.
140. Gasche C, Berstad A, et al. Guidelines on the diagnosis and management of iron deficiency and anemia in inflammatory bowel diseases. *Inflamm Bowel Dis* 2007;13(12):1545-53.
141. WHO. Iron deficiency anaemia: assessment, prevention and control; 2001.
142. Liguori L. Iron protein succinylate in the treatment of iron deficiency: controlled, double-blind, multicenter clinical trial on over 1,000 patients. *Int J Clin Pharmacol Ther Toxicol* 1993;31(3):103-23.
143. Coplin M, Schuette S, et al. Tolerability of iron: a comparison of bis-glycino iron II and ferrous sulfate. *Clin Ther* 1991;13(5):606-12.
144. Buffinton GD, Doe WF. Depleted mucosal antioxidant defences in inflammatory bowel disease. *Free Radic Biol Med* 1995;19(6):911-8.
145. Lih-Brody L, Powell SR, et al. Increased oxidative stress and decreased antioxidant defenses in mucosa of inflammatory bowel disease. *Dig Dis Sci* 1996;41(10):2078-86.
146. Simmonds NJ, Allen RE, et al. Chemiluminescence assay of mucosal reactive oxygen metabolites in inflammatory bowel disease. *Gastroenterology* 1992;103(1):186-96.
147. Millar AD, Rampton DS, et al. Effects of iron and iron chelation in vitro on mucosal oxidant activity in ulcerative colitis. *Aliment Pharmacol Ther* 2000;14(9):1163-8.
148. Erichsen K, Hausken T, et al. Ferrous fumarate deteriorated plasma antioxidant status in patients with Crohn disease. *Scand J Gastroenterol* 2003;38(5):543-8.
149. Lund EK, Wharf SG, et al. Oral ferrous sulfate supplements increase the free radical-generating capacity of feces from healthy volunteers. *Am J Clin Nutr* 1999;69(2):250-5.
150. Aghdassi E, Wendland BE, et al. Antioxidant vitamin supplementation in Crohn's disease decreases oxidative stress. a randomized controlled trial. *Am J Gastroenterol* 2003;98(2):348-53.
151. Uritski R, Barshack I, et al. Dietary iron affects inflammatory status in a rat model of colitis. *J Nutr* 2004;134(9):2251-5.
152. Erichsen K, Milde AM, et al. Low-dose oral ferrous fumarate aggravated intestinal inflammation in rats with DSS-induced colitis. *Inflamm Bowel Dis* 2005;11(8):744-8.
153. Carrier JC, Aghdassi E, et al. Exacerbation of dextran sulfate sodium-induced colitis by dietary iron supplementation: role of NF-kappaB. *Int J Colorectal Dis* 2006;21(4):381-7.
154. Carrier J, Aghdassi E, et al. Iron supplementation increases disease activity and vitamin E ameliorates the effect in rats with dextran sulfate sodium-induced colitis. *J Nutr* 2002;132(10):3146-50.
155. Carrier J, Aghdassi E, et al. Effect of oral iron supplementation on oxidative stress and colonic inflammation in rats with induced colitis. *Aliment Pharmacol Ther* 2001;15(12):1989-99.
156. Reifen R, Matas Z, et al. Iron supplementation may aggravate inflammatory status of colitis in a rat model. *Dig Dis Sci* 2000;45(2):394-7.
157. Reifen R, Nissenkorn A, et al. 5-ASA and lycopene decrease the oxidative stress and inflammation induced by iron in rats with colitis. *J Gastroenterol* 2004;39(6):514-9.
158. Oldenburg B, van Berge Henegouwen GP, et al. Iron supplementation affects the production of pro-inflammatory cytokines in IL-10 deficient mice. *Eur J Clin Invest* 2000;30(6):505-10.
159. Barollo M, D'Inca R, et al. Effects of iron manipulation on trace elements level in a model of colitis in rats. *World J Gastroenterol* 2005;11(28):4396-9.
160. Barollo M, D'Inca R, et al. Effects of iron deprivation or chelation on DNA damage in experimental colitis. *Int J Colorectal Dis* 2004;19(5):461-6.
161. Stein JM, Hartmann F, et al. [Pathophysiological-based diagnosis and therapy of iron-deficient anaemia in inflammatory bowel disease]. *Z Gastroenterol* 2009;47(2):228-36.
162. Silverstein SB, Rodgers GM. Parenteral iron therapy options. *Am J Hematol* 2004;76(1):74-8.
163. Gloire G, Legrand-Poels S, et al. NF-kappaB activation by reactive oxygen species: fifteen years later. *Biochem Pharmacol* 2006;72(11):1493-505.
164. Bonizzi G, Karin M. The two NF-kappaB activation pathways and their role in innate and adaptive immunity. *Trends Immunol* 2004;25(6):280-8.
165. Li N, Karin M. Is NF-kappaB the sensor of oxidative stress? *Faseb J* 1999;13(10):1137-43.
166. Anderson MT, Staal FJ, et al. Separation of oxidant-initiated and redox-regulated steps in the NF-kappa B signal transduction pathway. *Proc Natl Acad Sci U S A* 1994;91(24):11527-31.

167. Shrivastava A, Aggarwal BB. Antioxidants differentially regulate activation of nuclear factor-kappa B, activator protein-1, c-jun amino-terminal kinases, and apoptosis induced by tumor necrosis factor: evidence that JNK and NF-kappa B activation are not linked to apoptosis. *Antioxid Redox Signal* 1999;1(2):181-91.
168. Hayakawa M, Miyashita H, et al. Evidence that reactive oxygen species do not mediate NF-kappaB activation. *Embo J* 2003;22(13):3356-66.
169. Korn SH, Wouters EF, et al. Cytokine-induced activation of nuclear factor-kappa B is inhibited by hydrogen peroxide through oxidative inactivation of IkappaB kinase. *J Biol Chem* 2001;276(38):35693-700.
170. Nakano H, Nakajima A, et al. Reactive oxygen species mediate crosstalk between NF-kappaB and JNK. *Cell Death Differ* 2006;13(5):730-7.
171. Papa S, Bubici C, et al. The NF-kappaB-mediated control of the JNK cascade in the antagonism of programmed cell death in health and disease. *Cell Death Differ* 2006;13(5):712-29.
172. She H, Xiong S, et al. Iron activates NF-kappaB in Kupffer cells. *Am J Physiol Gastrointest Liver Physiol* 2002;283(3):G719-26.
173. Li L, Frei B. Iron chelation inhibits NF-kappaB-mediated adhesion molecule expression by inhibiting p22(phox) protein expression and NADPH oxidase activity. *Arterioscler Thromb Vasc Biol* 2006;26(12):2638-43.
174. Stone RM. How I treat patients with myelodysplastic syndromes. *Blood* 2009;113(25):6296-303.
175. Richardson DR, Kalinowski DS, et al. Cancer cell iron metabolism and the development of potent iron chelators as anti-tumour agents. *Biochim Biophys Acta* 2009;1790(7):702-17.
176. Kontoyiannis D, Pasparakis M, et al. Impaired on/off regulation of TNF biosynthesis in mice lacking TNF AU-rich elements: implications for joint and gut-associated immunopathologies. *Immunity* 1999;10(3):387-98.
177. Kontoyiannis D, Boulougouris G, et al. Genetic dissection of the cellular pathways and signaling mechanisms in modeled tumor necrosis factor-induced Crohn's-like inflammatory bowel disease. *J Exp Med* 2002;196(12):1563-74.
178. Apostolaki M, Manoloukos M, et al. Role of beta7 integrin and the chemokine/chemokine receptor pair CCL25/CCR9 in modeled TNF-dependent Crohn's disease. *Gastroenterology* 2008;134(7):2025-35.
179. Rath HC, Herfarth HH, et al. Normal luminal bacteria, especially Bacteroides species, mediate chronic colitis, gastritis, and arthritis in HLA-B27/human beta2 microglobulin transgenic rats. *J Clin Invest* 1996;98(4):945-53.
180. Ruiz PA, Shkoda A, et al. IL-10 gene-deficient mice lack TGF-beta/Smad-mediated TLR2 degradation and fail to inhibit proinflammatory gene expression in intestinal epithelial cells under conditions of chronic inflammation. *Ann N Y Acad Sci* 2006;1072:389-94.
181. Ruiz PA, Shkoda A, et al. IL-10 gene-deficient mice lack TGF-beta/Smad signaling and fail to inhibit proinflammatory gene expression in intestinal epithelial cells after the colonization with colitogenic *Enterococcus faecalis*. *J Immunol* 2005;174(5):2990-9.
182. Baumeister P, Luo S, et al. Endoplasmic reticulum stress induction of the Grp78/BiP promoter: activating mechanisms mediated by YY1 and its interactive chromatin modifiers. *Mol Cell Biol* 2005;25(11):4529-40.
183. Martinez I, Wallace G, et al. Diet-induced metabolic improvements in a hamster model of hypercholesterolemia are strongly linked to alterations of the gut microbiota. *Appl Environ Microbiol* 2009;75(12):4175-84.
184. Cole JR, Wang Q, et al. The Ribosomal Database Project: improved alignments and new tools for rRNA analysis. *Nucleic Acids Res* 2009;37(Database issue):D141-5.
185. Schumann K, Herbach N, et al. Iron absorption and distribution in TNF(DeltaARE/+) mice, a model of chronic inflammation. *J Trace Elem Med Biol*;24(1):58-66.
186. Sturm A, Lensch M, et al. Human galectin-2: novel inducer of T cell apoptosis with distinct profile of caspase activation. *J Immunol* 2004;173(6):3825-37.
187. Kirino Y, Takeno M, et al. Tumor necrosis factor alpha acceleration of inflammatory responses by down-regulating heme oxygenase 1 in human peripheral monocytes. *Arthritis Rheum* 2007;56(2):464-75.
188. Kaser A, Blumberg RS. Endoplasmic reticulum stress and intestinal inflammation. *Mucosal Immunol*;3(1):11-6.

189. Werner T, Haller D. Intestinal epithelial cell signalling and chronic inflammation: From the proteome to specific molecular mechanisms. *Mutat Res* 2007;622(1-2):42-57.
190. Mullner EW, Neupert B, et al. A specific mRNA binding factor regulates the iron-dependent stability of cytoplasmic transferrin receptor mRNA. *Cell* 1989;58(2):373-82.
191. Casey JL, Hentze MW, et al. Iron-responsive elements: regulatory RNA sequences that control mRNA levels and translation. *Science* 1988;240(4854):924-8.
192. Wallander ML, Leibold EA, et al. Molecular control of vertebrate iron homeostasis by iron regulatory proteins. *Biochim Biophys Acta* 2006;1763(7):668-89.
193. Beinert H, Kennedy MC, et al. Aconitase as Ironminus signSulfur Protein, Enzyme, and Iron-Regulatory Protein. *Chem Rev* 1996;96(7):2335-2374.
194. Dandekar T, Stripecke R, et al. Identification of a novel iron-responsive element in murine and human erythroid delta-aminolevulinic acid synthase mRNA. *Embo J* 1991;10(7):1903-9.
195. Zheng L, Kennedy MC, et al. Binding of cytosolic aconitase to the iron responsive element of porcine mitochondrial aconitase mRNA. *Arch Biochem Biophys* 1992;299(2):356-60.
196. Fukushima K, Fiocchi C. Paradoxical decrease of mitochondrial DNA deletions in epithelial cells of active ulcerative colitis patients. *Am J Physiol Gastrointest Liver Physiol* 2004;286(5):G804-13.
197. Roediger WE. The colonic epithelium in ulcerative colitis: an energy-deficiency disease? *Lancet* 1980;2(8197):712-5.
198. Grisham MB, Granger DN. Neutrophil-mediated mucosal injury. Role of reactive oxygen metabolites. *Dig Dis Sci* 1988;33(3 Suppl):6S-15S.
199. Babbs CF. Oxygen radicals in ulcerative colitis. *Free Radic Biol Med* 1992;13(2):169-81.
200. Pravda J. Radical induction theory of ulcerative colitis. *World J Gastroenterol* 2005;11(16):2371-84.
201. Kruidenier L, Kuiper I, et al. Intestinal oxidative damage in inflammatory bowel disease: semi-quantification, localization, and association with mucosal antioxidants. *J Pathol* 2003;201(1):28-36.
202. Keilin D, Hartree EF. Catalase, peroxidase and metmyoglobin as catalysts of coupled peroxidatic reactions. *Biochem J* 1955;60(2):310-25.
203. Keilin D, Hartree EF. Properties of catalase. Catalysis of coupled oxidation of alcohols. *Biochem J* 1945;39(4):293-301.
204. Batandier C, Fontaine E, et al. Determination of mitochondrial reactive oxygen species: methodological aspects. *J Cell Mol Med* 2002;6(2):175-87.
205. Furuyama K, Kaneko K, et al. Heme as a magnificent molecule with multiple missions: heme determines its own fate and governs cellular homeostasis. *Tohoku J Exp Med* 2007;213(1):1-16.
206. Ponka P. Tissue-specific regulation of iron metabolism and heme synthesis: distinct control mechanisms in erythroid cells. *Blood* 1997;89(1):1-25.
207. Muhlenhoff U, Lill R. Biogenesis of iron-sulfur proteins in eukaryotes: a novel task of mitochondria that is inherited from bacteria. *Biochim Biophys Acta* 2000;1459(2-3):370-82.
208. Bai J, Cederbaum AI. Mitochondrial catalase and oxidative injury. *Biol Signals Recept* 2001;10(3-4):189-99.
209. Lupertz R, Chovolou Y, et al. Catalase overexpression impairs TNF-alpha induced NF-kappaB activation and sensitizes MCF-7 cells against TNF-alpha. *J Cell Biochem* 2008;103(5):1497-511.
210. Ward PP, Paz E, et al. Multifunctional roles of lactoferrin: a critical overview. *Cell Mol Life Sci* 2005;62(22):2540-8.
211. Mikogami T, Marianne T, et al. Effect of intracellular iron depletion by picolinic acid on expression of the lactoferrin receptor in the human colon carcinoma cell subclone HT29-18-C1. *Biochem J* 1995;308 ( Pt 2):391-7.
212. Tsuji S, Yamashita M, et al. Differential structure and activity between human and mouse intelectin-1: human intelectin-1 is a disulfide-linked trimer, whereas mouse homologue is a monomer. *Glycobiology* 2007;17(10):1045-51.
213. Puren AJ, Razeghi P, et al. Interleukin-18 enhances lipopolysaccharide-induced interferon-gamma production in human whole blood cultures. *J Infect Dis* 1998;178(6):1830-4.
214. Takeuchi M, Nishizaki Y, et al. Immunohistochemical and immuno-electron-microscopic detection of interferon-gamma-inducing factor ("interleukin-18") in mouse intestinal epithelial cells. *Cell Tissue Res* 1997;289(3):499-503.

215. Jorquera R, Tanguay RM. Fumarylacetoacetate, the metabolite accumulating in hereditary tyrosinemia, activates the ERK pathway and induces mitotic abnormalities and genomic instability. *Hum Mol Genet* 2001;10(17):1741-52.
216. Jorquera R, Tanguay RM. Cyclin B-dependent kinase and caspase-1 activation precedes mitochondrial dysfunction in fumarylacetoacetate-induced apoptosis. *Faseb J* 1999;13(15):2284-98.
217. Jorquera R, Tanguay RM. The mutagenicity of the tyrosine metabolite, fumarylacetoacetate, is enhanced by glutathione depletion. *Biochem Biophys Res Commun* 1997;232(1):42-8.
218. Tanguay RM, Jorquera R, et al. Tyrosine and its catabolites: from disease to cancer. *Acta Biochim Pol* 1996;43(1):209-16.
219. Bergeron A, Jorquera R, et al. Involvement of endoplasmic reticulum stress in hereditary tyrosinemia type I. *J Biol Chem* 2006;281(9):5329-34.
220. Fisher AL, Page KE, et al. The *Caenorhabditis elegans* K10C2.4 gene encodes a member of the fumarylacetoacetate hydrolase family: a *Caenorhabditis elegans* model of type I tyrosinemia. *J Biol Chem* 2008;283(14):9127-35.
221. Wang P, Heitman J. The cyclophilins. *Genome Biol* 2005;6(7):226.
222. Stames MA, Rutherford SL, et al. Cyclophilins: a new family of proteins involved in intracellular folding. *Trends Cell Biol* 1992;2(9):272-6.
223. Kaser A, Blumberg RS. Endoplasmic reticulum stress in the intestinal epithelium and inflammatory bowel disease. *Semin Immunol* 2009;21(3):156-63.
224. Lawless MW, Mankan AK, et al. Expression of hereditary hemochromatosis C282Y HFE protein in HEK293 cells activates specific endoplasmic reticulum stress responses. *BMC Cell Biol* 2007;8:30.
225. de Almeida SF, Picarote G, et al. Chemical chaperones reduce endoplasmic reticulum stress and prevent mutant HFE aggregate formation. *J Biol Chem* 2007;282(38):27905-12.
226. Isom HC, McDevitt EI, et al. Elevated hepatic iron: A confounding factor in chronic hepatitis C. *Biochim Biophys Acta* 2009.
227. Nunez MT, Osorio A, et al. Iron-induced oxidative stress up-regulates calreticulin levels in intestinal epithelial (Caco-2) cells. *J Cell Biochem* 2001;82(4):660-5.
228. Ferruzza S, Scarino ML, et al. Biphasic effect of iron on human intestinal Caco-2 cells: early effect on tight junction permeability with delayed onset of oxidative cytotoxic damage. *Cell Mol Biol (Noisy-le-grand)* 2003;49(1):89-99.
229. Ferruzza S, Scacchi M, et al. Iron and copper alter tight junction permeability in human intestinal Caco-2 cells by distinct mechanisms. *Toxicol In Vitro* 2002;16(4):399-404.
230. Nunez MT, Tapia V, et al. Iron-induced oxidative damage in colon carcinoma (Caco-2) cells. *Free Radic Res* 2001;34(1):57-68.
231. Lukinova N, Iacovelli J, et al. Iron chelation protects the retinal pigment epithelial cell line ARPE-19 against cell death triggered by diverse stimuli. *Invest Ophthalmol Vis Sci* 2009;50(3):1440-7.
232. Courtois F, Seidman EG, et al. Membrane peroxidation by lipopolysaccharide and iron-ascorbate adversely affects Caco-2 cell function: beneficial role of butyric acid. *Am J Clin Nutr* 2003;77(3):744-50.
233. Meddings JB. Review article: Intestinal permeability in Crohn's disease. *Aliment Pharmacol Ther* 1997;11 Suppl 3:47-53; discussion 53-6.
234. Issenman RM, Jenkins RT, et al. Intestinal permeability compared in pediatric and adult patients with inflammatory bowel disease. *Clin Invest Med* 1993;16(3):187-96.
235. Peeters M, Ghooys Y, et al. Increased permeability of macroscopically normal small bowel in Crohn's disease. *Dig Dis Sci* 1994;39(10):2170-6.
236. Prasad S, Mingrino R, et al. Inflammatory processes have differential effects on claudins 2, 3 and 4 in colonic epithelial cells. *Lab Invest* 2005;85(9):1139-62.
237. Ryan P, Kelly RG, et al. Bacterial DNA within granulomas of patients with Crohn's disease--detection by laser capture microdissection and PCR. *Am J Gastroenterol* 2004;99(8):1539-43.
238. Darfeuille-Michaud A, Boudeau J, et al. High prevalence of adherent-invasive *Escherichia coli* associated with ileal mucosa in Crohn's disease. *Gastroenterology* 2004;127(2):412-21.
239. Ganz T. Iron in innate immunity: starve the invaders. *Curr Opin Immunol* 2009;21(1):63-7.
240. Kabyemela ER, Fried M, et al. Decreased susceptibility to *Plasmodium falciparum* infection in pregnant women with iron deficiency. *J Infect Dis* 2008;198(2):163-6.

241. Koka S, Foller M, et al. Iron deficiency influences the course of malaria in *Plasmodium berghei* infected mice. *Biochem Biophys Res Commun* 2007;357(3):608-14.
242. Qin J, Li R, et al. A human gut microbial gene catalogue established by metagenomic sequencing. *Nature*;464(7285):59-65.
243. Florin TH. A role for sulfate-reducing bacteria in ulcerative colitis. *Gastroenterology* 1990;98:A170.
244. Macfarlane S, Furrie E, et al. Mucosal bacteria in ulcerative colitis. *Br J Nutr* 2005;93 Suppl 1:S67-72.
245. Favre C, Neut C, et al. Fecal beta-D-galactosidase production and Bifidobacteria are decreased in Crohn's disease. *Dig Dis Sci* 1997;42(4):817-22.
246. Inness VL, McCartney AL, et al. Molecular characterisation of the gut microflora of healthy and inflammatory bowel disease cats using fluorescence in situ hybridisation with special reference to *Desulfovibrio* spp. *J Anim Physiol Anim Nutr (Berl)* 2007;91(1-2):48-53.
247. Kleessen B, Kroesen AJ, et al. Mucosal and invading bacteria in patients with inflammatory bowel disease compared with controls. *Scand J Gastroenterol* 2002;37(9):1034-41.
248. Sartor RB. Probiotic therapy of intestinal inflammation and infections. *Curr Opin Gastroenterol* 2005;21(1):44-50.
249. Foster SL, Richardson SH, et al. Elevated iron status increases bacterial invasion and survival and alters cytokine/chemokine mRNA expression in Caco-2 human intestinal cells. *J Nutr* 2001;131(5):1452-8.
250. Holbein BE. Enhancement of *Neisseria meningitidis* infection in mice by addition of iron bound to transferrin. *Infect Immun* 1981;34(1):120-5.
251. Kulnigg S, Gasche C. Systematic review: managing anaemia in Crohn's disease. *Aliment Pharmacol Ther* 2006;24(11-12):1507-23.
252. Erichsen K, Ulvik RJ, et al. Oral ferrous fumarate or intravenous iron sucrose for patients with inflammatory bowel disease. *Scand J Gastroenterol* 2005;40(9):1058-65.
253. Seril DN, Liao J, et al. Dietary iron supplementation enhances DSS-induced colitis and associated colorectal carcinoma development in mice. *Dig Dis Sci* 2002;47(6):1266-78.
254. Gasche C, Waldhoer T, et al. Prediction of response to iron sucrose in inflammatory bowel disease-associated anemia. *Am J Gastroenterol* 2001;96(8):2382-7.
255. Bodemar G, Kechagias S, et al. Treatment of anaemia in inflammatory bowel disease with iron sucrose. *Scand J Gastroenterol* 2004;39(5):454-8.
256. Lindgren S, Wikman O, et al. Intravenous iron sucrose is superior to oral iron sulphate for correcting anaemia and restoring iron stores in IBD patients: A randomized, controlled, evaluator-blind, multicentre study. *Scand J Gastroenterol* 2009;1-8.
257. Bernstein CN, Leslie WD. Review article: Osteoporosis and inflammatory bowel disease. *Aliment Pharmacol Ther* 2004;19(9):941-52.
258. Huybers S, Apostolaki M, et al. Murine TNF(DeltaARE) Crohn's disease model displays diminished expression of intestinal Ca<sup>2+</sup> transporters. *Inflamm Bowel Dis* 2008;14(6):803-11.

## ACKNOWLEDGEMENTS

Mein aufrichtiger Dank gilt Prof. Dr. Dirk Haller für seine ewig währende Begeisterung an der Wissenschaft, die nicht endenden neuen Ideen, die intensiven und bereichernden Diskussionen, aber vor allem für das entgegengebrachte Vertrauen in die eigenen Fähigkeiten und dafür, dass es in der Arbeitsgruppe immer gemenschelt hat.

Ebenso möchte ich mich sehr herzlich bei Prof. Dr. Klaus Schümann bedanken, mein persönlicher Eisenguru, vor allem für die stete Bereitschaft alle Fragen über Eisen zu beantworten und für seine lustigen E-Mails, die mich oftmals haben schmunzeln lassen.

Danke an Prof. Dr. Hannelore Daniel für die Übernahme des Vorsitz der Prüfungskommission und die überaus erfolgreiche Nutzung der MALDI-TOF MS.

Ein ganz großes Dankeschön geht an Prof. Dr. Jens Walter und Inés Martínez für die Durchführung der Pyrosequenzierung, die Auswertung der Daten und das Aufbereiten für die Publikation.

Vielen lieben Dank an Tina Hallas, für die Unterstützung bei meinen U-Boot Experimenten, die sie manchmal zur Verzweiflung gebracht haben und der Aktion „Die Tonne des Grauens“ (ich werde dies nicht näher erläutern). An dieser Stelle danke ich aufrichtig allen Mäusen, die für meine wissenschaftlichen Experimente ihr Leben lassen mussten (meist durch Tina's Hand).

Dafür, dass die letzten 4 Jahre trotz einiger wissenschaftlicher Rückschläge immer wieder sehr viel Spaß gemacht haben möchte ich mich von Herzen bedanken bei meinen Kollegen und Freunden: Anna Shkoda, Pedro Ruiz, Micha Hoffmann, Anja Messlik (my only Hanni), Thomas Clavel (wo wären wir ohne Zopf und Geduldspiele zum Geburtstag – danke!), Gabriele Hörmannspurger (besonders das Koffer tragen in den USA), Eva Rath (kommt Zeit, kommt Rat(h)), Katharina Rank, Marie Anne von Schilde (my sports buddy), Natalie Steck (klein aber oho!), Emanuel (Emu) Berger, Nico Gebhardt (wo wäre ich ohne meinen lebendigen Molaritätenrechner – FCB!!), Benjamin Tiemann, Lisa Gruber, Katharina Heller, Pia Baur, Sigrid Kisling, Ingrid Schmöller, Job Mapesa, Silvia Pitariu, Susan Chang, Anna Zenchuk, Sonja Böhm und Brita Sturm...dafür, dass wir ein tolles Team waren.

Ein extra Dank an Stefan Wagner, der mehr als ein Jahr mit mir auf dem Eisentrip war. Versuch CK9 bleibt unvergessen!

Ich habe das große Glück, liebe Freunde an meiner Seite zu haben, die vermutlich nie verstanden haben was ich da eigentlich getan habe, die mich aber immer auf ihre eigene Weise unterstützt haben. Vielen nicht-in-Worte-fassbaren Dank an: Laura & Alexander, Iris & Mathias, Chrissi, Dagmar, Michi, Flo & LX, Christina & Schanzi, Torsten & Christian.

Zuletzt bedanke ich mich aus tiefstem Herzen bei meinen Eltern Dieter und Gerda Werner, bei meinem Bruder Tom, Susi, Lena, Benjamin und Frank, weil ihr mein Leben täglich bereichert, mir Liebe, Wärme und Geborgenheit gebt und weil wir eine super Familie sind. Mein lieber Frank (G), ohne deinen Humor und deine unermüdete, positive Art wäre Vieles schwerer.

## CURRICULUM VITAE

### **Persönliche Daten**

**Geburtstag und -ort:**

22.03.1979 in München

**Familienstand:**

ledig, keine Kinder

**Staatsangehörigkeit:**

deutsch

### **Berufstätigkeit und Studium**

seit Mai 2006

**Doktorandin**

am Lehrstuhl für Biofunktionalität der Lebensmittel

**Titel der Promotion:**

„Iron as environmental factor in the pathogenesis of Crohn’s disease-like ileitis“

09/2004 – 05/2006

**Studium der Ernährungswissenschaft (Master of Science)**

an der Technischen Universität München /

Freising-Weihenstephan

**Vertiefungsfach:**

Biomedizin

**Masterarbeit:**

„Proteomanalyse von Patienten mit chronisch entzündlichen Darmerkrankungen (Morbus Crohn und Colitis ulcerosa)“

**Abschluss:**

|                   |   |
|-------------------|---|
|                   | Master of Science   |
| 10/2001 – 08/2004 | <b>Studium der Ernährungswissenschaft (Bachelor of Science)</b><br><br>an der Technischen Universität München /<br><br>Freising-Weihenstephan<br><br><b>Bachelorarbeit:</b><br><br>„Wirkung eines Phytopharmakons (Iberogast®) auf die Kontraktilität des isolierten Meerschweinchenmagens“<br><br><b>Abschluss:</b><br><br>Bachelor of Science |
| 11/2000 – 08/2001 | <b>Assistentin des Geschäftsführers der Bavaria Sonor GmbH</b>  |
| 07/2000 – 10/2000 | <b>Teamassistentin der Geschäftsleitung der Bavaria Sonor GmbH</b><br>(100% Tochter der Bavaria Film GmbH)  |
| 09/1998 – 06/2000 | <b>Ausbildung zur Industriekauffrau</b><br><br>bei Bavaria Film GmbH, München   |

## **Schulischer Werdegang**

|                   |  |
|-------------------|--|
| 09/1989 – 06/1998 | <b>Werner-von-Siemens Gymnasium München</b><br><br><b>Abschluss :</b><br><br>Allgemeine Hochschulreife |
| 09/1985 – 09/1989 | <b>Grundschule am Karl-Marx-Ring, München</b>  |

## **Nebentätigkeiten**

08/2005 – 08/2007

**Assistentin von Dimitrij Saldanha**

Saldanha Consulting

03/2001 – 03/2006

**Aerobictrainerin**

Trainingswelten, Femme Fitness, VHS Ottobrunn etc.

10/2001 – 10/2002

**D.A.S.-Versicherung**

Call-Center Notruf-Hotline

09/1995 – 03/1998

**Verkaufstätigkeiten**

bei Bombastic-Fashion, Planet-Fashion

## **Praktika**

10/2003

**Betriebliches Praktikum**

im Kranken- und Altenpflagedienst Katharina Rastel

09/2003

**Betriebliches Praktikum**

im Krankenhaus Harlaching in der Ernährungsmedizin und Diätetik

## ERKLÄRUNG

Hiermit erkläre ich, dass ich die vorliegende Doktorarbeit selbständig angefertigt habe. Es wurden nur die in der Arbeit ausdrücklich benannten Quellen und Hilfsmittel benutzt. Wörtlich oder sinngemäß übernommenes Gedankengut habe ich als solches kenntlich gemacht.

-----  
Ort, Datum

-----  
Unterschrift